



ETH zürich

Institute of Structural Engineering
Chair of Timber Structures
ETH Zürich

CHARRING MODELS FOR TIMBER

Alperen Gürer

Supervisors

Prof. Dr. Andrea Frangi

Prof. Dr. Bart Merci

Chamith Karannagodage

Master thesis submitted in the Erasmus+ Study Programme
International Master of Science in Fire Safety Engineering

May 2023

This page is intentionally left blank.

Disclaimer

This master's dissertation is submitted in partial fulfilment of the requirements for the degree of The International Master of Science in Fire Safety Engineering (IMFSE). This master's dissertation has never been submitted for any degree or examination to any other University/programme. The author declares that this master's dissertation is original work except where stated. This declaration constitutes an assertion that full and accurate references and citations have been included for all material, directly included and indirectly contributing to the master's dissertation. The author gives permission to make this master's dissertation available for consultation and to copy parts of this master's dissertation for personal use. In the case of any other use, the limitations of the copyright have to be respected, in particular with regard to the obligation to state expressly the source when quoting results from this master's dissertation. The master's dissertation supervisor must be informed when data or results are used.

Read and approved,



Alperen Gürer

May 11, 2023

CHARRING MODELS FOR TIMBER

Author: Alperen Gürer
aguerer@ethz.ch

Supervisors

Prof. Dr. Andrea Frangi
Prof. Dr. Bart Merci
Chamith Karannagodage

May 2023

Abstract

In this thesis, charring models of timber have been inspected and three of them are chosen for comparison. Those are the Brandon's model (FSUW book), Eurocode Model (prEN 1995-1-2:20YY + EN 1991-1-2) and Combined Model (Cumulative temperature charring model (prEN 1995-1-2:20YY) + DIN EN 1991-1-2/NA). The combined model does not exist in current codes, it is a combination of two different codes. The comparison is made by using three sets of experimental data which are from FSUW book, RISE research paper and compartment tests conducted in ETH Zurich. The first two sets are conducted on full scale compartments, the latter one conducted in small scale compartments.

The models' predicted values for compartment temperature and char depth at the end of the fire are compared with the ones measured in the experiments. Also, a sensitivity analysis is done to see the effect of selected parameters such as combustion factor and time dependent modification factor (α). Afterwards, a new method of using two different time dependent modification factors for the combined model is created and compared with the older version which uses only one α value for entire duration of fire. The results suggest that using the updated version of combined model which has two α values gives closest predictions to the experimental measurements. However, additional analyses with different compartment tests can be useful to get more precise results. Further study on the topic of using more than two α values is suggested to be an interesting and important improvement.

Keywords

charring, timber, fire modelling, fire, fire safety, mass timber

VERKOHLUNGSMODELLE FÜR HOLZ

Autor: Alperen Gürer
aguerer@ethz.ch

Betreuerin

Prof. Dr. Andrea Frangi
Prof. Dr. Bart Merci
Chamith Karannagodage

Mai 2023

Zusammenfassung

In dieser Arbeit wurden Verkohlungsmodelle von Holz untersucht und drei davon sind für einen Vergleich ausgewählt worden. Dabei handelt es sich um das Brandon-Modell (FSUW-Buch), das Eurocode-Modell (prEN 1995-1-2:20YY + EN 1991-1-2) und das Kombinationsmodell (Kumulatives Temperatur-Verkohlungsmodell (prEN 1995-1-2:20YY) + DIN EN 1991-1-2/NA). Das Kombinationsmodell existiert nicht in den aktuellen Vorschriften, es ist eine Kombination aus zwei verschiedenen Vorschriften. Der Vergleich erfolgt anhand von drei Datensätzen aus Experimenten, die dem FSUW-Buch entnommen, einer Forschungsarbeit von RISE und Abteilungstests, die an der ETH Zürich durchgeführt wurden, stammen. Die ersten beiden Datensätze stammen aus Tests in lebensgroßen Abteilungen, der letzte aus Tests in kleinen Abteilungen.

Die von den Modellen vorhergesagten Werte für die Abteilungstemperatur und die Verkohlungstiefe am Ende des Feuers werden mit den gemessenen Werten aus den Experimenten verglichen. Außerdem wird eine Sensitivitätsanalyse durchgeführt, um den Effekt ausgewählter Parameter wie dem Verbrennungsfaktor und dem zeitabhängigen Modifikationsfaktor (α) zu sehen. Anschließend wird eine neue Methode zur Verwendung von zwei verschiedenen zeitabhängigen Modifikationsfaktoren für das Kombinationsmodell erstellt und mit der älteren Version verglichen, die nur einen α -Wert für die gesamte Dauer des Feuers verwendet. Die Ergebnisse deuten darauf hin, dass die Verwendung der aktualisierten Version des Kombinationsmodells, das zwei α -Werte hat, im Vergleich zu den experimentellen Messungen die genauesten Vorhersagen liefert. Allerdings könnten zusätzliche Analysen mit verschiedenen Abteilungstests nützlich sein, um genauere Ergebnisse zu erzielen. Weitere Studien zum Thema der Verwendung von mehr als zwei α -Werten werden als interessante und wichtige Verbesserung vorgeschlagen.

Schlagworte

verkohlung, holz, brandmodellierung, feuer, brandschutz, massivholz

AHŞAP İÇİN KÖMÜRLEŞME MODELLERİ

Yazar: Alperen Gürer
aguerer@ethz.ch

Danışmanlar

Prof. Dr. Andrea Frangi
Prof. Dr. Bart Merci
Chamith Karannagodage

Mayıs 2023

Özet

Bu tezde, ahşabın kömürleşme modelleri incelenmiş ve bunlardan üçü karşılaştırma için seçilmiştir. Bunlar Brandon'ın modeli (FSUW kitabı), Eurocode Modeli (prEN 1995-1-2:20YY + EN 1991-1-2) ve Kombine Model (Kümülatif sıcaklık yanma modeli (prEN 1995-1-2:20YY) + DIN EN 1991-1-2/NA)'dir. Kombine model, mevcut kodlarda bulunmamaktadır, bu iki farklı kodun birleşiminden oluşur. Karşılaştırma, FSUW kitabından, RISE araştırma makalesinden ve ETH Zürih'te gerçekleştirilen kompartıman testlerinden elde edilen üç set deneysel veri kullanılarak yapılmıştır. İlk iki set, tam ölçekli kompartıman üzerinde gerçekleştirilirken, sonuncusu küçük ölçekli kompartıman üzerinde gerçekleştirilmiştir.

Modellerin, yangın sonundaki kompartıman sıcaklığı ve kömürleşme derinliği için tahmin ettiği değerler, deneylerde ölçülenlerle karşılaştırılmıştır. Ayrıca, yanma faktörü ve zamana bağımlı modifikasyon faktörü (α) gibi seçilen parametrelerin etkisini görmek için bir duyarlılık analizi yapılmıştır. Daha sonra, kombine model için iki farklı zaman bağımlı modifikasyon faktörünün kullanılmasına yönelik yeni bir yöntem oluşturulmuş ve tüm yangın süresi için yalnızca bir α değeri kullanan daha eski versiyonla karşılaştırılmıştır. Sonuçlar, iki α değerine sahip olan kombine modelin güncellenmiş versiyonunun kullanılmasının, deneysel ölçümlere en yakın tahminleri verdiğini öne sürmektedir. Ancak, farklı kompartıman testleri ile ek analizler, daha kesin sonuçlar almak için yararlı olabilir. İki'den fazla α değeri kullanma konusundaki daha ileri çalışmaların, ilginç ve önemli bir gelişme olacağı önerilmektedir.

Anahtar Kelimeler

kömürleşme, ahşap, yangın modelleme, yangın , yangın güvenliği, lamine ahşap

Acknowledgements

In the journey of crafting this thesis, I owe a wealth of gratitude to several people who have contributed immensely.

My family, consisting of my dear Mom, Dad, and Brother, have been a constant source of love, support, and encouragement. Aybike, your invaluable assistance and motivation was integral in my commitment to my undergraduate studies, leading me to this point.

I am immensely grateful to Prof. Dr. Bart Merci for his supervision and guidance provided during the creation of this thesis. I extend my heartfelt appreciation to Prof. Dr. Andrea Frangi and Chamith Karannagodage, whose guidance and counsel throughout the creation of this thesis was instrumental. Their insights were always interesting, beneficial, and readily available. Special recognition goes to The Chair of Structural Engineering - Timber Structures at ETH Zurich for graciously hosting me in their office and diligently answering all my questions. I also wish to express my gratitude to Basler & Hofmann for providing accommodation during the course of my thesis. Your support was immeasurable, and for this, I am deeply thankful.

Lastly, I would like to express my gratitude to the team at IMFSE for their role in developing such a fascinating Master's programme. Also I am profoundly thankful to the European Union and to the sponsor companies, for their continuous financial support to the programme.

Contents

1	Introduction & Objectives	1
1.1	Objectives	3
2	Methodology	4
2.1	The Temperature Prediction Models	6
2.1.1	EN 1991-1-2 Annex A	6
2.1.1.1	Heating Phase	6
2.1.1.2	Cooling Phase	10
2.1.2	DIN EN 1991-1-2/NA Appendix AA	11
2.1.2.1	Ventilation Controlled Case	14
2.1.2.2	Fuel Controlled Case	16
2.1.2.3	Creating the Curve	17
2.2	The Char Depth Prediction Models	19
2.2.1	Brandon Brandon's method	19
2.2.2	Design model for parametric temperature-time curves	22
2.2.2.1	Design charring rate	23
2.2.2.2	Notional design charring rate	24
2.2.2.3	Design charring depth	26
2.2.2.4	Design total fire load density	27
2.2.2.5	Design structural fire load density	28
2.2.2.6	Iterative Process	28
2.2.3	Cumulative temperature charring model	29
2.3	The Models	29
2.3.1	Brandon's model (FSUW)	29
2.3.2	Eurocode Model (prEN 1995-1-2:20YY + EN 1991-1-2)	30
2.3.3	Cumulative temperature charring model + DIN EN 1991-1-2/NA	30
2.3.4	Comparison of Models	31
2.4	Experiments	33
2.4.1	Fire Safe Use of Wood in Buildings	33

2.4.2	Fire safe implementation of visible mass timber in tall buildings compartment fire testing	35
2.4.3	Compartment Fires Tests conducted in ETH Zurich	40
2.4.3.1	Standard compartment	41
2.4.3.2	Large compartment	42
2.4.3.3	Movable Fuel	43
3	Results & Discussion	45
3.1	Char Depth Predictions for FSUW and RISE Tests	46
3.2	Temperature Predictions for FSUW and RISE Tests	48
3.3	Char Depth Predictions for ETH Zurich Tests	50
3.4	Temperature Predictions for ETH Zurich Tests	52
3.5	Sensitivity Analysis	53
3.5.1	Combustion Factor	54
3.5.2	Time Dependent Modification Factor (α)	56
3.5.3	Ratio Between the Heat Release and Char Depth	58
3.5.4	Rate of Heat Release of Timber Members per Unit Area Related to the Charring Rate	60
3.6	Time dependent modification factor (α) Analysis	62
3.7	Choosing time dependent modification factor (α)	63
3.8	Using two time dependent modification factors (α)	64
3.9	Two time dependent modification factors (α) comparison	65
3.10	Creating time dependent modification factor (α) - Time Graphs	68
4	Conclusion	74
4.1	Recommendations for future work	76
5	Bibliography	78
Appendix A	Graphs for the Other Tests	81
A.1	FSUW Tests	81
A.1.1	Test 2	81
A.1.2	Test 3	82
A.1.3	Test 4	83
A.2	RISE Tests	84
A.2.1	Test 6	84
A.2.2	Test 7	85
A.2.3	Test 8	86
A.2.4	Test 9	87

A.3	ETH Zurich Tests	88
A.3.1	Test C2	88
A.3.2	Test C3	89
A.3.3	Test C4	90
A.3.4	Test C5	91
A.3.5	Test C6	92
A.3.6	Test C7	93
A.3.7	Test C8	94
A.3.8	Test C10	95
A.3.9	Test C11	96
A.3.10	Test C12	97
A.4	Time dependent modification factor (α) Analysis	98
A.4.1	Test 6	98
A.4.2	Test 7	99
A.4.3	Test 8	100
A.4.4	Test 9	101
A.5	Choosing time dependent modification factor (α)	102
A.5.1	Test 6	102
A.5.2	Test 7	103
A.5.3	Test 8	104
A.5.4	Test 9	105
A.6	Using two time dependent modification factors (α)	106
A.6.1	Test 6	106
A.6.2	Test 7	107
A.6.3	Test 8	108
A.6.4	Test 9	109
A.7	Two time dependent modification factors (α) comparison	110
A.7.1	Test 6	110
A.7.2	Test 7	112
A.7.3	Test 8	114
A.7.4	Test 9	116
A.7.5	Test C2	118
A.7.6	Test C3	119
A.7.7	Test C4	120
A.7.8	Test C5	121
A.7.9	Test C6	122
A.7.10	Test C7	123
A.7.11	Test C8	124

A.7.12 Test C10	125
A.7.13 Test C11	126
A.7.14 Test C12	127
A.8 Creating time dependent modification factor (α) - Time Graphs	128
A.8.1 Test 6	128
A.8.2 Test 7	131
A.8.3 Test 8	134
A.8.4 Test 9	137

List of Tables

2.1	Indicative values for the reliability index β_{fi} and the associated probability of failure p_f (Reference period 1 year) for different uses	14
2.2	Parameters for the fire development phase and maximum heat release rate HRR_f per unit area during the full developed phase for different uses (characteristic values)	15
2.3	Modification factors for charring	25
2.4	Basic design charring rate β_0	26
2.5	Modification of Brandon's model	30
2.6	Comparison of Models	32
2.7	Overview of compartment test properties and results of FSUW	34
2.8	Summary of RISE Tests	38
2.9	Overview of fuel load for ETH Zurich Tests	43
2.10	Overview of compartment test properties of ETH Zurich Tests	44

List of Figures

1.1	The Design of Cross Laminated Timber copied from Reid Middleton (2017)	2
1.2	Burning of Timber copied from Klippel, M. and Frangi, A. (2011)	3
2.1	Schematic representation of the temperature-time curve according to the simplified natural fire model with the points (t_i, Θ_i) described by equations and the curve segments in between copied from NABau (2015-09)	11
2.2	Floor Plan for Tests 5, 6, 7 and 8 copied from Brandon <i>et al.</i> (2021)	36
2.3	Floor Plan for Test 9 copied from Brandon <i>et al.</i> (2021)	37
2.4	Standard compartment for ETH Zurich Tests (cm) copied from Glauser <i>et al.</i> (2021)	41
2.5	Large compartment for ETH Zurich Tests (cm) copied from Glauser <i>et al.</i> (2021)	42
3.1	Char Depth Predictions for FSUW and RISE Tests	47
3.2	Temperature for Test 1	48
3.3	Temperature for Test 5	49
3.4	Char Depth Predictions for ETH Zurich Tests	51
3.5	Temperature for Test C9	52
3.6	Sensitivity Analysis of Combustion Factor on Char Depth	54
3.7	Sensitivity Analysis of Combustion Factor on Maximum Temperature	55
3.8	Sensitivity Analysis of Time Dependent Modification Factor on Char Depth	56
3.9	Sensitivity Analysis of Time Dependent Modification Factor on Maximum Temperature	57
3.10	Sensitivity Analysis of Ratio Between the Heat Release and Char Depth on Char Depth	58
3.11	Sensitivity Analysis of Ratio Between the Heat Release and Char Depth on Maximum Temperature	59
3.12	Sensitivity Analysis of Rate of Heat Release of Timber Members per Unit Area Related to the Charring Rate on Char Depth	60
3.13	Sensitivity Analysis of Rate of Heat Release of Timber Members per Unit Area Related to the Charring Rate on Maximum Temperature	61

3.14	Alpha Analysis for Test 5	62
3.15	Choosing Alpha for Test 5	63
3.16	Combined Alpha Method for Test 5	64
3.17	Combined Alpha Method for Test 5	65
3.18	Temperatures for two time dependent modification factor for Test 5 . . .	66
3.19	Temperatures for two time dependent modification factor for Test C9 . .	67
3.20	Alpha - Time Graph for Test 5	68
3.21	Alpha - Time Graph Zoomed for Test 5	70
3.22	Alpha - Time Graph for Test 5	71
3.23	Streamlined Alpha - Time Graph for Test 5	72
3.24	Simplified Alpha - Time Graph for Test 5	73
4.1	Schematic representation of proposed updated version of the temperature-time curve according to the simplified natural fire model with the points (t_i, Θ_i) described by equations and the curve segments in between	76
A.1	Temperature for Test 2	81
A.2	Temperature for Test 3	82
A.3	Temperature for Test 4	83
A.4	Temperature for Test 6	84
A.5	Temperature for Test 7	85
A.6	Temperature for Test 8	86
A.7	Temperature for Test 9	87
A.8	Temperature for Test C2	88
A.9	Temperature for Test C3	89
A.10	Temperature for Test C4	90
A.11	Temperature for Test C5	91
A.12	Temperature for Test C6	92
A.13	Temperature for Test C7	93
A.14	Temperature for Test C8	94
A.15	Temperature for Test C10	95
A.16	Temperature for Test C11	96
A.17	Temperature for Test C12	97
A.18	Alpha Analysis for Test 6	98
A.19	Alpha Analysis for Test 7	99
A.20	Alpha Analysis for Test 8	100
A.21	Alpha Analysis for Test 9	101
A.22	Choosing Alpha for Test 6	102
A.23	Choosing Alpha for Test 7	103

A.24 Choosing Alpha for Test 8	104
A.25 Choosing Alpha for Test 9	105
A.26 Combined Alpha Method for Test 6	106
A.27 Combined Alpha Method for Test 7	107
A.28 Combined Alpha Method for Test 8	108
A.29 Combined Alpha Method for Test 9	109
A.30 Combined Alpha Method for Test 6	110
A.31 Temperatures for two time dependent modification factor for Test 6 . . .	111
A.32 Combined Alpha Method for Test 7	112
A.33 Temperatures for two time dependent modification factor for Test 7 . . .	113
A.34 Combined Alpha Method for Test 8	114
A.35 Temperatures for two time dependent modification factor for Test 8 . . .	115
A.36 Combined Alpha Method for Test 9	116
A.37 Temperatures for two time dependent modification factor for Test 9 . . .	117
A.38 Temperatures for two time dependent modification factor for Test C2 . .	118
A.39 Temperatures for two time dependent modification factor for Test C3 . .	119
A.40 Temperatures for two time dependent modification factor for Test C4 . .	120
A.41 Temperatures for two time dependent modification factor for Test C5 . .	121
A.42 Temperatures for two time dependent modification factor for Test C6 . .	122
A.43 Temperatures for two time dependent modification factor for Test C7 . .	123
A.44 Temperatures for two time dependent modification factor for Test C8 . .	124
A.45 Temperatures for two time dependent modification factor for Test C10 .	125
A.46 Temperatures for two time dependent modification factor for Test C11 .	126
A.47 Temperatures for two time dependent modification factor for Test C12 .	127
A.48 Alpha - Time Graph for Test 6	128
A.49 Streamlined Alpha - Time Graph for Test 6	129
A.50 Simplified Alpha - Time Graph for Test 6	130
A.51 Alpha - Time Graph for Test 7	131
A.52 Streamlined Alpha - Time Graph for Test 7	132
A.53 Simplified Alpha - Time Graph for Test 7	133
A.54 Alpha - Time Graph for Test 8	134
A.55 Streamlined Alpha - Time Graph for Test 8	135
A.56 Simplified Alpha - Time Graph for Test 8	136
A.57 Alpha - Time Graph for Test 9	137
A.58 Streamlined Alpha - Time Graph for Test 9	138
A.59 Simplified Alpha - Time Graph for Test 9	139

Nomenclature

Abbreviations

HRR_f Maximum heat release rate per unit area

CLT Cross Laminated Timber

ETH Swiss Federal Institute of Technology (Eidgenössische Technische Hochschule)

FASY Beech (*Fagus sylvatica*)

FSUW Fire Safe Use of Wood in Buildings

FXEX European ash (*Fraxinus excelsior*)

GLT Glue Laminated Timber

Glulam Glued-laminated

GLVL Glue Laminated Veneer Lumber

HRR Heat Release Rate

IBK Institute of Structural Engineering, ETH Zurich (Institut für Baustatik und Konstruktion)

ISO International Organization for Standardization

LVL Laminated Veneer Lumber

MBO Musterbauordnung, code for fire protection and stability of buildings in Germany

OSB Oriented Strand Board

QCXA White oak (*Quercus alba*)

QCXE Oak (*Quercus petraea*, *Quercus robur*)

QCXR Northern red oak (*Quercus rubra*)

RISE Research Institutes of Sweden

Upper-case Roman letters

$\dot{Q}_{\max,d}$ Design value of the maximum heat release rate for fire

$\dot{Q}_{\max,f,d}$ Design value of the maximum heat release rate for fuel-controlled fires

$\dot{Q}_{\max,f,k}$ Characteristic value of the maximum heat release rate for fuel-controlled fires

$\dot{Q}_{\max,k}$ Characteristic value of the maximum heat release rate for fire

$\dot{Q}_{\max,v,d}$ Design value of the maximum heat release rate for ventilation-controlled fires

$\dot{Q}_{\max,v,k}$ Characteristic value of the maximum heat release rate for ventilation-controlled fires

A_f Floor area

A_i Surface area of the enclosing component i

A_j Area of enclosure surface j , openings not included

A_t	Total area of enclosure
A_v	Total area of vertical openings on all walls
A_w	Area of the ventilation openings
O_{lim}	Limit opening factor
Q_d	Total fire load in the fire compartment
Q_2	Fire load for the phase 2
Q_3	Fire load for the phase 3
Q_{fo}	Heat release rate of a possible flashover
$Q_{x,d}$	Design fuel load for the case x
A_{CLT}	Area of exposed timber
O	Opening factor
V	Coefficient of variation of the fire load density

Lower-case Roman letters

b_i	Heat storage capacity of the enclosing component i
b_i	Thermal absorptivity of layer i
b_j	Thermal property of enclosure surface j
c_i	Specific heat of layer i

$d_{char,t}$	Design charring depth of linear timber member at the end of the parametric fire
d_{char}	Char depth
d_{char}^i	Char depth at the iteration i
h_w	Average height of the ventilation openings
h_{eq}	Weighted average of window heights on all walls
k_2	Protection factor
k_3	Post-protection factor
k_4	Consolidation factor
k_ρ	Density factor
k_{con}	Connection factor
k_g	Gap factor
k_{gd}	Grain direction factor
k_h	Conversion Factor
k_h	Thickness factor
k_i	Applicable modification factors for charring
$k_{3,1}$	Post-protection factor
$k_{3,2}$	Post-protection factor

$k_{s,n,1}$	Combined section and conversion factor for the fire exposed side
$k_{s,n,2}$	Combined section and conversion factor for the lateral side
$q_{d,fi}$	Design value of the fire load density related to the floor area
$q_{d,t}$	Design value of the fire load density related to the total area
$q_{d,fi,t}$	Design compartment fire load density related to the surface area
$q_{d,st,t}$	Structural fire load density related to the surface area
$q_{d,tot,t}$	Design total fire load density related to the surface area
$q_{f,k}$	Characteristic fire load density
$q_{t,d}^{i+1}$	Total fire load at the $(i + 1)^{\text{th}}$ iteration
$q_{x,d}$	Design fuel load density for case x
s_{10}	Rate of heat release of timber members per unit area related to the charring rate
s_i	Thickness of layer i
s_{lim}	Limit thickness
t^*	Modified time
t_0	initial time
t_1	Time at end of the phase 1
t_2	Time at end of the phase 2

t_3	Time for the phase 3
t_α	Factor describing the fire development
t_i	Time for the phase i
t_o	Time at which the charring is assumed to start reducing
$t_{1,fo}$	Time of a possible flashover
$t_{1,x}$	Time at end of the phase 1 for case x
$t_{2,x}$	Time at end of the phase 2 for case x
$t_{3,x}$	Time for phase 3 for case x
t_4	Time for the suggested phase 4
t_{max}^*	Modified time for maximum temperature
t_{max}^1	Time at which the gas temperature starts to decline
t_{lim}	Limit time
t_{max}	Time for maximum temperature
b	Heat storage capacity of the entire enclosing components
b	Thermal absorptivity for the total enclosure
b	Width of the linear timber member
c	Specific heat

e	Euler's number
h	Depth of the cross-section of the linear timber member
k	Multiplication factor
m	Combustion factor
q	Fire load density
q_{mfl}	Movable fire load per unit compartment internal surface area
t	Time
x	Decay phase factor

Upper-case Greek letters

β	Charring rate associated with standard fire resistance test
β_0	Basic design charring rate
β_{fi}	Reliability index
β_n	Notional charring rate for rectangular members
β_o	One-dimensional charring rate for flat surfaces
β_{par}	Parametric char rate
Γ	Heating rate factor
Γ_{lim}	Limit heating rate factor

Θ	Temperature
Θ_0	Initial temperature
Θ_1	Temperature at end of the phase 1
Θ_2	Temperature at end of the phase 2
Θ_3	Temperature for the phase 3
Θ_i	Temperature for phase i
$\Theta_{1,f}$	Temperature for the phase 1 for fuel controlled fires
$\Theta_{1,v}$	Temperature for the phase 1 for ventilation controlled fires
$\Theta_{2,f}$	Temperature for the phase 2 for fuel controlled fires
$\Theta_{2,v}$	Temperature for the phase 2 for ventilation controlled fires
$\Theta_{2,x}$	Maximum temperature at phase 2 for case x
$\Theta_{3,f}$	Temperature for the phase 3 for fuel controlled fires
$\Theta_{3,v}$	Temperature for the phase 3 for ventilation controlled fires
$\Theta_{3,x}$	Maximum temperature for phase 3 for case x
Θ_4	Temperature for the suggested phase 4
Θ_{\max}	Maximum temperature
Θ_g	Gas temperature in the fire compartment

Lower-case Greek letters

α Sensitivity factor

α_1 Ratio between the heat release and char depth

$\alpha_{st}(\alpha)$ Time dependent modification factor

χ Combustion efficiency

$\gamma_{fi,Q}$ Partial safety factor

λ Thermal conductivity

λ_i Thermal conductivity of layer i

ρ Density

ρ_f Probability of failure

ρ_i Density of layer i

1 Introduction & Objectives

The wood has a lengthy history as a building material, and its use as a structural component in residential construction was common in many countries. In recent years, there has been a resurgence of global interest in using timber as a structural and design material for various building types. The growing demand for timber structures can be attributed to factors such as aesthetic appeal, environmental sustainability, prefabrication, accelerated construction, cost-effectiveness, and earthquake resistance. (Buchanan and Ostman (2022))

According to the International Energy Agency (IEA) and United Nations Environment Program, nearly 40% of global carbon emissions originate from the construction process and operation of buildings. The decarbonization of the buildings and construction sector is not on track to reach the goals of the Paris Agreement by 2050. (IEA (2023)) (United Nations Environment Programme (2022))

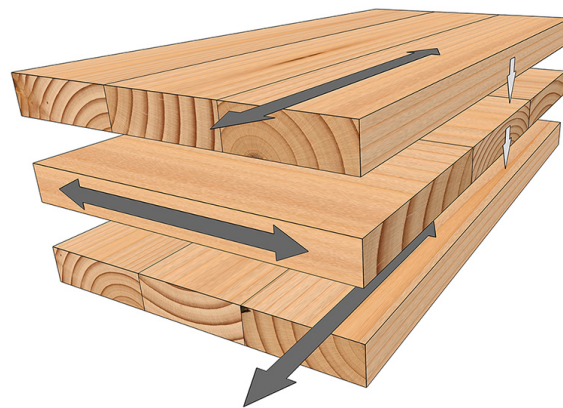
According to the Paris Agreement, global carbon emissions need to be reduced by 50% by 2050 compared to the global carbon emissions of 1990 to keep the global average temperature rise well below 2 °C. (Horowitz (2016))

In order to achieve the decarbonization goal, augmenting the use of timber in built environment is essential. However, several concerns have been raised regarding the use of timber as a structural material. Due to its lightweight nature and status as a natural biomaterial, issues like durability and acoustic performance in timber buildings have been questioned, particularly in comparison to non-combustible materials when it comes to fire safety. However, advanced engineered wood products such as cross laminated timber (CLT) now allow for the construction of sizable and intricate timber structures. Cutting-edge engineering methods make it possible to build timber buildings that were previously achievable only with concrete and steel, thus challenging the foundations of current fire codes.

Cross laminated timber (CLT) is a fairly recent and new mass timber material that has been attracting interest in the construction sector (Karacabeyli and Douglas (2013)). Originating in Europe during the 1990s, considerable research and development have contributed to the growing adoption of CLT in construction projects globally. The primary factors driving CLT's increasing popularity include its technical proficiency and eco-friendly characteristics, which enable timber to be employed in a broader array of applications than was previously achievable.

CLT is a panel which is composed of many layers. These layers are created by placing solid timber boards side-by-side. Then these layers are stacked crosswise with right angles and bonded by adhesives to create a solid panel. This process can be seen in the Figure 1.1. The dimensions of CLT panels can differ based on the manufacturer; however, they can be produced as large as 18 meters in length, 5 meters in width, and up to 500 mm thick. These proportions make them well-suited for use in floors, walls, and roofs (Abed *et al.* (2022)).

Figure 1.1: The Design of Cross Laminated Timber copied from Reid Middleton (2017)



However, there are still many doubts and unknowns in mass timber such as char fall off in CLT. The fall off occurs when the adhesive bond between the layers fail. The main reason of this is the augmentation of temperature in glue line. Other unknown in this field is the phenomenon of self-extinction of the timber, there are studies conducted in this topic. However, improvements in predicting char depth and occurrence of self-extinction will help a lot for the practice of designing of mass timber. The motivation of this thesis is dealing with this issue and improving the knowledge in char depth prediction in timber.

1.1 Objectives

In recent years, there has been a growing interest in the use of timber as a construction material due to its sustainability and renewable nature. One of the main challenges in the design of the timber structures is understanding their behaviour under fire, particularly the charring process of timber.

Various models have been developed to predict the char depth in compartment fires, but there remains a need for improved understanding and more accurate predictive tools. This thesis aims to address this gap by investigating the charring behaviour of timber and evaluating the performance of existing models. It will also explore potential enhancements to these models, ultimately contributing to the safe and efficient design of timber structures in fire scenarios.

Figure 1.2: Burning of Timber copied from Klippel, M. and Frangi, A. (2011)



2 Methodology

A comprehensive literature review was conducted to identify existing research. It is seen that there are many related papers published on the topic of charring of timber. There are several models that has been developed to predict the char depth for a compartment fire. The book "Fire Safe Use of Wood in Building" (Buchanan and Ostman (2022)) provides a valuable overview of this subject.

Conventional compartment fire models utilize governing equations for mass and energy, solving them for distinct control volumes to determine fire gas temperatures and heat fluxes within the compartment. Incorporating pyrolysis of combustible surfaces into these calculations is considerably more complex, and there are limited models available for fire engineers.

The Fire Dynamics Simulator (FDS) has been employed to assess the response of mass timber structures, with its method validated against five full-scale compartment fire tests involving exposed cross-laminated timber (Barber *et al.* (2018)). The pyrolysis model requires input of timber's kinetic properties. In that study, char depths were predicted with an accuracy of 20% for fully developed fires. However, the model did not account for CLT char fall-off which is resulting from glue line failure, gypsum board fall-off, or charring of CLT behind the gypsum board. Additionally, the computational effort and time required were substantial.

The B-RISK zone model (Wade *et al.* (2016), Wade *et al.* (2018) and Wade (2019)) features optional sub-models for calculating the contribution of exposed mass timber to determine the fully developed fire environment within a compartment with varying levels of exposed timber on walls and ceilings. It assumes that the wood surfaces contribute to fuel mass based on the 300°C isotherm's position within the boundary surfaces. This approach is similar to the Brandon's Method which is which is discussed in section 2.2.1 of this thesis. In Brandon's Method the total fuel available to burn is updated at each time step to account for the timber surfaces' additional contribution. The model

also enables specifying the proportion of external burning to the compartment. Wade's validation of the model's gas temperature predictions against 19 full-scale experimental configurations demonstrated accurate estimates of peak temperature and burning duration. Recent developments have incorporated a detailed kinetic model for wood pyrolysis within the zone model framework (Wade *et al.* (2019))

Schmid and Frangi (2021) introduced a simplified engineering model to account for structural timber in compartment fires. Their Timber Charring and Heat Storage model (TiCHS-model) can evaluate the contribution of structural timber to the fire load within the compartment. The model employs an iterative approach, focusing on predicting the compartment environment, including temperature and gas properties. The predictions generally show good agreement, except when the fall-off of charring layers leads to a sudden change in combustion characteristics, causing the fire to regrow.

The chosen models for this thesis work are as below:

- Brandon Brandon's method (Chapter 3.8.1 from FSUW)
- Design model for parametric temperature-time curves (part A.4.4 of prEN 1995-1-2:20YY)
- Cumulative temperature charring model (part A.4.3.2 of prEN 1995-1-2:20YY)

FSUW: Fire Safe Use of Wood in Buildings (Buchanan and Ostman (2022))

prEN 1995-1-2:20YY: Eurocode 5 Design of timber structures Part 1-2: Structural fire design (CEN (2023-01))

The models that are used for prediction of gas temperature curve of the compartment are as below:

- EN 1991-1-2 Annex A
- DIN EN 1991-1-2/NA Appendix AA

EN 1991-1-2: Eurocode 1: Actions on Structures - Part 1-2: Actions on structures exposed to fire. (CEN (2002-10))

DIN EN 1991-1-2/NA : The German National Annex - Nationally determined parameters Eurocode 1: Actions on structures - Part 1-2: Actions on structures exposed to fire. (NABau (2015-09))

Daniel Brandon's method and design model for parametric temperature-time curves use EN 1991-1-2 Annex A to predict the gas temperatures inside the compartment. However for cumulative temperature charring model there is no temperature prediction method provided, the temperature is to be provided to the model to calculate the char depth. So in order to provide a temperature curve DIN EN 1991-1-2/NA Appendix AA is used with the cumulative temperature charring model.

Firstly the temperature prediction models will be discussed.

2.1 The Temperature Prediction Models

2.1.1 EN 1991-1-2 Annex A

According to the Eurocode 1: Actions on Structures Part 1-2: Actions on structures exposed to fire Annex A (EN 1991-1-2 Annex A) the fire curves given are valid for fire compartments up to 500 m² of floor area, without openings in the roof and for a maximum compartment height of 4 m. It is assumed that the fire load of the compartment is completely burnt out.

2.1.1.1 Heating Phase

The fire curve in the heating phase is defined as below,

$$\Theta_g = 20 + 1325 \left(1 - 0.324e^{-0.2t^*} - 0.204e^{-1.7t^*} - 0.472e^{-19t^*} \right) \quad (2.1.1)$$

where

Θ_g is the gas temperature in the fire compartment [°C]

$$t^* = t \cdot \Gamma \quad [\text{h}] \quad (2.1.2)$$

with

t	time	[h]
Γ	$= \frac{[O/b]^2}{(0.04/1160)^2}$	[-]
b	thermal absorptivity for the total enclosure = $\sqrt{\rho c \lambda}$	[J/m ² s ^{1/2} K]
	with the following limits: $100 \leq b \leq 2200$	
ρ	density of boundary of enclosure	[kg/m ³]
c	specific heat of boundary of enclosure	[J/kgK]
λ	thermal conductivity of boundary of enclosure	[W/(mK)]
O	opening factor: $\frac{A_v \sqrt{h_{eq}}}{A_t}$	[m ^{1/2}]
	with the following limits: $0.02 \leq O \leq 0.20$	
A_v	total area of vertical openings on all walls	[m ²]
h_{eq}	weighted average of window heights on all walls	[m]
A_t	total area of enclosure (walls, ceiling and floor, including openings)	[m ²]

It is stated that for the calculation of the b factor, the density ρ , the specific heat c and the thermal conductivity λ of the boundary may be taken at ambient temperature.

To account for an enclosure surface with different layers of material b factor will be calculated as below:

$$\text{— If } b_1 < b_2, b = b_1 \quad (2.1.3)$$

— If $b_1 > b_2$, a limit thickness s_{lim} is calculated for the exposed material according to:

$$s_{lim} = \sqrt{\frac{3600 t_{max} \lambda_1}{c_1 \rho_1}} \text{ with } t_{max} \text{ given by Equation 2.1.9.} \quad [\text{m}] \quad (2.1.4)$$

$$\text{If } s_1 > s_{lim} \text{ then } b = b_1 \quad (2.1.5)$$

$$\text{If } s_1 < s_{lim} \text{ then } b = \frac{s_1}{s_{lim}} b_1 + \left(1 - \frac{s_1}{s_{lim}}\right) b_2 \quad (2.1.6)$$

where

index 1 denotes the layer that is in direct contact with the fire, index 2 indicates the layer immediately following it, and so on.

s_i is the thickness of layer i

$$b_i = \sqrt{(\rho_i c_i \lambda_i)}$$

ρ_i is the density of layer i

c_i is the specific heat of layer i

λ_i is the thermal conductivity of layer i

To account for different b factors in walls, ceiling and floor, $b = \sqrt{(\rho c \lambda)}$ should be calculated from Equation 2.1.7:

$$b = \frac{\sum (b_j A_j)}{A_t - A_v} \quad (2.1.7)$$

where

A_j is the area of enclosure surface j , openings not included

b_j is the thermal property of enclosure surface j according to Equation 2.1.3, Equation 2.1.5 and Equation 2.1.6

(5) The maximum temperature Θ_{\max} in the heating phase happens for $t^* = t_{\max}^*$

$$t_{\max}^* = t_{\max} \cdot \Gamma \quad [\text{h}] \quad (2.1.8)$$

with

$$t_{\max} = \max \left[\left(0.2 \cdot 10^{-3} \cdot q_{d,t}/0 \right); t_{\text{lim}} \right] \quad [\text{h}] \quad (2.1.9)$$

where

$q_{d,t}$ is the design value of the fire load density related to the total area A_t of the enclosure whereby $q_{d,t} = q_{d,fi} \cdot A_f/A_t$ [MJ/m²]. The following limits should be observed: $50 \leq q_{d,t} \leq 1000$ [MJ/m²]

$q_{d,fi}$ is the design value of the fire load density related to the floor area A_f [MJ/m²] which taken from Annex E of the EN 1991-1-2

t_{lim} should be determined from Equation 2.1.10 expressed in [h].

It should be noted that if the fire is fuel controlled the time t_{\max} corresponding to the maximum temperature is given by t_{lim} . If t_{\max} is given by $(0,2 \cdot 10^{-3} \cdot q_{d,t}/O)$, the fire is ventilation controlled.

When $t_{\max} = t_{\text{lim}}$, Equation 2.1.2 should be replaced by:

$$t^* = t \cdot \Gamma_{\text{lim}} \quad [\text{h}] \quad (2.1.10)$$

with

$$\Gamma_{\text{lim}} = \frac{[O_{\text{lim}}/b]^2}{(0.04/1160)^2} \quad (2.1.11)$$

where

$$O_{\text{lim}} = 0.1 \cdot 10^{-3} \cdot q_{d,t}/t_{\text{lim}} \quad (2.1.12)$$

If ($O > 0.04$ and $q_{d,t} < 75$ and $b < 1160$), Γ_{lim} in Equation 2.1.11 should be multiplied

by k given by:

$$k = 1 + \left(\frac{O - 0.04}{0.04} \right) \left(\frac{q_{d,t} - 75}{75} \right) \left(\frac{1160 - b}{1160} \right) \quad (2.1.13)$$

In case of slow fire growth rate, $t_{lim} = 25$ min; in case of medium fire growth rate, $t_{lim} = 20$ min and in case of fast fire growth rate, $t_{lim} = 15$ min.

If advice is needed on fire growth rate refer to the Table E.6 of EN 1991-1-2.

2.1.1.2 Cooling Phase

The fire curves in the cooling phase should be calculated from the equations, respectively:

$$\Theta_g = \Theta_{max} - 625 (t^* - t_{max}^* \cdot x) \quad \text{for } t_{max}^* \leq 0.5 \quad (2.1.14)$$

$$\Theta_g = \Theta_{max} - 250 (3 - t_{max}^*) (t^* - t_{max}^* \cdot x) \quad \text{for } 0.5 < t_{max}^* < 2 \quad (2.1.15)$$

$$\Theta_g = \Theta_{max} - 250 (t^* - t_{max}^* \cdot x) \quad \text{for } t_{max}^* \geq 2 \quad (2.1.16)$$

where t^* should be determined from Equation 2.1.2.

$$t_{max}^* = (0.2 \cdot 10^{-3} \cdot q_{t,d}/O) \cdot \Gamma \quad (2.1.17)$$

$$x = \begin{cases} 1.0, & \text{if } t_{max} > t_{lim} \\ t_{lim} \cdot \Gamma / t_{max}^*, & \text{if } t_{max} = t_{lim} \end{cases}$$

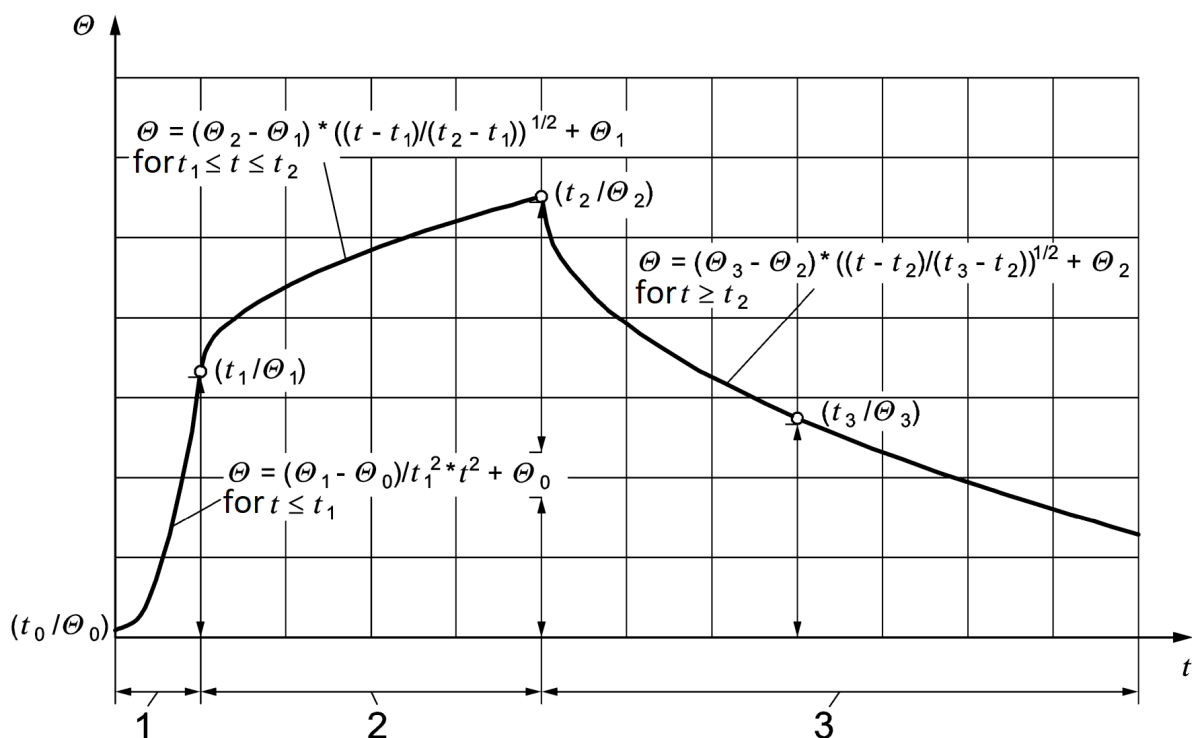
By using this process given by the Eurocode 1: Actions on Structures - Part 1-2: Actions on structures exposed to fire Annex A, the temperature inside the compartment can be calculated for entire duration of the fire.

2.1.2 DIN EN 1991-1-2/NA Appendix AA

Appendix AA of The German National Annex - Nationally determined parameters - Eurocode 1: Actions on structures - Part 1-2: General actions -Actions on structures exposed to fire (DIN EN 1991-1-2/NA) (NABau (2015-09)) gives a different method to calculate temperature of a compartment fire.

By taking advantage of the temporal congruence with the heat release rate, the temperature time curve of the natural fire can be described in all phases, from the fire growth phase to the fully developed fire phase and the decay phase (see Figure 2.1).

Figure 2.1: Schematic representation of the temperature-time curve according to the simplified natural fire model with the points (t_i, Θ_i) described by equations and the curve segments in between copied from NABau (2015-09)



The curve sections for the three aforementioned phases are limited by distinctive points at the times t_0 , t_1 , t_2 and t_3 , which result from the course of the heat release rate. In determining the associated temperature values Θ_1 , Θ_2 , and Θ_3 , a distinction must be made between ventilation-controlled fires and fire load-controlled fires.

In order to determine whether the fire is ventilation or fire load controlled the Equation 2.1.18 is used.

$$\dot{Q}_{\max,k} = \text{MIN} \{ \dot{Q}_{\max,v,k}; \dot{Q}_{\max,f,k} \} \quad (2.1.18)$$

where

$\dot{Q}_{\max,v,k}$ is the characteristic value of the maximum heat release rate for ventilation-controlled fires

$\dot{Q}_{\max,f,k}$ is the characteristic value of the maximum heat release rate for fuel-controlled fires

For ventilation-controlled fires in residential, office and similar uses, the characteristic value of the maximum heat release rate may be determined in simplified form using Equation 2.1.19.

$$\dot{Q}_{\max,v,k} = 1.21 \cdot A_w \cdot \sqrt{h_w} \quad \text{in MW} \quad (2.1.19)$$

where

A_w the area of the ventilation openings in m^2

h_w the average height of the ventilation openings in m

For fire load-controlled fires in residential, office and similar uses, the characteristic value of the heat release rate can be determined in simplified form using Equation 2.1.20.

$$\dot{Q}_{\max,f,k} = 0.25 \cdot A_f \quad \text{in MW} \quad (2.1.20)$$

where

A_f the maximum fire area in m^2 , usually the floor area of the fire compartment

As stated in Equation 2.1.18, the characteristic value of the maximum heat release rate is the smaller of the two maximum heat release rates for the ventilation-controlled fire and the fire load-controlled fire.

The design values of the highest heat release rate $\dot{Q}_{\max,v,k}$ are defined by:

$$\dot{Q}_{\max,v,d} = \dot{Q}_{\max,v,k} \cdot \gamma_{fi,Q} \quad (2.1.21)$$

$$\dot{Q}_{\max,f,d} = \dot{Q}_{\max,f,k} \cdot \gamma_{fi,Q} \quad (2.1.22)$$

$$\dot{Q}_{\max,d} = \dot{Q}_{\max,k} \cdot \gamma_{fi,Q} \quad (2.1.23)$$

where

$\gamma_{fi,Q}$ the partial safety factor according to Equation 2.1.24

$$\gamma_{fi} = \frac{1 - V \cdot 0,78 \cdot [0,5772 + \ln(-\ln(\Phi(\alpha \cdot \beta_{fi})))]}{1 - V \cdot 0,78 \cdot [0,5772 + \ln(-\ln(0,9))]} \quad (2.1.24)$$

where

V The coefficient of variation of the fire load density is taken as 0.3

α The sensitivity factor (as a measure of the influence of scattering) taken as 0.6

β_{fi} The reliability index is chosen as 4.2 from the Table 2.1 depending on the use and the consequences of damage in the event of a component failure. As no further details are available, the values for medium damage should be used.

Table 2.1: Indicative values for the reliability index β_{fi} and the associated probability of failure p_f (Reference period 1 year) for different uses

Line	Use	Damage Consequences					
		High		Medium		Small	
		β	p_f	β	p_f	β	p_f
		1a	1b	2a	2B	3a	3b
1	Residential building, office building and similar uses Building classes according to MBO	4.7	1.3E-6	4.2	1.3E-5	3.7	1.1E-4
2	Hospital, nursing home						
3	Lodging establishment, hotel						
4	School						
5	Point of sale	5.2	1.0E-7	4.7	1.3E-6	4.2	1.3E-5
6	Meeting place						
7	Skyscraper						
8	Agricultural buildings	-	-	4.2	1.3E-5	3.7	1.1E-4

2.1.2.1 Ventilation Controlled Case

In ventilation controlled fires, for a reference fire load density of $q = 1300 \text{ MJ/m}^2$:

$$t_1 = t_\alpha \cdot \sqrt{\dot{Q}_{\max,v,d}} \quad \text{in s} \quad (2.1.25)$$

$$\Theta_{1,v} = -8.75 \cdot 1/O - 0.1 \cdot b + 1175 \quad \text{in } ^\circ\text{C} \quad (2.1.26)$$

$$t_2 = t_1 + \frac{Q_2}{\dot{Q}_{\max,v,d}} \quad \text{in s} \quad \text{with } Q_2 = 0.7 \cdot Q_d - \frac{t_1^3}{3 \cdot t_\alpha^2} \quad (2.1.27)$$

$$\Theta_{2,v} = (0.004 \cdot b - 17) \cdot 1/O - 0.4 \cdot b + 2175 \quad \text{in } ^\circ\text{C} \quad \leq 1340^\circ\text{C} \quad (2.1.28)$$

$$t_3 = t_2 + \frac{2 \cdot Q_3}{\dot{Q}_{\max,v,d}} \quad \text{in s} \quad \text{with } Q_3 = 0.3 \cdot Q_d \quad (2.1.29)$$

$$\Theta_{3,v} = -5.0 \cdot 1/O - 0.16 \cdot b + 1060 \quad \text{in } ^\circ\text{C} \quad (2.1.30)$$

where

t_α is the factor describing the fire development according to Table 2.2

b is the heat storage capacity of the entire enclosing components in $\frac{\text{J}}{\text{m}^2 \cdot \sqrt{\text{s}} \cdot \text{K}}$ according to Equation 2.1.31

$O = A_w \sqrt{h_w} / A_t$ is the opening factor in $\text{m}^{1/2}$

A_w is the area of the ventilation openings in m^2

h_w is the average height of the ventilation openings in m

A_t is the total area of the enclosing components with opening surfaces in m^2

$Q_d = q \cdot A_f$, the total fire load in the fire compartment in MJ with the reference fire load density $q = 1300/\text{MJ}/\text{m}^2$

Table 2.2: Parameters for the fire development phase and maximum heat release rate HRR_f per unit area during the full developed phase for different uses (characteristic values)

Line	Use	Fire Spread	t_α (s)	HRR_f (MW/m ²)
		1	2	3
1	Residential building	Middle	300	0.25
2	Office building	Middle	300	0.25
3	Hospital (room)	Middle	300	0.25
4	Hotel (room)	Middle	300	0.25
5	Library	Middle	450	0.50
6	School (classroom)	Middle	300	0.15
7	Point of sale, shopping center	Fast	150	0.25
8	Place of assembly (theater, cinema)	Fast	150	0.50
9	Transportation (public area)	Slow	600	0.25

The heat storage capacity (b) can be calculated as an average weighted over the areas of the enclosing components. To take into account the different heat storage capacity b_i from walls, ceiling and floor, b can be determined according to equation

$$b = \left(\left(\sum_{i=1}^n (b_i \cdot A_i) \right) / (A_t - A_w) \right) \quad (2.1.31)$$

where

b_i is the heat storage capacity of the enclosing component i , in $\frac{\text{J}}{\text{m}^2 \cdot \sqrt{\text{s}} \cdot \text{K}}$

A_i is the surface area of the enclosing component i , in m^2

2.1.2.2 Fuel Controlled Case

In fuel controlled fires, for a reference fire load density of $q = 1300 \text{ MJ/m}^2$:

$$t_1 = t_\alpha \cdot \sqrt{\dot{Q}_{\max,f,d}} \quad \text{in s} \quad (2.1.32)$$

$$\Theta_{1,f} = \begin{cases} 24000 \cdot k + 20 & \text{in } ^\circ\text{C} \quad \text{for } k \leq 0.04 \\ 980^\circ\text{C} & \text{for } k > 0.04 \end{cases} \quad (2.1.33)$$

$$t_2 = t_1 + \frac{Q_2}{\dot{Q}_{\max,f,d}} \quad \text{in s} \quad \text{with } Q_2 = 0.7 \cdot Q_d - \frac{t_1^3}{3 \cdot t_\alpha^2} \quad (2.1.34)$$

$$\Theta_{2,f} = \begin{cases} 33000 \cdot k + 20 & \text{in } ^\circ\text{C} \quad \text{for } k \leq 0.04 \\ 1340^\circ\text{C} & \text{for } k > 0.04 \end{cases} \quad (2.1.35)$$

$$t_3 = t_2 + \frac{2 \cdot Q_3}{\dot{Q}_{\max,f,d}} \quad \text{in s} \quad \text{with } Q_3 = 0.3 \cdot Q_d \quad (2.1.36)$$

$$\Theta_{3,f} = \begin{cases} 16000 \cdot k + 20 & \text{in } ^\circ\text{C} \quad \text{for } k \leq 0.04 \\ 660^\circ\text{C} & \text{for } k > 0.04 \end{cases} \quad (2.1.37)$$

where

$$k = \left(\frac{\dot{Q}_{\max,f,d}^2}{A_w \cdot \sqrt{h_w} (A_t - A_w) \cdot b} \right)^{1/3} \quad (2.1.38)$$

2.1.2.3 Creating the Curve

Based on the temperature-time curve for the reference fuel load density ($q = 1300 \text{ MJ/m}^2$), temperature-time curves for any fuel load density $q_{x,d} \leq 1300 \text{ MJ/m}^2$ can be determined. The rising part of the temperature-time curve during the fire growth phase and fully developed fire phase (Area 1 and Area 2 in Figure 2.1) is independent of the fuel load density. The time $t_{2,x}$ at which the maximum temperature $\Theta_{2,x}$ is reached depends on the fuel load. It can be directly determined from the approach for the heat release rate.

- For $Q_1 < 0.7 \cdot Q_{x,d}$

$$t_{2,x} = t_1 + \frac{(0.7 \cdot Q_{x,d}) - (t_1^3 / (3 \cdot t_\alpha^2))}{\dot{Q}_{\max,d}} \quad \text{in s} \quad (2.1.39)$$

The associated temperature $\Theta_{2,x}$ is determined as follows :

$$\Theta_{2,x} = (\Theta_2 - \Theta_1) \cdot \sqrt{\frac{(t_{2,x} - t_1)}{(t_2 - t_1)}} + \Theta_1 \quad \text{in } ^\circ\text{C} \quad (2.1.40)$$

where

t_α is factor for describing the fire growth rate

$$Q_1 = \frac{t_1^3}{3 \cdot t_\alpha^2} \quad \text{in MW};$$

$$Q_{x,d} = q_{x,d} \cdot A_f \quad \text{with } q_{x,d} \quad \text{from Equation 2.1.41}$$

$$q_{x,d} = \chi \cdot q_{f,k} \cdot \gamma_{fi,q} \quad \text{in MJ/m}^2 \quad (2.1.41)$$

where

$q_{f,k}$ the characteristic fire load density, related to the base area A_f of the fire compartment or the utilization unit in MJ/m^2 ;

χ the combustion efficiency; for mixed fire loads typical of office, residential and similar uses in building construction with a predominant proportion of cellulose-containing materials, a flat rate $\chi = 0.8$ may be assumed.

$\gamma_{fi,q}$ a partial safety factor that takes into account the probability of occurrence of a fully developed fire in the fire compartment as well as the required reliability of the structural components. It is calculated by Equation 2.1.24

- For $Q_1 \geq 0.7 \cdot Q_{x,d}$

$$t_{1,x} = \sqrt[3]{0.7 \cdot Q_{x,d} \cdot 3 \cdot t_{\alpha}^2} \quad \text{in s} \quad (2.1.42)$$

The associated temperature $\Theta_{2,x}$ is determined as follows :

$$\Theta_{2,x} = \frac{(\Theta_1 - 20)}{t_1^2} \cdot t_{1,x}^2 + 20 \quad \text{in } ^\circ\text{C} \quad (2.1.43)$$

The temperature $\Theta_{3,x}$ at time $t_{3,x}$ for different fire load densities $q_{x,d}$ lies on a logarithmic function from $(t = 0; \Theta_0)$ to $(t_3; \Theta_3)$:

$$\Theta_{3,x} = \Theta_3 \cdot \frac{\log_{10} \left(\frac{t_{3,x}}{60} + 1 \right)}{\log_{10} \left(\frac{t_3}{60} + 1 \right)} \quad \text{in } ^\circ\text{C} \quad (2.1.44)$$

where

$$t_{3,x} = \frac{0.6 \cdot Q_{x,d}}{\dot{Q}_{\max,d}} + t_{2,x} \quad \text{in s} \quad (2.1.45)$$

In the range between $t = 0$ and t_1 (Area 1 according to Figure 2.1) the temperature increases quadratically

$$\Theta(t) = \frac{(\Theta_1 - 20)}{t_1^2} \cdot t^2 + 20 \quad \text{in } ^\circ\text{C} \quad \text{for } 0 \leq t \leq t_1 \quad (2.1.46)$$

In Area 2, the temperature increase is described by Equation 2.1.47

$$\Theta(t) = (\Theta_{2,x} - \Theta_1) \cdot \sqrt{\frac{(t - t_1)}{(t_{2,x} - t_1)}} + \Theta_1 \quad \text{in } ^\circ\text{C} \quad \text{for } t_1 \leq t \leq t_2 \quad (2.1.47)$$

The decreasing branch in Area 3 is described by Equation 2.1.48

$$\Theta(t) = (\Theta_{3,x} - \Theta_{2,x}) \cdot \sqrt{\frac{(t - t_{2,x})}{(t_{3,x} - t_{2,x})}} + \Theta_{2,x} \quad \text{in } ^\circ\text{C} \quad \text{for } t > t_2 \quad (2.1.48)$$

The time of a possible flashover, $t_{1, fo}$, at which the heat release rate suddenly rises to its maximum, can be determined by using Equation 2.1.49

$$t_{1, fo} = \sqrt{t_{\alpha}^2 \cdot \dot{Q}_{fo}} \quad \text{in s} \quad (2.1.49)$$

where \dot{Q}_{fo} can be determined according to Equation 2.1.50

$$\dot{Q}_{fo} = 0.0078 \cdot A_t + 0.378 \cdot A_w \cdot \sqrt{h_w} \quad \text{in MW} \quad (2.1.50)$$

2.2 The Char Depth Prediction Models

2.2.1 Brandon Brandon's method

Brandon (2018a) suggested an engineering method that combines parametric fire equations with an iterative procedure to calculate the char depth by modifying the fuel density at each iteration. The char rate was based on an empirical model which is created by using numerous parametric fire experiments. However, this suggested method can only be applied when engineered timber lamella's glue line integrity is maintained and any protective board encapsulation products used to protect the timber do not fail or become detached. An empirical relationship between the char rate and the heating rate has been proposed by Brandon. This was based on fire experiments in modern furnaces which are controlled by using the plate thermometers. These tests updated a correlation previously developed by Hadvig (1981) and the updated correlation is currently included in Eurocode 5, Appendix A.

The parametric char rate β_{par} (mm/min) is given by

$$\beta_{par} = \beta \Gamma^{0.25} \quad [\text{mm/min}] \quad (2.2.1)$$

where

β is the charring rate associated with standard fire resistance tests according to ISO 834 (International Organization for Standardization (2014)) and corresponds to either the

one-dimensional β_o charring rate for flat surfaces or the notional charring rate β_n for rectangular members, as described in EN 1995-1-2.

Γ heating rate factor that depends on the thermal properties of the compartment and the opening factor O

$$\Gamma = \frac{\left(\frac{O}{\sqrt{k\rho c}}\right)^2}{\left(\frac{0.04}{1160}\right)^2} \quad [-] \quad (2.2.2)$$

where

ρ = density (kg/m³),

c = specific heat (kJ/kg·K),

k = thermal conductivity (kW/m·K) of the compartments boundaries

O is the opening factor calculated by

$$O = \frac{A_v}{A_t} \sqrt{h_v} \quad [m^{1/2}] \quad (2.2.3)$$

where

A_t is the total area of floors, walls and ceiling, including openings (m²)

A_v is the area of openings (m²)

h_v is the weighted average height of the compartment openings (m)

At t_o charring is assumed to start reducing. t_o is calculated by using Equation 2.2.4

$$t_o = 0.009 \frac{q_{t,d}}{O} \quad [\text{min}] \quad (2.2.4)$$

where

$q_{t,d}$ is the design fire load per unit area of internal surfaces excluding the openings (MJ/m²).

Charring is assumed to completely stop at time $3t_0$. Therefore the final char depth is calculated as

$$d_{\text{char}} = 2\beta_{\text{par}} t_0 \quad [\text{mm}] \quad (2.2.5)$$

The gas temperature starts to decline at time t_{max}^1 which is calculated by Equation 2.2.6 (from EN 1991-1-2 Annex A)

$$t_{\text{max}}^1 = \max [0.0002q_{t,d}/O; t_{\text{lim}}] \quad [\text{hour}] \quad (2.2.6)$$

where

$$t_{\text{lim}} = \begin{cases} 0.333 \text{ hour (20 min)} & \text{for a medium fire growth rate} \\ 0.417 \text{ hour (25 min)} & \text{for a slow fire growth rate} \\ 0.25 \text{ hour (15 min)} & \text{for a fast fire growth rate} \end{cases}$$

The contribution of structural timber is calculated by an iterative process using the following Equation 2.2.7 where $q_{t,d}^{i+1}$ is the total fire load at the $(i + 1)^{\text{th}}$ iteration, including the moveable fire load q_{mfl} , which is the moveable fire load per unit compartment internal surface area, including the openings (MJ/m²). t_{max}^1 is constant and does not change for subsequent iterations.

$$q_{t,d}^{i+1} = q_{\text{mfl}} + \frac{A_{\text{CLT}}\alpha_1 (d_{\text{char}}^i - 0.7\beta_{\text{par}}t_{\text{max}}^1)}{A_t} \quad [\text{MJ/m}^2] \quad (2.2.7)$$

where

A_t = internal compartment surface area, including openings (m²)

A_{CLT} = area of exposed timber (m²)

α_1 = ratio between the heat release and char depth and is taken as 5.39 MJ/m² per mm of char depth

The value 5.39 MJ/m^2 per mm is experimentally determined by Schmid *et al.* (2016). This was derived from cone calorimeter experiments at an irradiance of 75 kW/m^2 flux for char depths exceeding 10 mm.

The parameter $0.7\beta_{\text{par}}t_{\text{max}}$ is an estimate of the energy stored in the char depth and char depth burning outside the compartment during the fully developed stage (of a duration t_{max}^1).

To validate the method based on a selected number of compartment experiments, Brandon produced the comparison of the predicted and experimental char depth. (Brandon (2018b))

The experiments had opening factors ranging from 0.03 to $0.10 \text{ m}^{0.5}$, and the method may not be applicable if the opening factor falls outside this range. Additionally, this method can only be used when the glue line integrity of engineered timber lamella remains intact, protective board encapsulation products shield the underlying timber do not fail or fall off, and where the exposed adjacent wooden surfaces are not facing each other.

Once the char depth calculation stabilizes to a stable value, the designer can consider this to be an approximation of the maximum char depth on the exposed wood surfaces within the compartment. However, this does not account for localized effects and hot spots where smouldering combustion may continue which requires further analysis.

2.2.2 Design model for parametric temperature-time curves

This model is given by the part A.4.4 of prEN 1995-1-2:20YY. There it is stated that this model shall only be applied with the model of the parametric temperature-time curves given in EN 1991-1-2, Annex A.

Other restrictions are as below,

- The minimum distance between initially unprotected walls made of timber members should be 3.5 m
- Timber members of the compartment should fulfil one or more of the following requirements:
 - products which are encapsulated for the entire fire duration

- initially unprotected structural timber products
- initially unprotected timber products which maintain bond line integrity of face bonds in fire.
- The rules given in this model shall only be applied to calculate the load bearing capacity of timber members with initially unprotected sides made of structural timber, GLT, LVL, GLVL and CLT
- $0.02 \leq O \leq 0.10$
- $b \geq 4 \cdot d_{char,t}$ for linear timber members
- $h \geq 4 \cdot d_{char,t}$ for linear timber members

where

O is the opening factor given in EN 1991-1-2, Annex A, in $m^1/2$

b is the width of the linear timber member, in mm;

$d_{char,t}$ is the design charring depth of linear timber member at the end of the parametric fire according to Equation 2.2.10, in mm;

h is the depth of the cross-section of the linear timber member, in mm

- This method can be used for opening factors of $0.10 < O \leq 0.20$ under the condition that $O = 0.10$ is used consistently for all equations in this method and EN1991-1-2, Annex A.

2.2.2.1 Design charring rate

The design charring rate during the heating phase of the parametric fire curve should be calculated as follows:

$$\beta_{par} = \beta_n \cdot \Gamma^{0.25} \quad (2.2.8)$$

where

β_n is the notional design charring rate according to Equation 2.2.9, in mm/min

β_{par} is the design charring rate for the parametric fire, in mm/min

Γ is the factor accounting for the thermal properties of the boundaries of the enclosure of the compartment given in EN 1991-1-2, Annex A.

2.2.2.2 Notional design charring rate

The notional design charring rate β_n should be calculated in accordance with Equation 2.2.9 using the applicable modification factors for charring k_i given in Table 2.3 and the basic design charring rate β_0 given in Table 2.4:

$$\beta_n = \prod k_i \cdot \beta_0 \quad (2.2.9)$$

where

β_n is the notional design charring rate within one charring phase, in mm/min

$\prod k_i$ is the product of applicable modification factors for charring k_i given Table 2.3

β_0 is the basic design charring rate, in mm/min given in Table 2.4

Table 2.3: Modification factors for charring

Modification factor	Designation	Description	Reference (prEN 1995-1-2:20YY)
k_{con}	Connection factor	Effect of increased charring due to fasteners	5.4.2.2 (3) and (4)
k_{gd}	Grain direction factor	Effect of increased charring parallel to the grain	5.4.2.2 (5) and (5)
k_g	Gap factor	Effect of increased charring for plane timber members with gap	7.2.3 (2) and (3)
k_h	Thickness factor	Effect of limited thickness for wood panelling and wood-based panels	5.4.2.2 (7)
k_h	Conversion Factor	Effect of corner roundings and effect of cracks and fissures on the surface for linear timber members and allowing the conversion into a rectangular residual cross-section	7.2.2.(2) and (3)
$k_{s,n,1}$	Combined section and conversion factor for the fire exposed side	Effect of corner roundings as well as the superposition of heat flux for timber frame assemblies and allowing the conversion into a rectangular residual cross-section.	7.2.4(14)
$k_{s,n,2}$	Combined section and conversion factor for the lateral side		7.2.4(14)
k_p	Density factor	The effect of the density for wood-based panels	5.4.2.2 (8)
k_2	Protection factor		5.4.2.2 (9) and (10)
k_3	Post-protection factor		5.4.2.2(11)
$k_{3,1}$	Post-protection factor		7.2.4 Table 7.6
$k_{3,2}$	Post-protection factor		7.2.4 Table 7.6
k_4	Consolidation factor		5.4.2.2(12)

Table 2.4: Basic design charring rate β_0

Timber member or panel	β_0 [mm/min]
Timber member made of softwood ^{a,c,d}	0.65
Timber member made of hardwood ^a	
Beech ^e	0.70
Beech ^e LVL	0.65
Ash ^f	0.60
Oak ^g	0.50
Panel ^b	
Solid wood panelling and cladding, solid wood panel with only one layer	0.65
LVL panel ^c	0.65
Particleboard, fibreboard	0.72
OSB, solid wood panel with multiple layers	0.9
Plywood	1.0
^a Timber members according to 5.1(1) of prEN 1995-1-2:20YY, subgroup timber members ^b Panels according to 5.1(1) of prEN 1995-1-2:20YY, subgroup panels ^c LVL and GLVL with a characteristic density of $\geq 480 \text{ kg/m}^3$ ^d Table B.2 in EN 14081-1 ^e FASY in EN 14081-1 ^f FXEX in EN 14081-1 ^g QCXA, QCXE, QCXR in EN 14081-1	

EN-14081-1:2016+A1:2019: Timber structures - Strength graded structural timber with rectangular cross section - Part 1: General requirements (CEN (2019-05))

2.2.2.3 Design charring depth

The design charring depth to determine the structural fire load is calculated as follows:

$$d_{char,t} = 2 \cdot \beta_{par} \cdot t_0 \quad (2.2.10)$$

with

$$t_0 = 0.009 \cdot \frac{q_{d,tot,t}}{o} \quad (2.2.11)$$

where

$d_{char,t}$ is the design charring depth to determine the structural fire load, in mm

β_{par} is the design charring rate for the parametric fire, in mm/min

O is the opening factor according to EN 1991-1-2, Annex A, in $m^{1/2}$

$q_{d,tot,t}$ is the design total fire load density related to the surface area A_t , in MJ/m^2

t_0 is the time until a constant charring rate is assumed, in min

NOTE: The design charring depth $d_{char,t}$ is the result of an iteration process

2.2.2.4 Design total fire load density

The design total fire load density should be calculated as follows:

$$q_{d,tot,t} = q_{d,fi,t} + q_{d,st,t} \quad (2.2.12)$$

where

$q_{d,tot,t}$ is the design total fire load density related to the surface area A_t , in MJ/m^2

$q_{d,fi,t}$ is the design compartment fire load density according to EN 1991-1-2 related to the surface area A_t , in MJ/m^2 ;

$q_{d,st,t}$ is the structural fire load density related to the surface area A_t , in MJ/m^2 .

NOTE: The design total fire load density $q_{d,tot,t}$ for the first iteration is calculated only with the compartment fire load density $q_{d,fi,t}$ assuming that the structural fire load density $q_{d,st,t} = 0$.

2.2.2.5 Design structural fire load density

The design structural fire load density should be calculated as follows:

$$q_{d,st,t} = m \cdot 60 \cdot s_{10} \cdot d_{char,t} \cdot \alpha_{st} \cdot \frac{A_{st}}{A_t} \quad (2.2.13)$$

where

$q_{d,st,t}$ is the design structural fire load density related to the surface area A_t , in MJ/m²

m is the combustion factor according to EN 1991-1-2

$d_{char,t}$ is the design charring depth to determine the structural fire load, in mm

s_{10} is the rate of heat release of timber members per unit area related to the charring rate, $s_{10} = 0.12$, in MW/m² per mm/min

α_{st} is the time dependent modification factor. It should be set to 1.0 unless specified differently

A_{st} is the combusting surface of timber members, in m²

A_t is the surface area of the design fire compartment, in m²

2.2.2.6 Iterative Process

The design total fire load density should be calculated iteratively by repeatedly calculating the design charring depth $d_{char,t}$, until the design charring depth at the end of the fire does not increase more than 0.5 mm.

NOTE: If the increase of the design charring depth of subsequent iterations remains higher than 0.5 mm for a large number of iterations, the calculation suggests a long or infinite fire duration. Design adjustments to reduce the structural fire load density, e.g. by reduction of the unprotected timber members or/and changes to the compartment or ventilation geometry can result in a shorter fire duration.

2.2.3 Cumulative temperature charring model

According to the part A.4.3.2 of prEN 1995-1-2:20YY, the design charring depth of unprotected timber members is calculated by equation below.

$$d_{char,t} = \left(\frac{\int_0^t (T^2) dt}{1.35 \cdot 10^5} \right)^{\frac{1}{1.6}} \quad (2.2.14)$$

2.3 The Models

2.3.1 Brandon's model (FSUW)

The char depth is calculated as explained in Section 2.2.1, also the gas temperature at time t (hours) is given by Equation 2.3.1 (from EN 1991-1-2 Annex A).

$$\theta_g = 20 + 1325 \left(1 - 0.324e^{-0.2t\Gamma} - 0.204e^{-1.7t\Gamma} - 0.472e^{-19t\Gamma} \right) \quad [^{\circ}\text{C}] \quad (2.3.1)$$

A modification is done to this model in order to take account of a problem that occurred in Test 9 which has huge opening ratio. (Section 2.4.2 and Table 2.8)

The problem was the negative impact of exposed timber in Brandon's method. It occurred because the opening ratio is 0.265 which is above the upper limit of 0.10.

In order to fix that the factor for the fuel burned in external environment and the energy stored in char is changed. Instead of taking it as constant value of 0.7, Equation 2.3.2 is used. This equation takes account of the opening ratio's effect on the fuel burned in external environment and also the energy stored in char. As the opening ratio increases the factor decreases as more fresh air therefore more oxygen can be supplied to the compartment.

$$0.7 * \text{MIN} \left(1, \left(0.0002 * q_{t,d} / O \right) / t_{lim} \right) \quad (2.3.2)$$

The change occurred after this modification can be seen in the Table 2.5.

Table 2.5: Modification of Brandon's model

	Before	After
Fire load (total area) without timber	125.24	125.24
Fire load (total area)	111.07	151.40

2.3.2 Eurocode Model (prEN 1995-1-2:20YY + EN 1991-1-2)

The char depth is calculated as explained in Section 2.2.2, also the gas temperature at time t (hours) is given by Equation 2.3.1.

2.3.3 Cumulative temperature charring model + DIN EN 1991-1-2/NA

As explained before cumulative temperature charring model requires the compartment temperature as input.

In order to get the temperature-time curve DIN EN 1991-1-2/NA Appendix AA is used. So the cumulative temperature charring model is combined with the German National Annex.

This combined process works as below,

1. Predict the temperature-time curve for only the moveable fuel load by using DIN EN 1991-1-2/NA Appendix AA
2. Predict the char depth by cumulative temperature charring model
3. Predict the additional fuel load by using prEN 1995-1-2:20YY
4. Predict the temperature-time curve for the total fuel load by using DIN EN 1991-1-2/NA Appendix AA
5. Repeat steps 2-3-4 until the char depth converges

From now on this model will be mentioned as combined model in order to keep the name simple.

2.3.4 Comparison of Models

Table 2.6 presents a comparative analysis of the three charring models: Brandon's Method (FSUW), prEN 1995-1-2: 20 YY, and the DIN EN 1991-1-2/NA model combined with a Cumulative Temperature Charring model.

As seen in the table, each model operates based on specific input parameters and has its own restrictions, which describe the circumstances under which they can be accurately applied.

Table 2.6: Comparison of Models

Model	Input Parameters	Restrictions	Output
Brandon's Method (FSUW)	<ul style="list-style-type: none"> - Specific heat capacity of compartment boundaries - Density of compartment boundaries - Thermal conductivity of compartment boundaries - Dimensions of compartment - Dimensions of openings - Number of openings - Fire Load (floor area) - Growth Rate - Area of Exposed CLT 	<ul style="list-style-type: none"> - Glue line stability of the engineered timber lamella is preserved - Any board coverings utilized to encapsulate the wood do not fail or become detached - A minimum distance of 3.5 m between initially unprotected walls made of timber members - $0.02 \leq O \leq 0.10$ - O is the opening factor given in EN 1991-1-2, Annex A 	<ul style="list-style-type: none"> - Time at which char rate reduces - The design charring depth at the end of the fire - Temperature-time curve
prEN 1995-1-2: 20 YY	<ul style="list-style-type: none"> - Ratio between the heat release and char depth - HRR of timber members per unit area related to the charring rate - Combustion factor 	<ul style="list-style-type: none"> - The depth of the cross-section of the linear timber member and the width of the linear timber member should be bigger than the design charring depth of linear timber member at the end of the parametric fire 	<ul style="list-style-type: none"> - The design charring depth at the end of the fire - Temperature-time curve
DIN EN 1991-1-2/NA + Cumulative temperature charring model	<ul style="list-style-type: none"> - Time dependent modification factor 	<ul style="list-style-type: none"> - Only be applied to timber members fulfilling one or more of the following requirements: - Products which are encapsulated for the entire fire duration - Initially unprotected structural timber products - Initially unprotected products which maintain bond line integrity of face bonds in fire 	<ul style="list-style-type: none"> - The design charring depth at the end of the fire - Temperature-time curve

2.4 Experiments

The experiments are chosen from three sources which are listed below:

- Fire Safe Use of Wood in Buildings, Buchanan and Ostman (2022)
- Fire safe implementation of visible mass timber in tall buildings compartment fire testing, Brandon *et al.* (2021)
- Compartment Fires Tests conducted in ETH Zurich, Glauser *et al.* (2021)

The first two experiment sets are for full scale compartments, however the third one is conducted on scaled down compartment. Due to this, the experiments are divided in two groups. In first group the full scale compartment tests, in the other group the scaled down compartment tests are inspected.

The tests are numbered separately for each group. In first group 9 tests exist, 4 of them are from Fire Safe Use of Wood in Buildings and the other 5 are from Fire safe implementation of visible mass timber in tall buildings compartment fire testing. In the second group 12 tests exist, all of them are from Compartment Fires Tests conducted in ETH Zurich.

2.4.1 Fire Safe Use of Wood in Buildings

This book is written by numerous contributors and edited by Andrew Buchanan and Birgit Östman. In section 3.8.1 of the book a series of experiments conducted in "Fire Safety Challenges of Tall Wood Buildings - Phase 2: Task 4 Engineering Analysis and Computer Simulations"(Brandon and RISE (2018)) is mentioned. The summary of these experiments can be seen in Table 2.7.

Table 2.7: Overview of compartment test properties and results of FSUW

Test	Compartment test properties					Experimental results				
	Dim.(m)	Opening dim(m)	Total unprot. surface (m^2)	Movable fuel load per floor area (M/m^2)	Time to flashover (min)	Time of char measured t_{ch} (min)	Char depth at t_{ch} lower limit (mm)	Char depth at t_{ch} upper limit (mm)	Method	
I-3	$4.6 \times 9.1 \times 2.7$	3.6×2	24.6	550	14	69	35	35	A	
I-4*	$4.6 \times 9.1 \times 2.7$	1.8×2	41.8	550	11	115	50	50	A	
A2	$9.1 \times 9.1 \times 2.7$	7.3×2.4	24.8	550	11	66	23	23	A	
A3	$9.1 \times 9.1 \times 2.7$	7.3×2.4	29.9	550	11	39	23	23	A	
K3	$3.5 \times 4.5 \times 2.5$	1.1×2	11.3	550	5	68	21	44	B	
QI	$2.7 \times 2.7 \times 2.8$	0.8×1.8	7.4	132	9	51	II	11	N.F.	
RI*	$2.7 \times 5.8 \times 2.4$	0.9×1.9	15.9	456	13	179	70	89	B	
R2	$2.7 \times 5.8 \times 2.4$	0.9×1.9	15.9	456	13	197	52	70	B	
R3	$2.7 \times 5.8 \times 2.4$	0.9×1.9	15.9	456	13	227	49	70	B	
SI	$3.5 \times 4.5 \times 2.5$	3×1.5	22.5	600	47	46	35	35	A	

* Tests involved delamination during the fully developed phase.

A = Char depth determined using thermocouple measurements. B = Char depth determined physically after the test.

From these experimental results, 4 tests are chosen. The chosen tests are shown in grey colour in the Table 2.7 and also they are listed below,

- I-3
- A2
- K3
- R2

This selection is based on the purpose of having different compartment geometries and different opening factors. Also the tests where there has been delamination are avoided as the prediction models' restrictions require that integrity of laminae.

2.4.2 Fire safe implementation of visible mass timber in tall buildings compartment fire testing

In the research study (Brandon *et al.* (2021)), five compartment fire experiments were carried out. These compartments had internal dimensions of 7.0 m x 6.85 m x 2.73 m. Four of the compartments (Tests 5, 6, 7, and 8) featured two ventilation openings measuring 2.25 m x 1.78 m (width x height), yielding an opening factor of 0.062 m^{1/2}. The selection of compartment dimensions and opening factors for this study was done by a probabilistic analysis and tall residential building data surveys. The final compartment test (Test 9) contained six larger openings, resulting in an opening factor of 0.25 m^{1/2}, which is approximately equivalent to the mid-range of opening factors for office compartments discovered in the survey.

The floor plan for Tests 5, 6, 7 and 8 is shown in Figure 2.2. The floor plan of Test 9 is shown in Figure 2.3.

These tests will be referred as RISE tests.

Figure 2.2: Floor Plan for Tests 5, 6, 7 and 8 copied from Brandon *et al.* (2021)

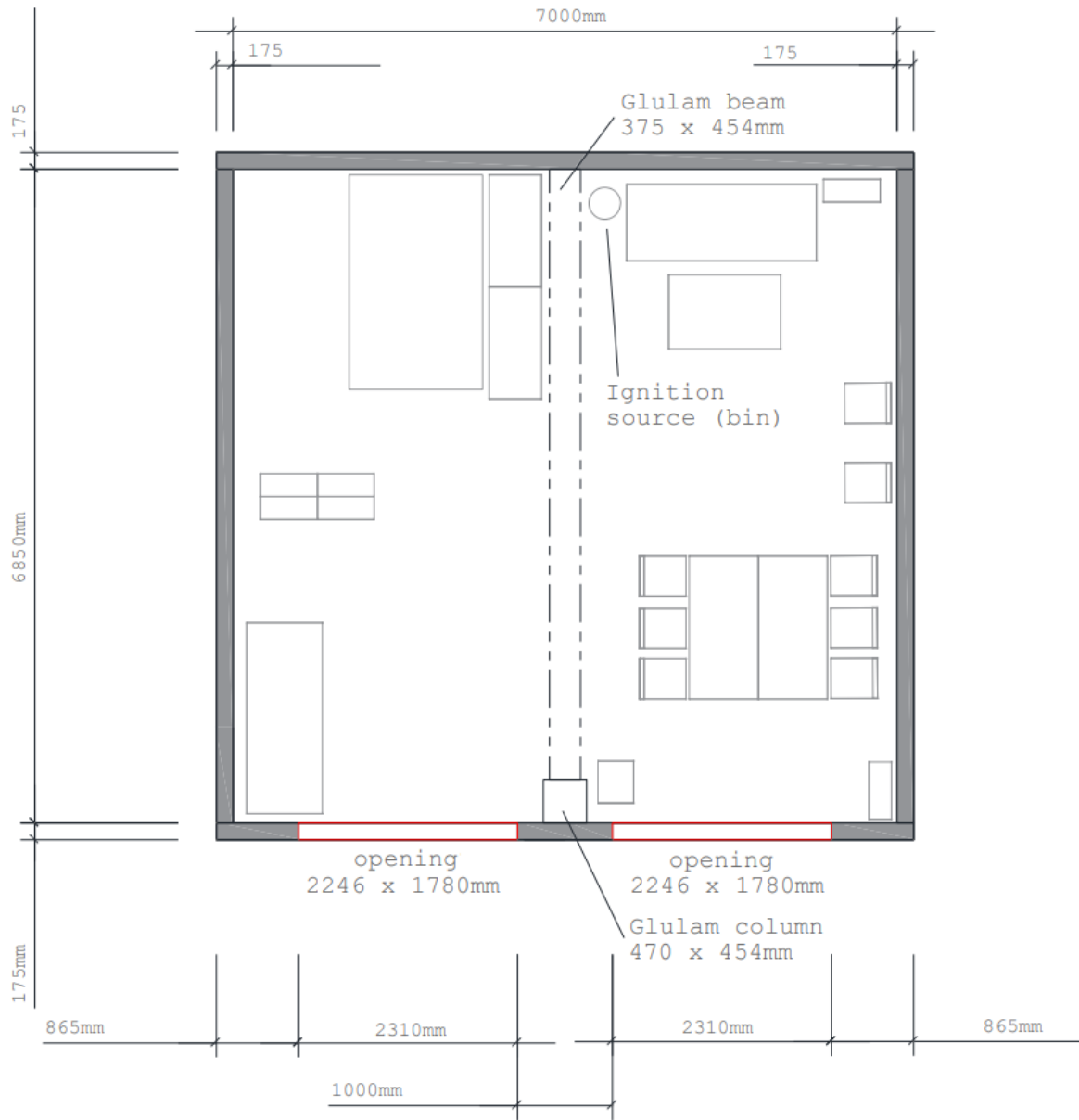
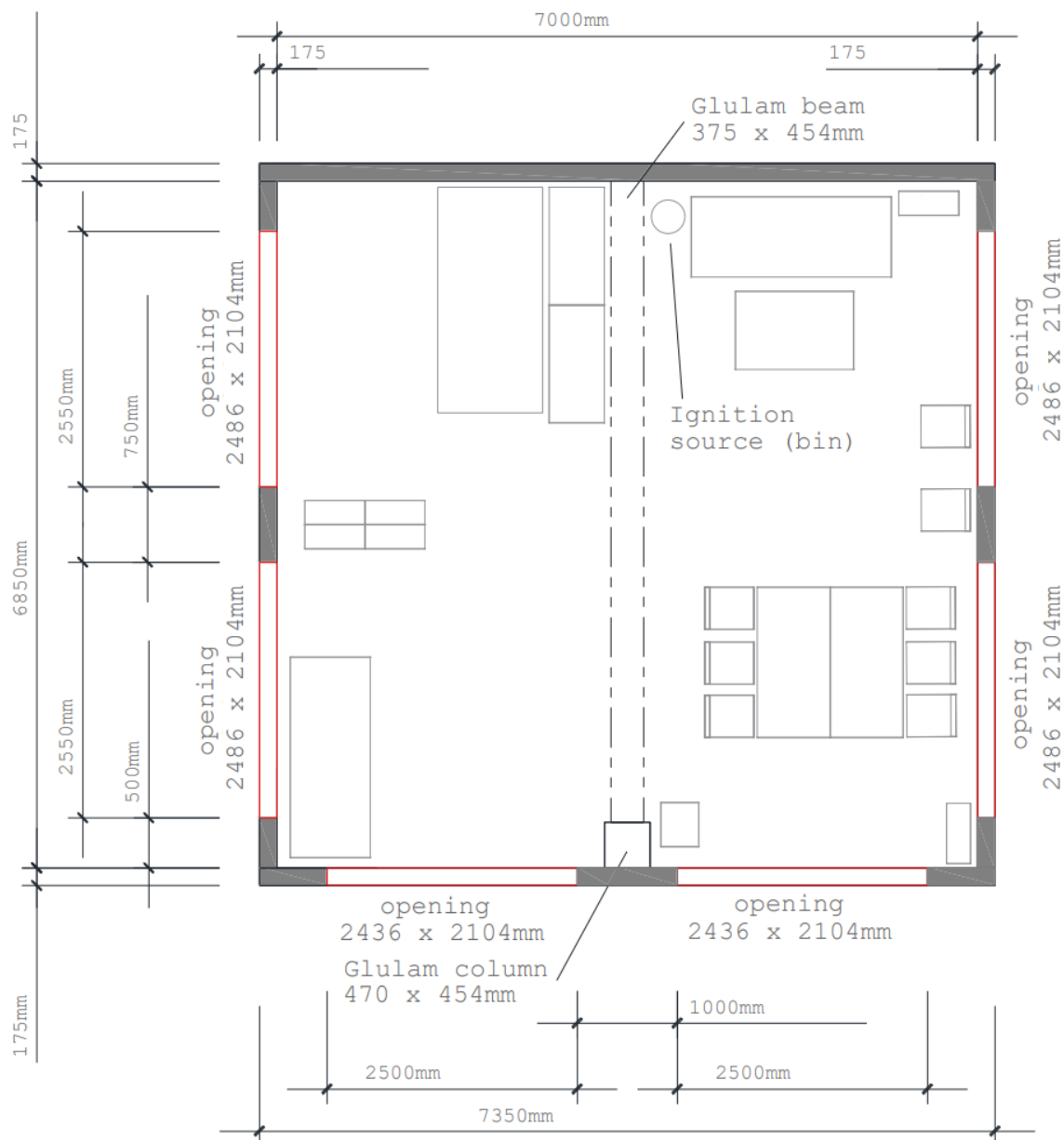


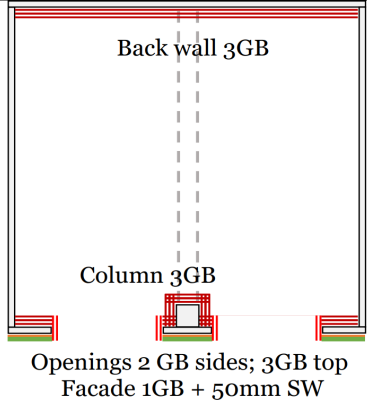
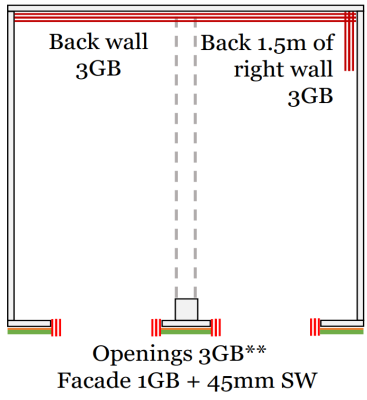
Figure 2.3: Floor Plan for Test 9 copied from Brandon *et al.* (2021)

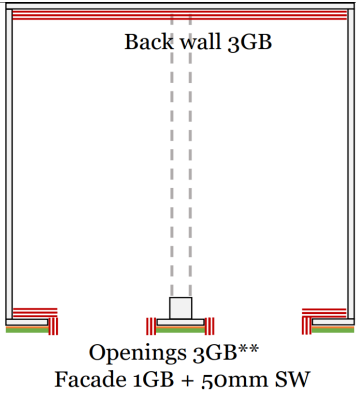
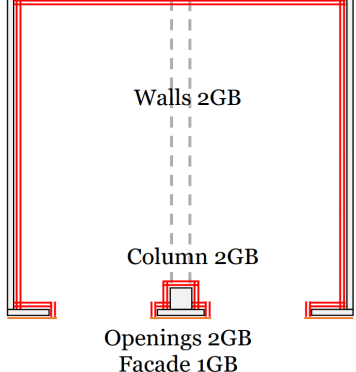
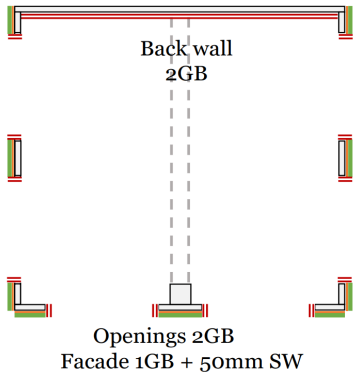
The compartment dimensions, opening sizes, and fuel load density were determined through a probabilistic analysis aimed at testing a severe fire scenario based on real building designs. The combination of compartment dimensions, fuel load density, and opening factor results in the 85th percentile of expected total char damage for fire scenarios in residential buildings where sprinklers are not activated, flashover occurs, and there is no fire service intervention.

The fuel used consisted of a mix of typical apartment furniture, particle board sheets on the floor to represent wood flooring, and additional wood cribs to represent stored fuel. The total mass of the movable fuel on the floor was measured using load cells beneath the floor for each test, totalling 1307 ± 10 kg. The ignition source was a metal bin filled with 635 g of crumbled A4 print paper.

Table 2.8 provides information on the locations and number of gypsum board protection layers, as well as the percentages of exposed surface areas. The figures also include the number of 15.9 mm thick Type X gypsum board layers (GB) implemented on interior surfaces. Schematic floor plans in a non - scaled format indicate the locations of protected surfaces.

Table 2.8: Summary of RISE Tests

Test name Window Opening size	Gypsum Board (GB) Protected interior surfaces	Exposed wood surfaces	Floor plan (schematic)
Test 5 - Two window openings - 8.0 m ² of exterior wall open	- Back wall and - Front wall protected by 3 layers of GB	- 100% of ceiling, 100% of beam, 100% of left wall, 100% of right wall exposed - No exposed wood wall surfaces meeting in a corner (91.2 m ²)	 Back wall 3GB Column 3GB Openings 2 GB sides; 3GB top Facade 1GB + 50mm SW
Test 6 - Two window openings - 8.0 m ² of exterior wall open	- Back wall and - Back 1.5 m length of right wall protected by 3 layers of GB	- 100% of ceiling, 100% of beam, 100% of left wall, 78% of right wall, 100% of front wall, 100% of column exposed - Two exposed wood wall surfaces meeting in a corner (front left and front right) (96.2 m ²)	 Back wall 3GB Back 1.5m of right wall 3GB Openings 3GB** Facade 1GB + 45mm SW

Test name Window Opening size	Gypsum Board (GB) Protected interior surfaces	Exposed wood surfaces	Floor plan (schematic)
Test 7 - Two window openings - 8.0 m ² of exterior wall open	- Back wall and - 0.7 m on the left and right-side edges of the front wall protected by 3 layers of GB	- 100% of ceiling, 100% of beam, 100% of left wall, 100% of right wall, 60% of front wall, 100% of column exposed - No exposed wood wall surfaces meeting in a corner (97.2 m ²)	
Test 8 - Two window openings - 8.0 m ² of exterior wall open	- All walls and - Column protected by 2 layers of GB	- 100% of ceiling, 100% of beam exposed - No exposed wood surfaces in walls (53.8 m ²)	
Test 9 - Six window openings - 31.2 m ² of exterior wall open	- Back wall protected by 2 layers of GB	- 100% of ceiling, 100% of beam, 100% of left wall, 100% of right wall, 100% of front wall, 100% of column exposed - Two exposed wood wall surfaces meeting in a corner (front left and front right) (77.9 m ²)	

Note: GB indicates gypsum boards, SW indicates stone wool

2.4.3 Compartment Fires Tests conducted in ETH Zurich

This project which consists of small scale compartment tests was part of three Master theses at the Institute of Structural Engineering (IBK) of ETH Zurich. (Glauser *et al.* (2021)) The boundaries of the compartment were either protected with fire protection panels or exposed to the fire. In Table 2.10 the summary of all tests performed in the project can be seen.

This set of experiments is chosen to analyse how the models perform in small scale compartments. However, note that these models are not created for these scenarios, they are created by using real full scale experimental data. So it should not be expected to get reasonable predictions.

The temperature measurements are taken by using a thermocouple tree which is located in the centre of the compartment. 9 thermocouples are placed along the tree in intervals of 5 cm. In case of a large compartment, three thermocouple trees are used. However in order to compare these measurements with the models' predictions an average of the measurements of thermocouples are calculated for each test.

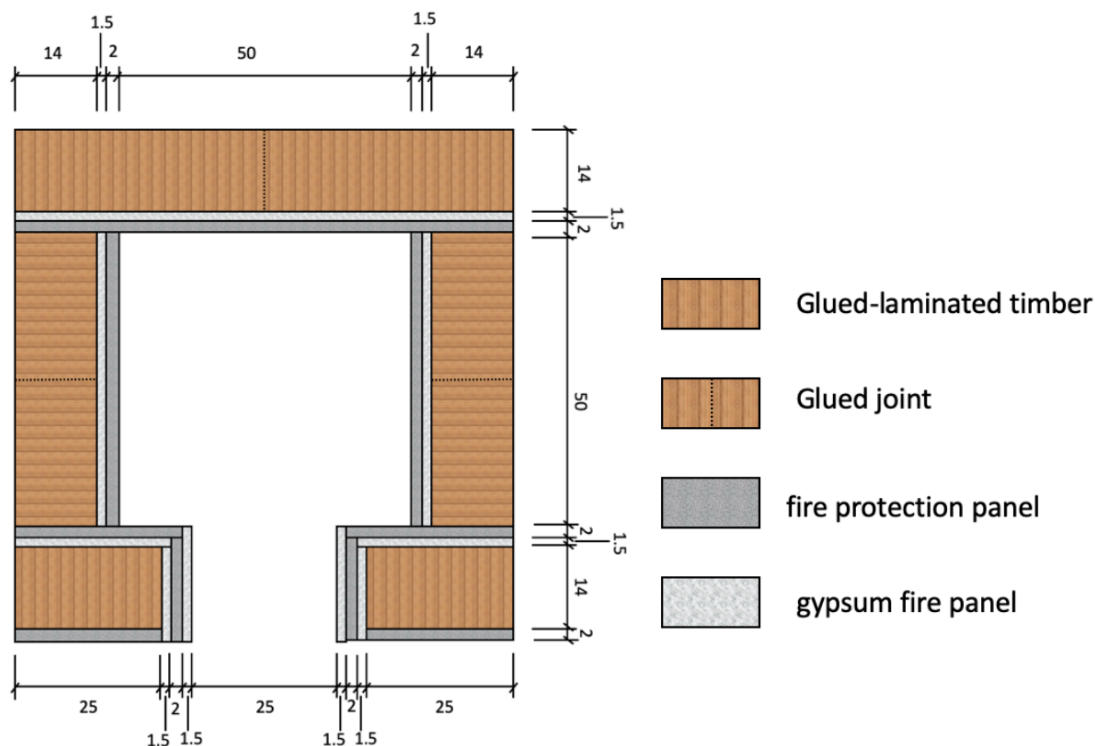
After the tests, the char layer depth measurements have been taken.

2.4.3.1 Standard compartment

The compartment is constructed from glued-laminated (Glulam) spruce. Each lamella has a thickness of 40 mm and is designed in a way that prevents detachment during a fire, with glue joints positioned perpendicularly to the specimen's exposed surface. Figure 2.4 illustrates the joints, dimensions, and orientation of the Glulam layers which is denoted by the texture.

The internal measurements of the compartments are consistently 0.5 m × 0.5 m × 0.5 m, irrespective of the presence of fire protection. When fire protection is employed, fire protection panels are utilized, consisting of a 1.5 cm thick gypsum fibreboard behind a 2 cm thick fire protection panel.

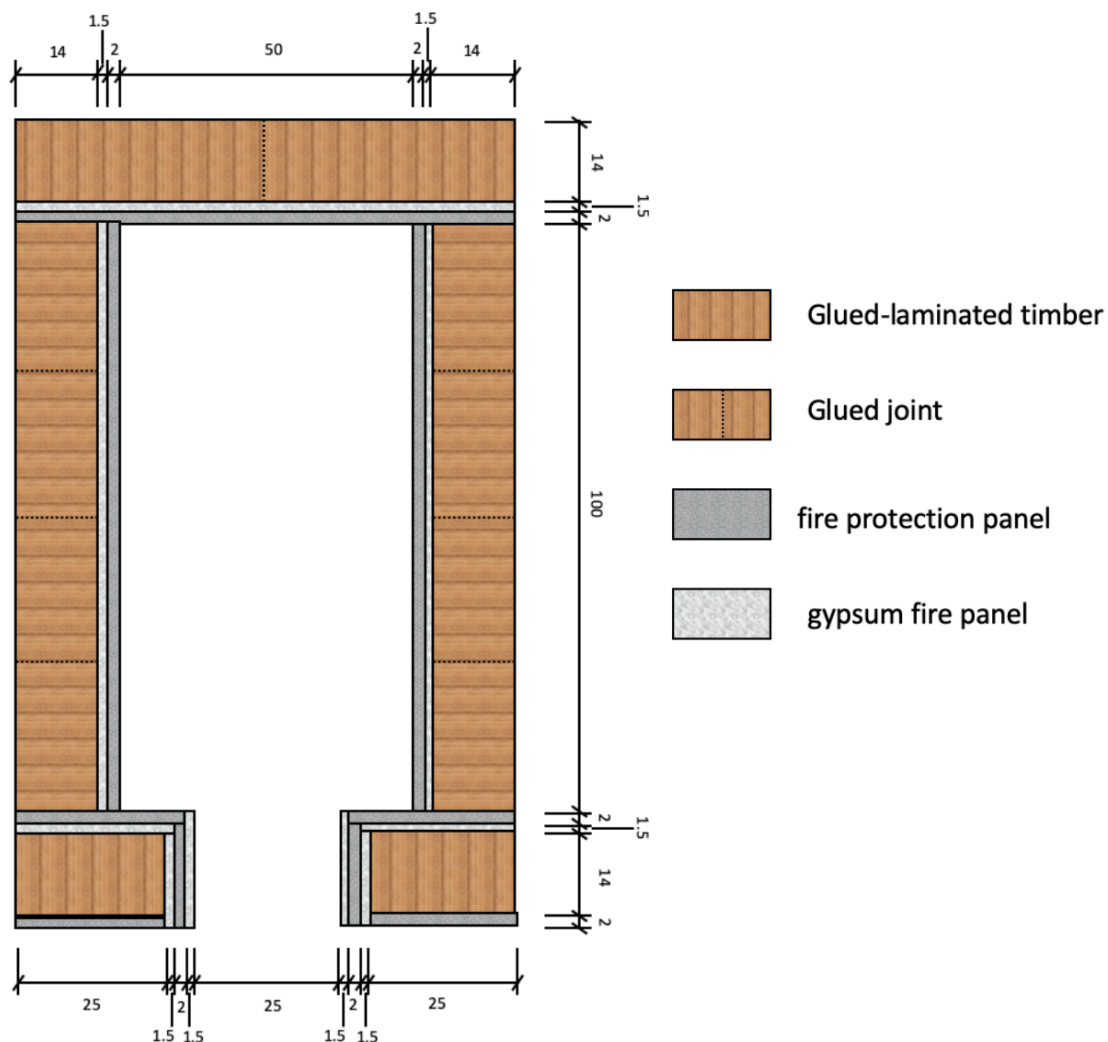
Figure 2.4: Standard compartment for ETH Zurich Tests (cm) copied from Glauser *et al.* (2021)



2.4.3.2 Large compartment

To examine the impact of compartment size, the compartment depth is adjusted from 0.5 m to 1 m in tests C5, C6, and C12. A diagram of the larger compartment is presented in Figure 2.5. Despite the augmented dimensions in comparison to the standard compartment, the materials and construction method remain identical to those of the standard compartment.

Figure 2.5: Large compartment for ETH Zurich Tests (cm) copied from Glauser *et al.* (2021)



2.4.3.3 Movable Fuel

Wood cribs served as movable fuel. There are two types of wood cribs used in these experiments. The standard crib consists of 12 layers with 5 sticks. It is important to mention that the modified wood crib was utilized for test C4, consisting of 18 layers, which is one and a half times the standard number of layers. The calculated weights of the two types of wood cribs and the resulting fuel load can be seen in Table 2.9

Table 2.9: Overview of fuel load for ETH Zurich Tests

	Standard	Modified
Weight of crib [kg]	2.2	3.3
Heat of Combustion [MJ/kg]	5	5
Fuel Load [MJ]	38.5	57.75

Table 2.10: Overview of compartment test properties of ETH Zurich Tests

test no.	Compartment size		Fuel		Exposed surface			Protected surface		
	standard	large	standard	modified	left	right	ceiling	left	right	ceiling
C2	x		1					x	x	x
C3	x		2					x	x	x
C4	x			1				x	x	x
C5		x	2					x	x	x
C6		x	4					x	x	x
C7	x		1				x	x	x	
C8	x		1		x	x	x			x
C9	x		1		x			x		x
C10	x		1		x	x			x	x
C11	x		1		x		x	x	x	
C12		x	1		x	x			x	x

3 Results & Discussion

As it is explained before, there are three sets of experiments that are used for the assessing and comparing the models.

The 4 experiments that have been chosen from FSUW book can be seen in Table 2.7

The 5 experiments that have been conducted in RISE study can be seen in Table 2.8

The 12 experiments that have been conducted in ETH Zurich study can be seen in Table 2.10

In order to keep this result section more understandable, first two sets of experiments which are conducted in full scale compartments will be presented separately from the third set which is conducted in small scale compartments. Firstly, the predictions for char depth and temperature will be discussed. Then sensitivity analysis for selected input parameters and an additional detailed analysis for the time dependent modification factor (α) will be shown. While doing the analyses EXCEL software and Python codes are used. To keep this section non repetitive, only one of the related graph will be shown. The rest of the graphs can be seen in the Appendix A.

3.1 Char Depth Predictions for FSUW and RISE Tests

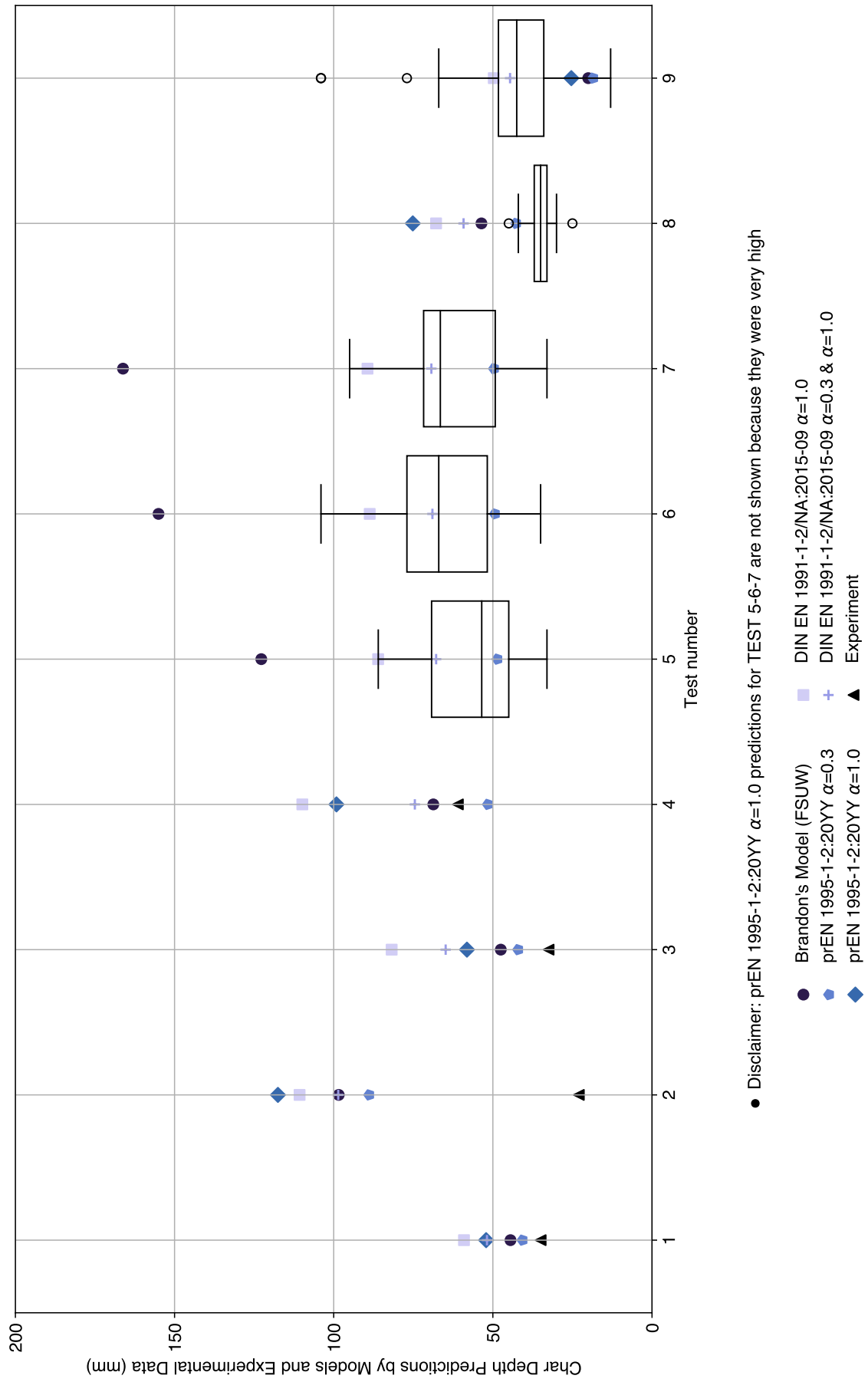
The FSUW tests' results are given as an upper and lower limit of char depths only. So for the first set of experiments (first 4 tests) only an average of upper and lower measured values is used as experimental measurement. These are shown in the Figure 3.1 as triangles. However, RISE tests' results are more detailed, many char depth measurements are given. So for this set of experiments the experimental measurements are shown by using box plots which can be seen in the Figure 3.1.

For the FSUW tests (Test 1-4), all of the char depth predictions of the models expect the prediction of prEN 1995-1-2:20YY with $\alpha = 0.3$ for Test 4 are in the safe side which means that they are giving a prediction value which is greater than the actual measurement from the experiments. However it should be noted that the experimental results shown as a single value in this graph as explained before.

For the RISE tests (Test 5-9) it is seen that the models except Brandon's Model (FSUW), give predictions which are in the range of the experimental measurements which are shown with box plot. However, prEN 1995-1-2:20YY with $\alpha = 0.3$ predicts a lower value than the mean of the experimental measurements. This can be explained by the model's low time dependent modification factor (α). When the time dependent modification factor (α) is small it means that more energy remains stored in char. Due to this lower temperatures are expected in the compartment which results in having smaller char depth values. The effect of this factor can be understood more clearly when it is seen that prEN 1995-1-2:20YY with $\alpha = 1.0$ predicts a very high char depths for the Tests 5,6 and 7.

For the RISE tests, combined model's new version (shown in the graph as DIN EN 1991-1-2/NA:2015-09 $\alpha = 0.3$ & $\alpha = 1.0$) which is explained in section 3.8, predicts char depth slightly above the experimental measurements' mean value. This means that this model which is created in this thesis performs as expected. The expectation from this new version of the combined model was to get realistic char depth predictions, and a safety factor can be added later on to these predictions accordingly.

Figure 3.1: Char Depth Predictions for FSUW and RISE Tests

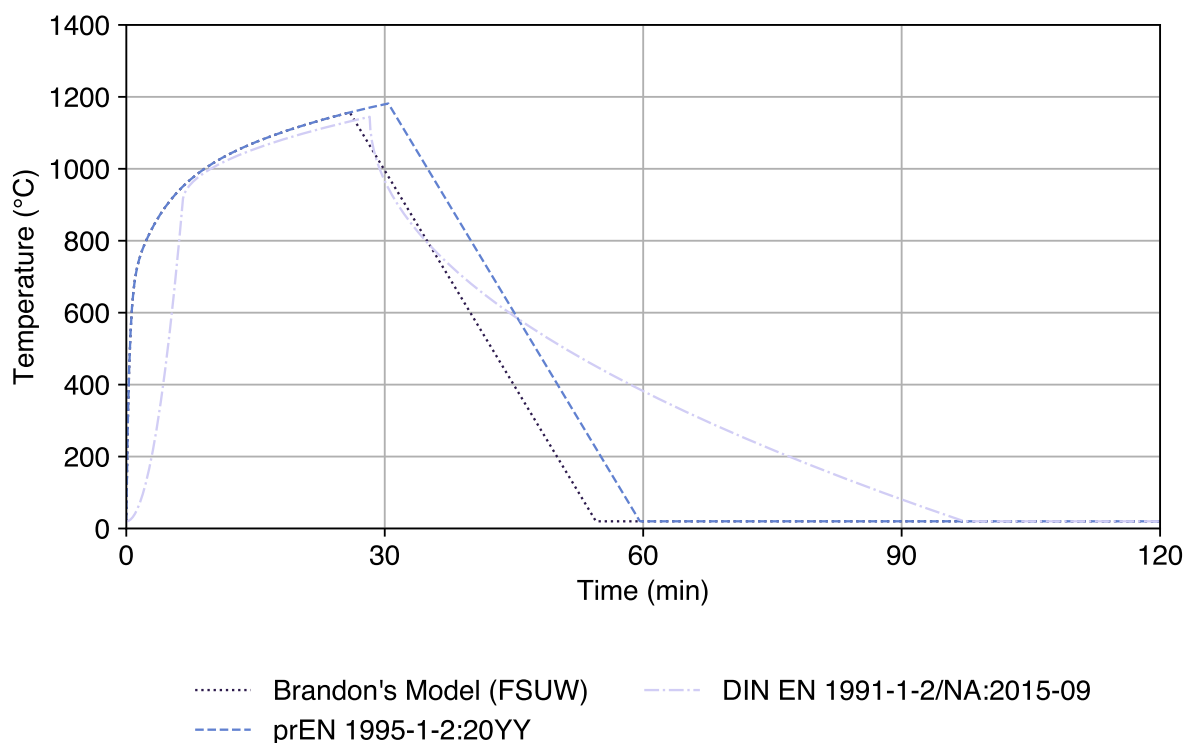


3.2 Temperature Predictions for FSUW and RISE Tests

In the experimental set from RISE, there exist both the temperature and char depth measurements. But as there is no experimental measurements for temperature for FSUW tests, only the temperature predictions for RISE tests can be compared with experimental measurements.

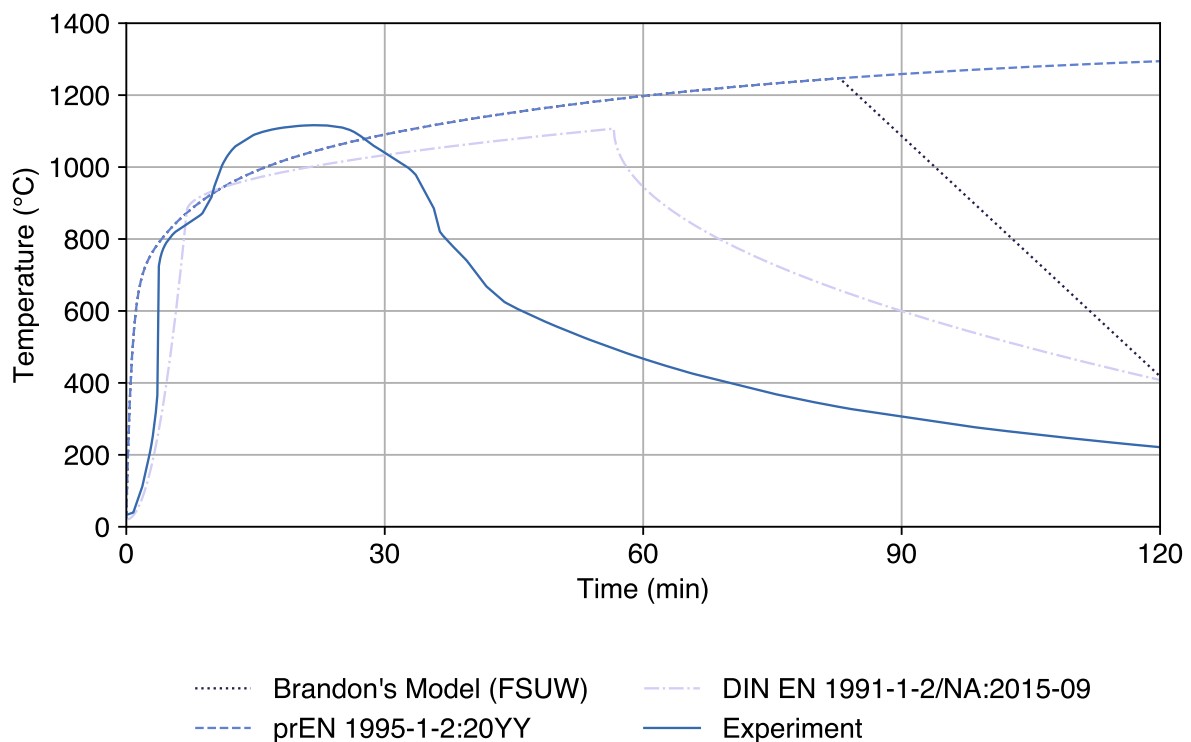
The comparisons for Test 1 and Test 5 can be seen in Figure 3.2 and Figure 3.3.

Figure 3.2: Temperature for Test 1



In the Test 1 there is no experimental measurement. The models can be compared with each other but a decision on performance can not be done. However, when the graph is inspected it can be seen that the combined model's (DIN EN 1991-1-2/NA:2015-09 + Cumulative Charring Model) decay phase behaves differently than the other 2 models. This can be explained by the fact that this model uses German national annex parametric temperature curve which has a curve equation defined for its decay phase instead of a line equation which is used for Eurocode parametric temperature curve (EN 1991-1-2).

Figure 3.3: Temperature for Test 5



In the Test 5, there is the experimental results also. So now the models can be compared with measurements. It is seen in the graphs that the all three of the models predicted the time to reach maximum temperature greater than the actual time required to reach maximum temperature. However, their predicted temperatures at the time for the actual maximum temperature is relatively close to the temperature at that time. In the decay phase, the Brandon's model and prEN 1995-1-2:20YY acts in an over conservative way which better than being under conservative. The issue that may be caused by being over conservative is to the negative effect on the economic concern of the design. Having said that, the combined model (DIN EN 1991-1-2/NA:2015-09) performs less conservative compared to the other two models. Therefore it can be said that this model is more economic while still being safe.

3.3 Char Depth Predictions for ETH Zurich Tests

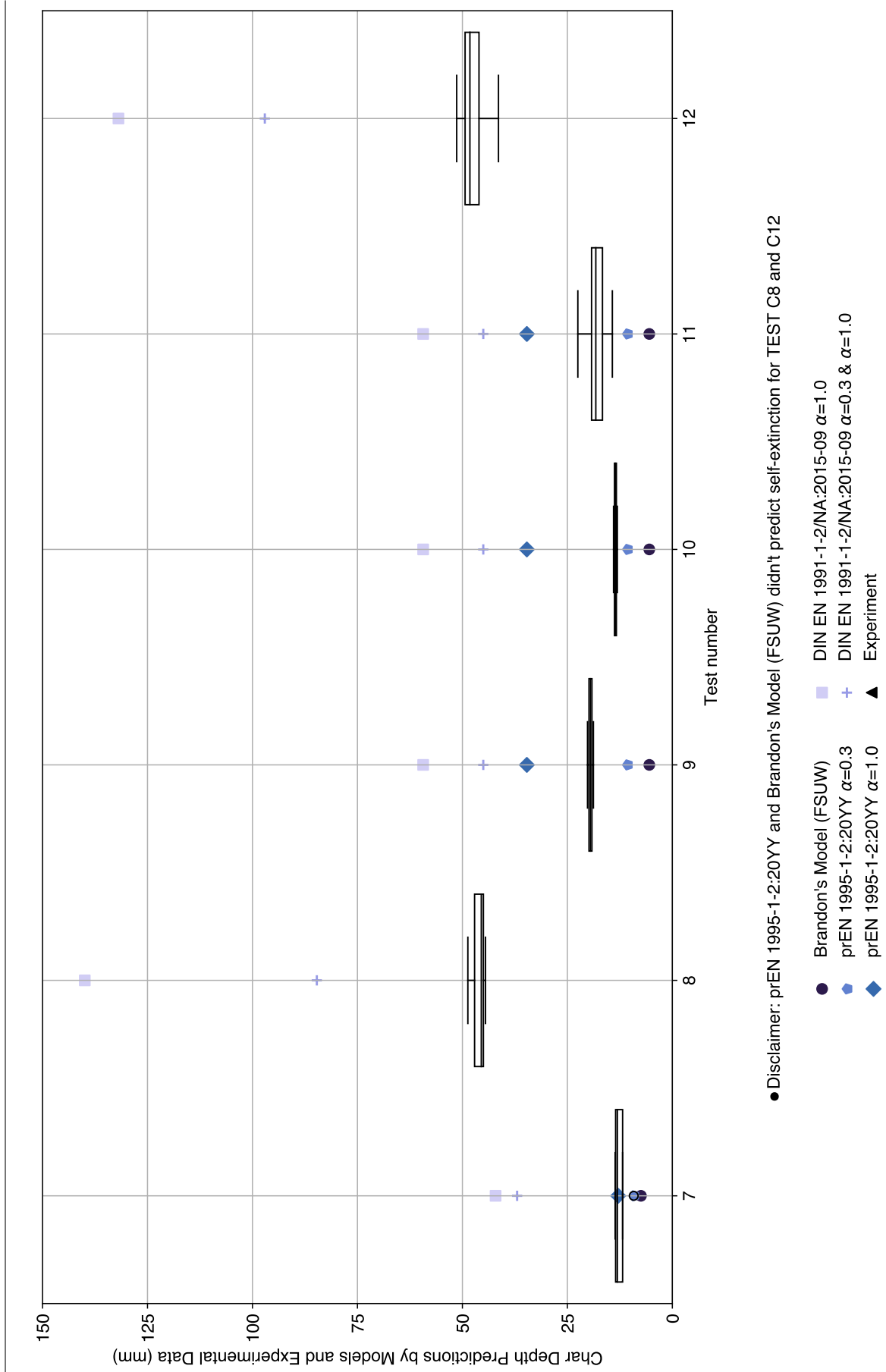
In the experiments conducted by ETH Zurich, the char depth measurements are taken. So for this set of experiments the experimental measurements are shown by using box plots which can be seen in the Figure 3.4. The first six of the tests are not shown as there is no exposed surface for those tests.

Overall, the Brandon's Model (FSUW) and prEN 1995-1-2:20YY with $\alpha = 0.3$ predicts a lower value than the actual experimental measurements. On the other hand, the combined model's 2 version (these are explained in section 3.8)

In Test C8 and C12, Brandon's Model (FSUW) and prEN 1995-1-2:20YY didn't predict self-extinction of timber. The reason of not achieving self-extinction for Test C8 is having only ceiling as protected surface which means that all other surfaces (left, right, back and front) are exposed to fire. Due to having more of the surfaces exposed, an increased positive feedback with radiation occurs between these compartment boundary surfaces. For the case of Test C12 the main reason is the compartment geometry which is shown in Figure 2.5. Also the effect of having left and right surfaces as exposed is important here.

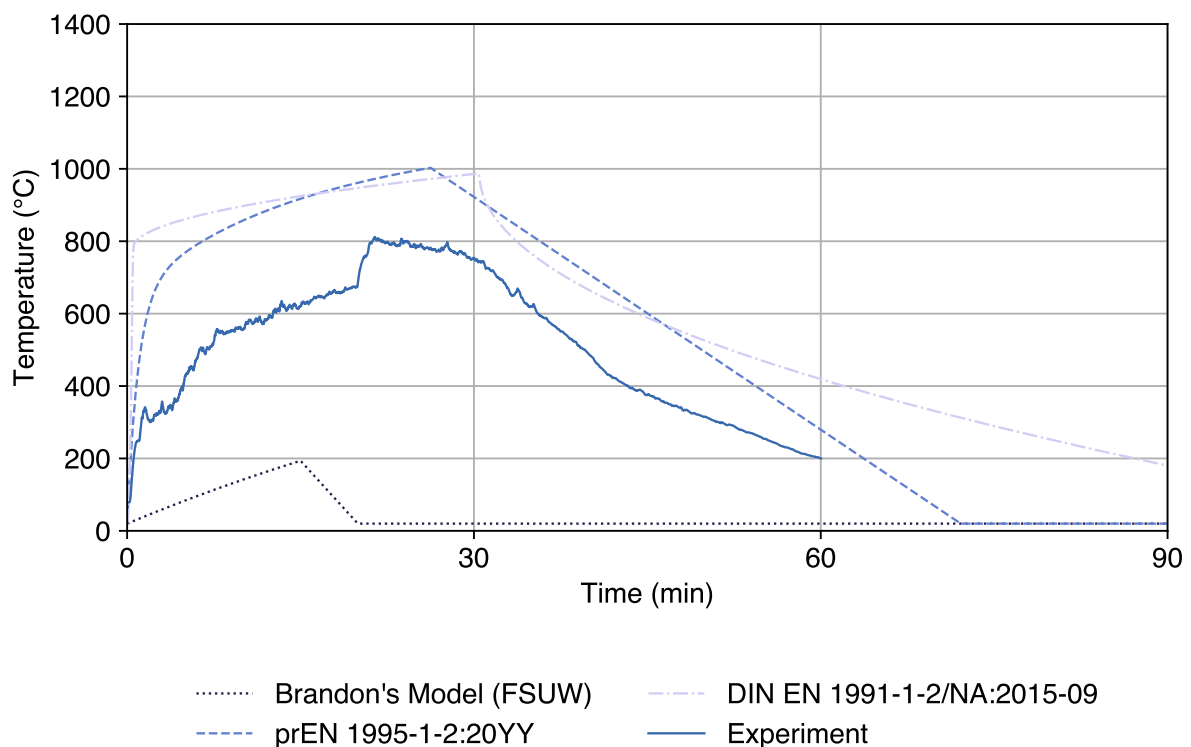
However, when the Test C10 is inspected, it can be seen that it has the same fuel and same exposed surfaces as the Test C12. Only the compartment size is different, so that is why the compartment geometry is said to be playing an important role while achieving the self-extinction or not achieving it. Due to this reason, an augmented care should be given while defining the boundaries of the compartment in these char prediction models.

Figure 3.4: Char Depth Predictions for ETH Zurich Tests



3.4 Temperature Predictions for ETH Zurich Tests

Figure 3.5: Temperature for Test C9



In the ETH Zurich Tests, the experimental results for temperature are given. This means that the models can be compared with measurements. It is seen in the graphs that the two of the models which are prEN 1995-1-2:20YY and combined model predicted the time to reach maximum temperature in a fairly close to the actual time required to reach maximum temperature. However their predictions are around 200 °C higher than the experimental measurement.

The other model, Brandon's model, underestimates the fire, both the duration of fire and the maximum temperature are predicted in a manner which is lower than the actual fire. It can be said that the Brandon's model is not suitable for the small scale compartments.

3.5 Sensitivity Analysis

In-depth sensitivity analyses can be crucial in understanding the performance and applicability of models. By adjusting the input parameters, one can evaluate the impact of each parameter on the overall model behaviour. This process not only helps in identifying the key factors that influence the charring of timber but also contributes to the optimization and refinement of the models.

For the purpose of this analysis, four key parameters are chosen:

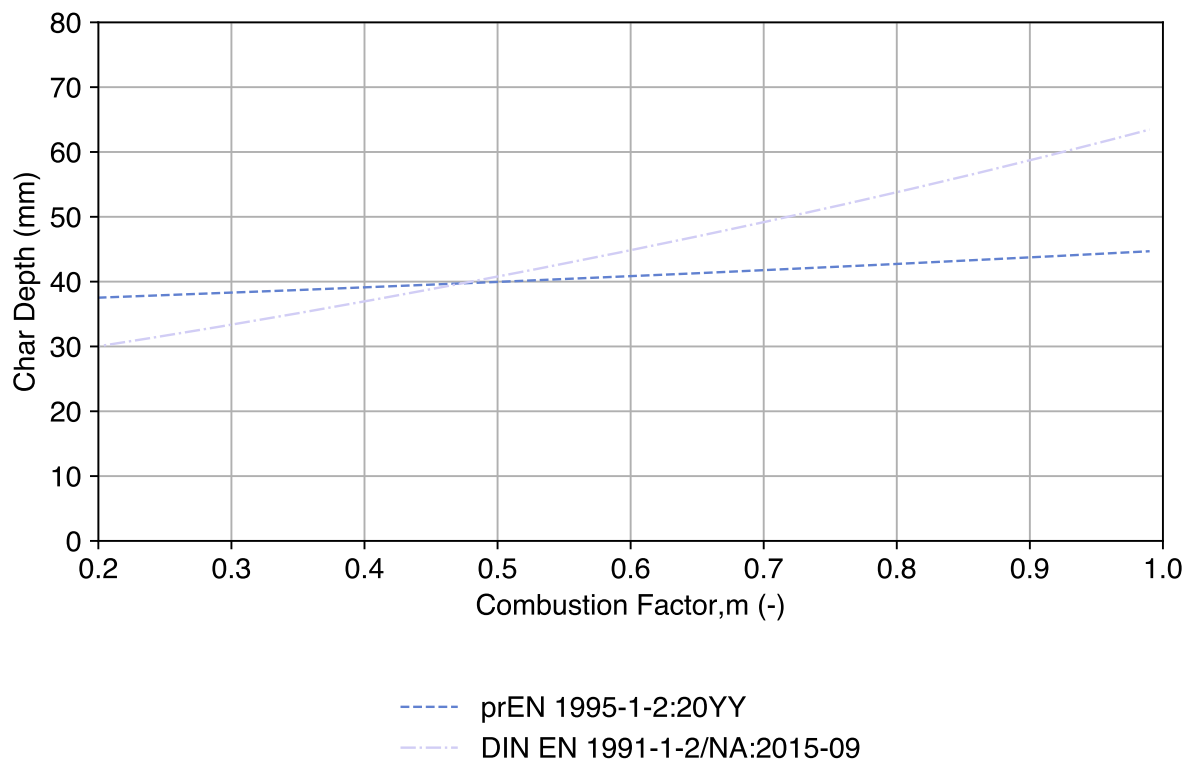
- Combustion factor
- Time Dependent Modification Factor
- Ratio Between the Heat Release and Char Depth
- Rate of Heat Release of Timber Members per Unit Area Related to the Charring Rate

These parameters were chosen over other potential factors, such as the geometry of the compartment, which can vary significantly from case to case. Although the geometry can influence the process, it does not provide consistent insights due to its variability. Hence, focusing on the parameters that remain consistent across various cases allows for a more standardized and meaningful analysis.

Moreover, current researches such as the recent study on quantifying the heat release from char oxidation in timber (MacLeod *et al.* (2023)) which is further inspecting the heat release from char shows the significance of the chosen parameters in the field of timber charring.

3.5.1 Combustion Factor

Figure 3.6: Sensitivity Analysis of Combustion Factor on Char Depth

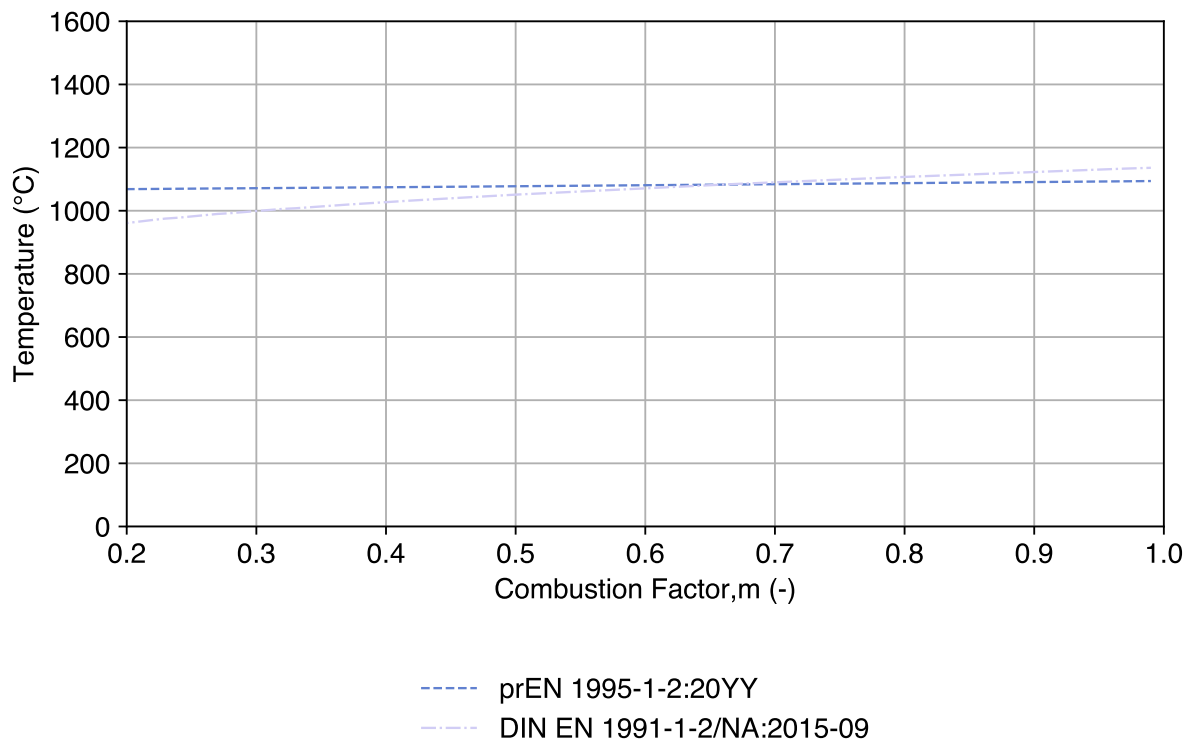


The combustion factor parameter is used in the prEN 1995-1-2:20YY and in the combined model (DIN EN 1991-1-2/NA:2015-09 + cumulative temperature charring model) which use Equation 2.2.13. However, it is not used in the Brandon's model (FSUW).

The effect of combustion factor on char depth can be seen in the Figure 3.6. The combined model has been affected by combustion factor more compared to the prEN 1995-1-2:20YY model. The reason behind this is the difference between the char depth calculations of these two models. The combined model's char depth calculation directly depends on temperature as because of its use of cumulative temperature charring model Equation 2.2.14 to predict char depth. However, the prEN 1995-1-2:20YY uses Equation 2.2.10 which depends on temperature in an indirect way.

Also combustion factor is used in calculation of $q_{x,d}$ in Equation 2.1.41. Due to these reasons the combustion factor effects the combined model more.

Figure 3.7: Sensitivity Analysis of Combustion Factor on Maximum Temperature

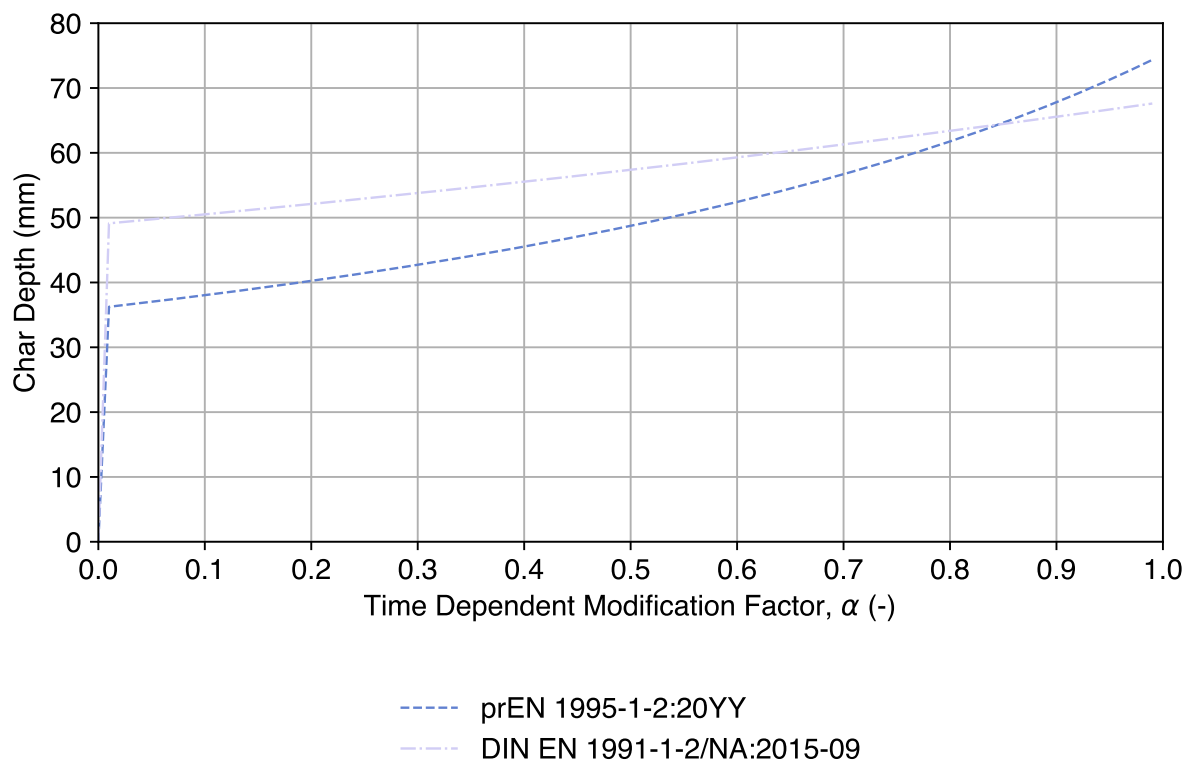


The temperature that has been mentioned in the part above (char depth discussion), is affected by combustion factor also because of the Equation 2.2.13 and Equation 2.1.9. The same behaviour is observed also for temperature, the combined model has been affected more by the change of the combustion factor. This can be seen in the Figure 3.7.

Also note that the sensitivity analysis for combustion factor is conducted between the values 0.2 to 1.0 of combustion factor. Because having less than 0.2 combustion efficiency will not be physically relevant as having greater than 1.0 will not be also.

3.5.2 Time Dependent Modification Factor (α)

Figure 3.8: Sensitivity Analysis of Time Dependent Modification Factor on Char Depth

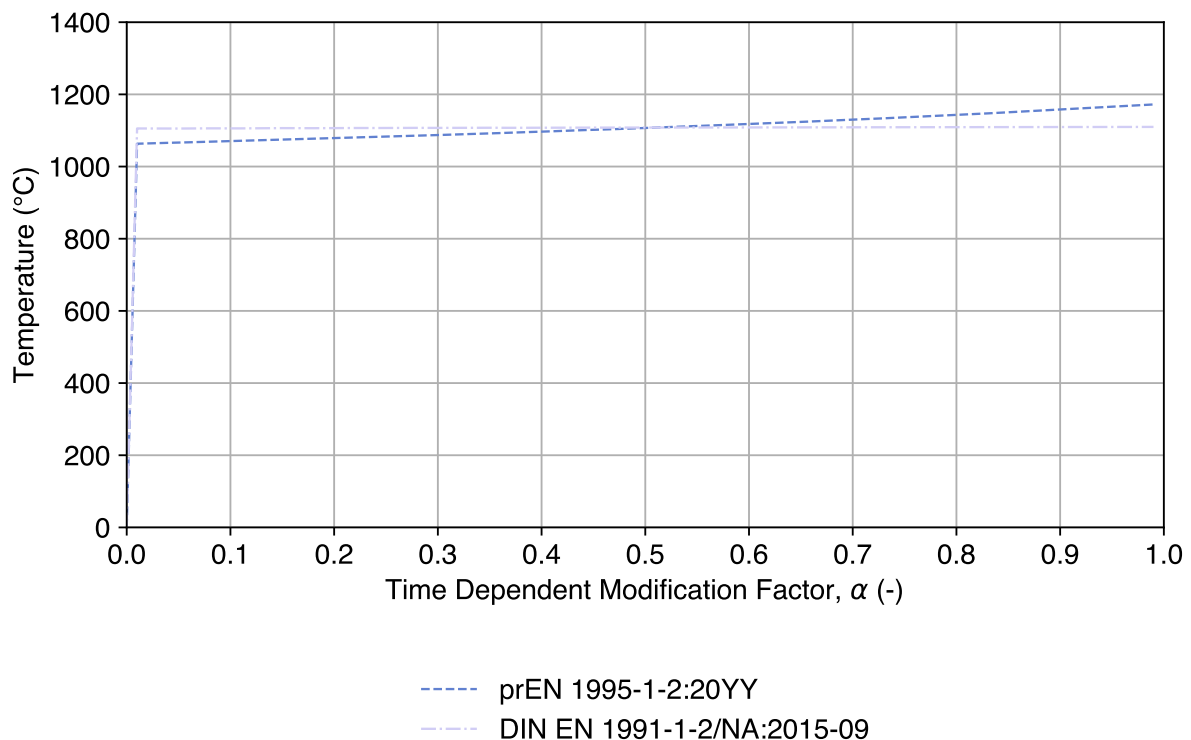


The time dependent modification factor (α) parameter is used in the prEN 1995-1-2:20YY and in the combined model (DIN EN 1991-1-2/NA:2015-09 + cumulative temperature charring model) which use Equation 2.2.13. However, it is not used in the Brandon's model (FSUW).

The effect of time dependent modification factor (α) on char depth can be seen in the Figure 3.8. The prEN 1995-1-2:20YY model has been affected by time dependent modification factor (α) more compared to the combined model. The reason of this can be explained by a similar process that is used in the discussion of sensitivity analysis of the combustion factor.

However as it can be seen the effect of time dependent modification factor (α) is more on the prEN 1995-1-2:20YY which is the opposite of the case of combustion factor. This can be explained by the lack of the time dependent modification factor (α) parameter in the calculation of $q_{x,d}$ in Equation 2.1.41.

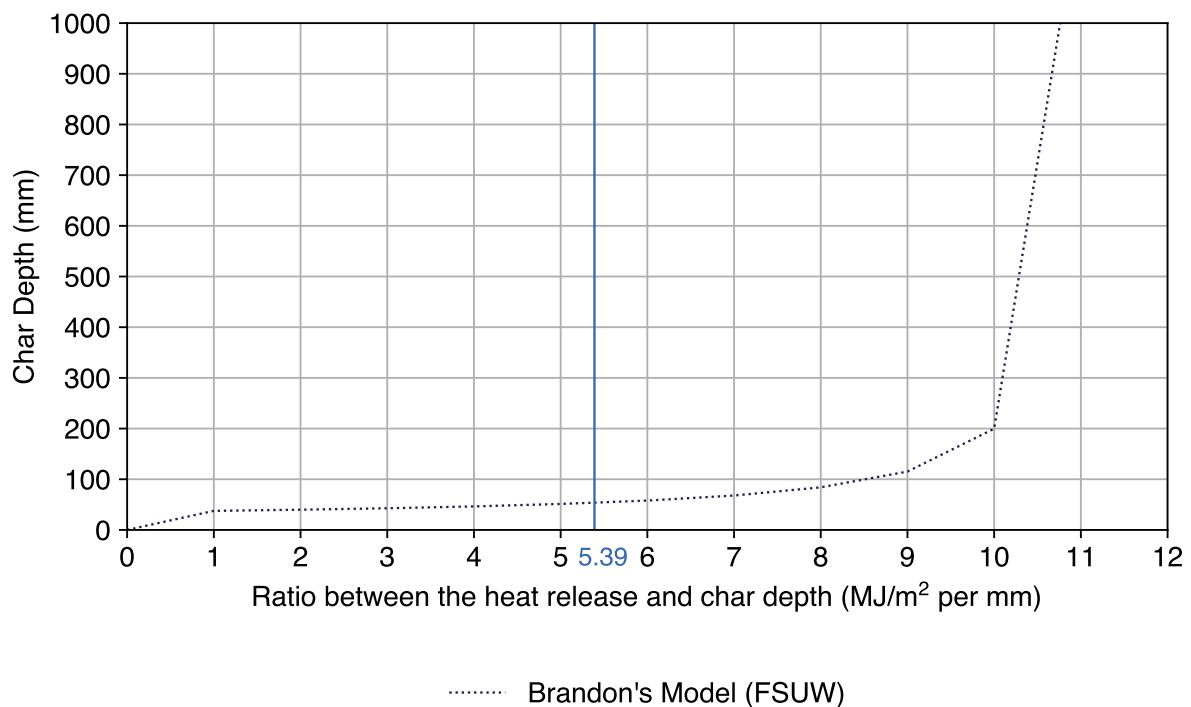
Figure 3.9: Sensitivity Analysis of Time Dependent Modification Factor on Maximum Temperature



In the temperature calculation which can be seen in the Figure 3.9, the effect of time dependent modification factor (α) is more in the prEN 1995-1-2:20YY.

3.5.3 Ratio Between the Heat Release and Char Depth

Figure 3.10: Sensitivity Analysis of Ratio Between the Heat Release and Char Depth on Char Depth



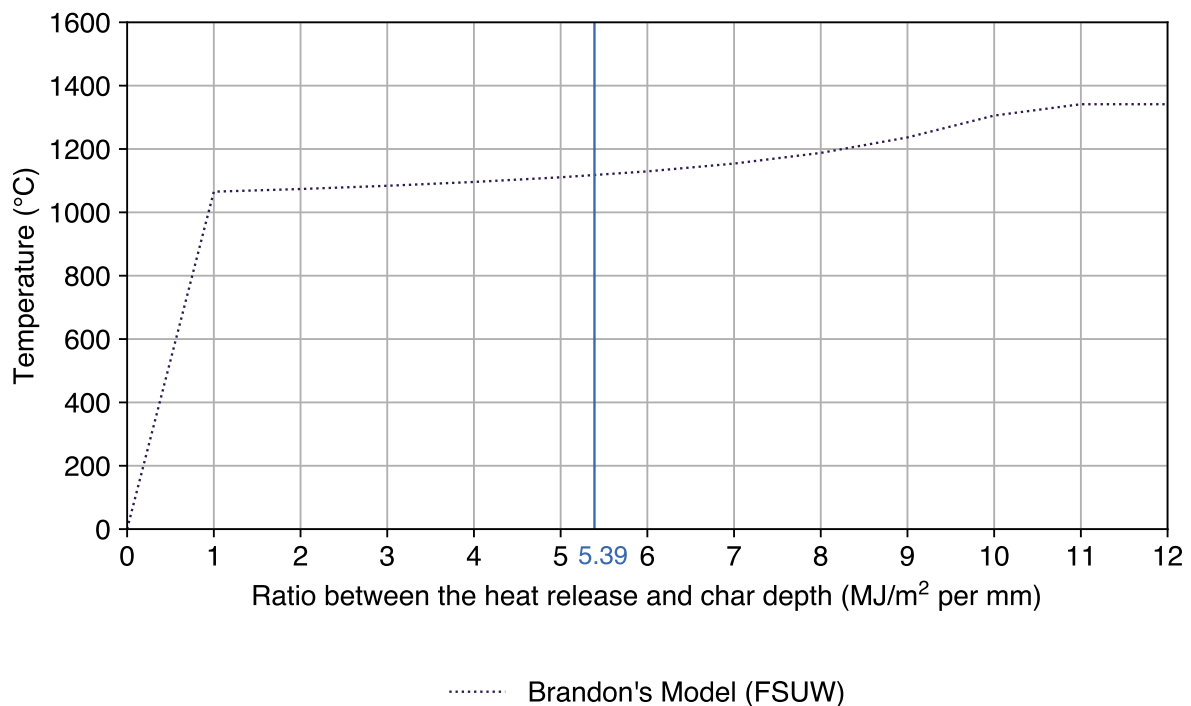
The ratio between the heat release and char depth parameter is used in the Brandon's model (FSUW). However, it is not used in the prEN 1995-1-2:20YY and in the combined model (DIN EN 1991-1-2/NA:2015-09 + cumulative temperature charring model).

The effect of this parameter on the char depth prediction can be seen in the Figure 3.10. The suggested value of 5.39 MJ/m² per mm is also shown in the same figure. This suggested value is experimentally determined by Schmid *et al.* (2016). This was derived from cone calorimeter experiments at an irradiance of 75 kW/m² flux for char depths exceeding 10 mm.

When the ratio becomes higher than 11 MJ/m² per mm, it is predicted that the auto-extinction will not occur. That is why the char depth prediction for the region after 11 does not exist.

However, for the ratio smaller than this limit, it is seen that as the ratio augments the char depth also augments. The reason behind this is can be seen by inspecting the Equation 2.2.7 which gives the $q_{t,d}$ value. This $q_{t,d}$ value is used in calculation of t_0 which is used in char depth calculation, Equation 2.2.5.

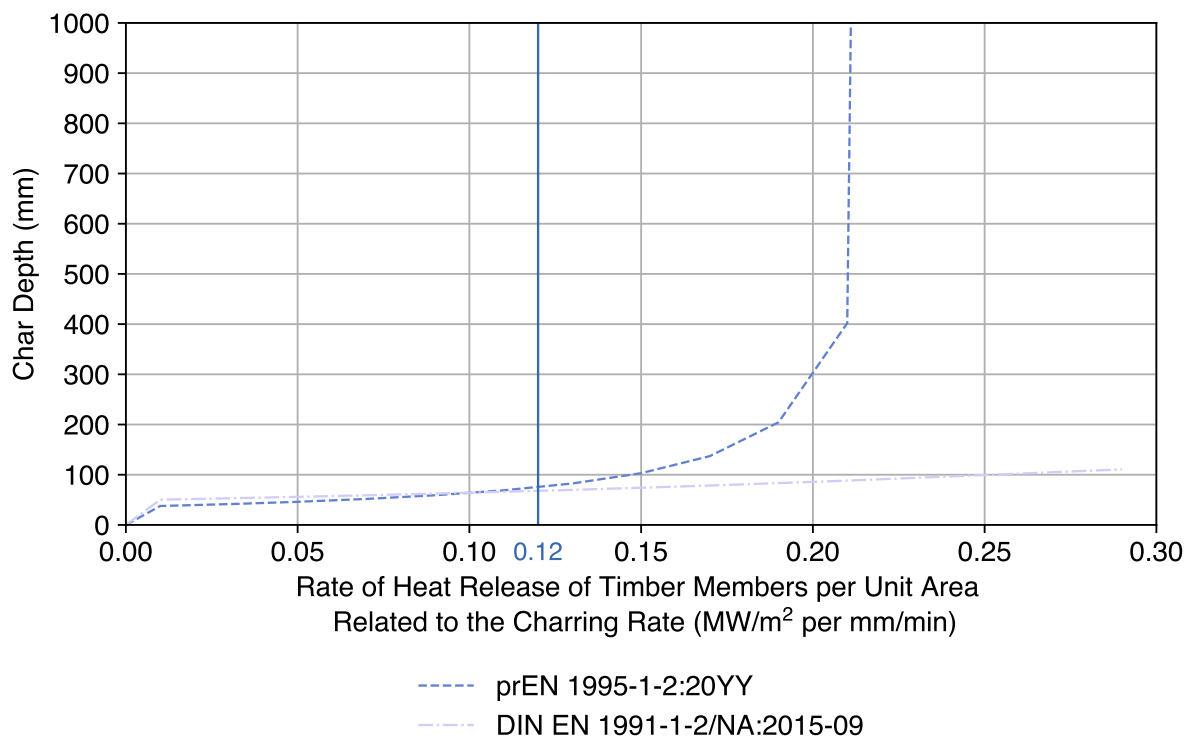
Figure 3.11: Sensitivity Analysis of Ratio Between the Heat Release and Char Depth on Maximum Temperature



As the char depth and temperature depends on each other, the same behaviour is seen in the temperature in Figure 3.11. As the ratio augments the temperature also augments.

3.5.4 Rate of Heat Release of Timber Members per Unit Area Related to the Charring Rate

Figure 3.12: Sensitivity Analysis of Rate of Heat Release of Timber Members per Unit Area Related to the Charring Rate on Char Depth



The rate of heat release of timber members per unit area related to the charring rate parameter is used in the prEN 1995-1-2:20YY and in the combined model (DIN EN 1991-1-2/NA:2015-09 + cumulative temperature charring model) which use Equation 2.2.13. However, it is not used in the Brandon's model (FSUW).

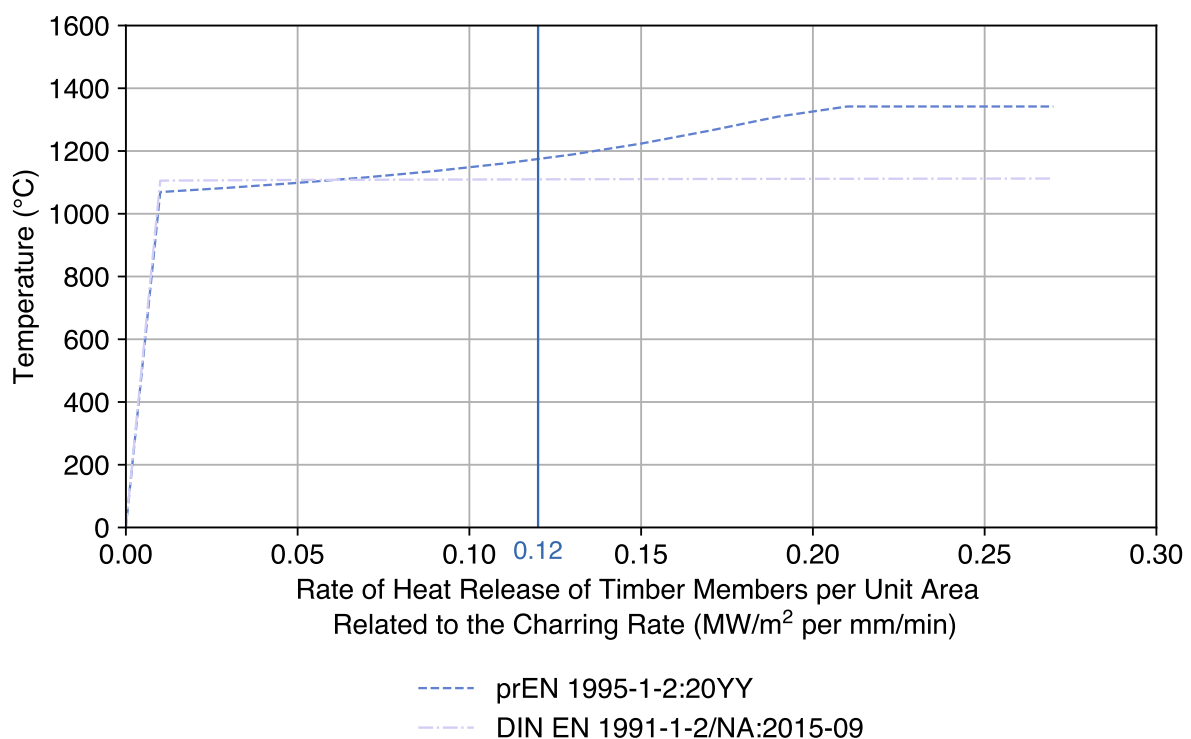
The effect of this parameter on the char depth prediction can be seen in the Figure 3.12. The suggested value of 0.12 MW/m² per mm/min is also shown in the same figure.

The rate of heat release of timber members per unit area related to the charring rate parameter effects the prEN 1995-1-2:20YY more than the combined model. Because the combined model uses this parameter only to convert the calculated char depth to structural fuel load. Then it uses this additional fuel load to calculate the temperature curve by using German National Annex, later the model uses this new temperature

curve to calculate the char depth again by using the cumulative temperature charring model. So the effect of the rate of heat release of timber members per unit area related to the charring rate, is an indirect effect.

However, for the prEN 1995-1-2:20YY model uses the additional structural fuel load in a more direct way. This discussion can be more easily understood if the process of predictions for these models are inspected by step by step.

Figure 3.13: Sensitivity Analysis of Rate of Heat Release of Timber Members per Unit Area Related to the Charring Rate on Maximum Temperature



As the char depth and temperature depends on each other, the same behaviour is seen in the temperature in Figure 3.13. As the ratio augments the temperature also augments for prEN 1995-1-2:20YY. However for the combined model the temperature stays nearly constant after around the value of 0.01 for this parameter. This can be explained by the equations used to create the temperature curve in the German National Annex.

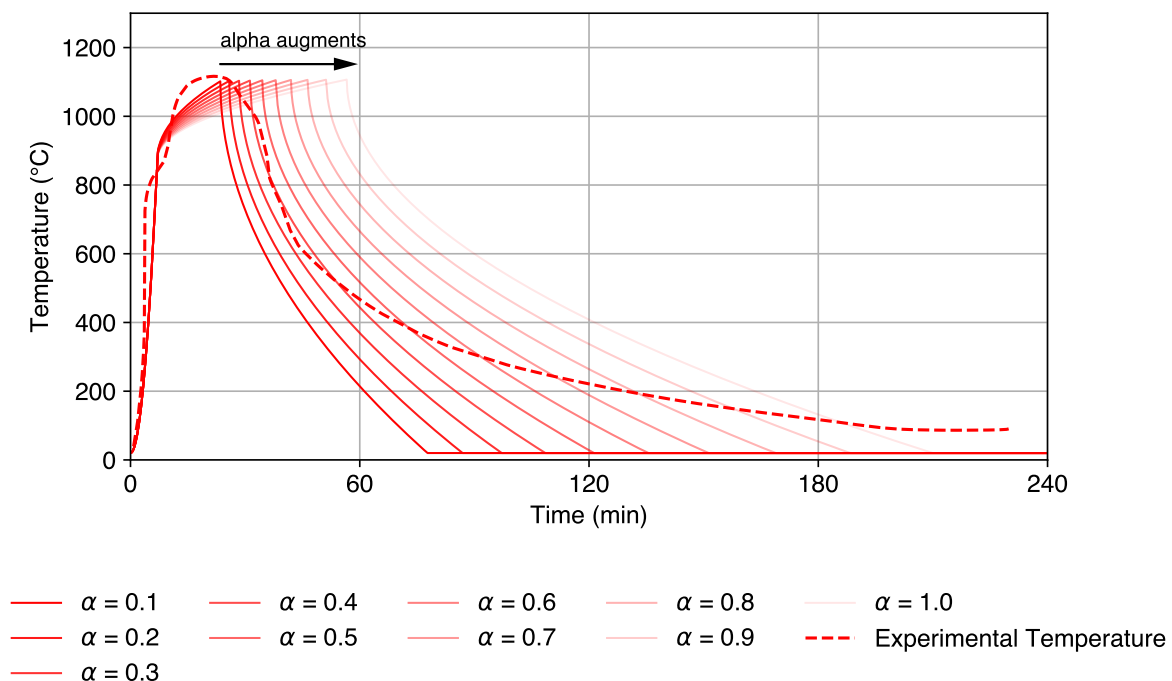
3.6 Time dependent modification factor (α) Analysis

Time dependent modification factor is an important parameter in charring models. Unlike other parameters, such as the "Rate of Heat Release of Timber Members per Unit Area Related to the Charring Rate", time dependent modification factor changes according to the phase of fire and therefore over time. This is where the "time dependent" part of the name comes from.

In order to examine the effects of different α values on the predictions, an α analysis is conducted where the temperature predictions for α values ranging from 0.1 to 1.0 are plotted over time. For this study the combined model is used as temperature-time curve is more easily modified in the DIN EN 1991-1-2/NA compared to EN 1991-1-2.

In the graphs below it can be seen that as the α value augments the position of the peak temperature shifts to right. This means that for a greater α value the time to reach maximum temperature will be greater also. Other remark from the graph is that for the growth phase all α values nearly have the same temperature predictions. However for the decay phase as the α augments the slope of the temperature curve decreases.

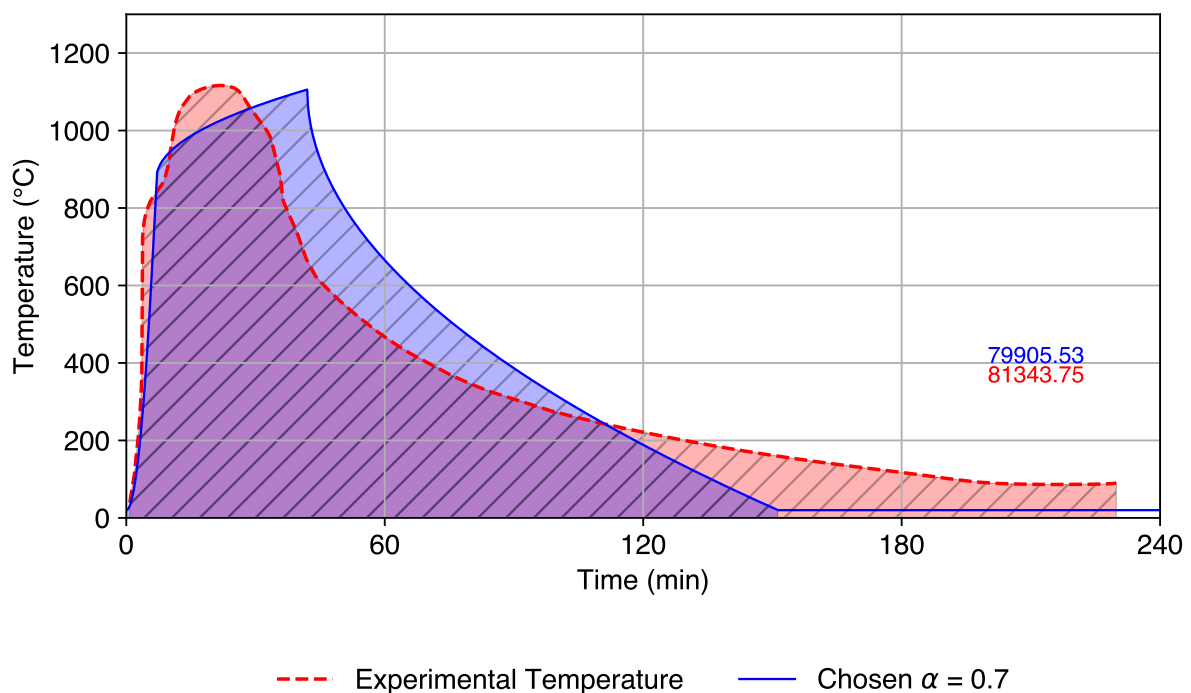
Figure 3.14: Alpha Analysis for Test 5



3.7 Choosing time dependent modification factor (α)

As it is seen in the above section, each of the α values give different predictions which shows similar behaviour. In order to choose one value for α , a study of comparing areas under curves is done. The motivation behind this study is to compare the energy release for each case. The areas are calculated for the part of the curve which is above 20 °C (Ambient temperature). The area under each α curve is compared with the area under the curve of experimental measurement. Then the α value which gives the closest result is chosen. The issue with this method is that it does not take into account the time required to reach the peak temperature. Thus, the α value will be chosen solely based on the area under the curve. Note that for this selection process the experimental temperature-time curve is needed. However the purpose of prediction model is to predict the temperature and therefore the char depth without doing an actual experiment. Due to this an α value which will cover the entire selection of tests will be determined and this α will be suggested as an input parameter for the prediction model. The results are shown in the Figure 3.15 below where the areas under curves are hatched and the values for these areas are shown on the right side of the curves. The chosen α value can be seen on the legend of the graph.

Figure 3.15: Choosing Alpha for Test 5

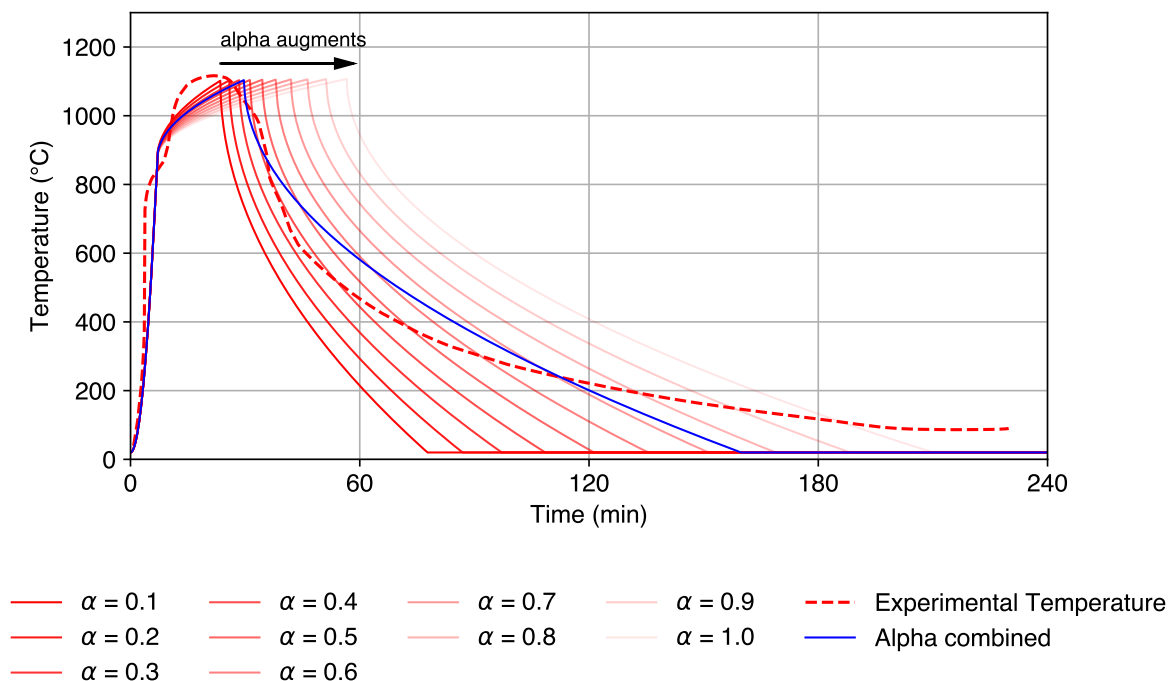


3.8 Using two time dependent modification factors (α)

As stated in above section the time to reach maximum temperature was not taken account of. In order to fix this issue a new method of using different α values is used. In this method, an α value is chosen for the period until the maximum temperature is reached. For the period after the maximum temperature a separate α value is chosen. After analysing the tests and predictions for each α value, the 2 α values are determined as 0.3 for the growth phase and 1.0 for the decay phase. These values are applied for each tests to see how the new predictions perform compared to experimental measurements.

The results can be seen in the graphs below where the predicted temperature - time curve for new method plotted against the older predictions which use only one α value for the entire time period. As it can be seen that there is an overall conformity between the predicted and experimental time to reach maximum temperature. Also for the decay phase the predicted curve performs well.

Figure 3.16: Combined Alpha Method for Test 5



3.9 Two time dependent modification factors (α) comparison

To compare the predictions of combined α 's method with experimental measurements, the previously used process of comparing areas under the curves has been chosen. The difference between the area under the predicted curve and the area under the experimental curve in the two α method is similar to that in the one α method. However, the two α method provides a better prediction of the time required to reach the maximum temperature.

Figure 3.17: Combined Alpha Method for Test 5

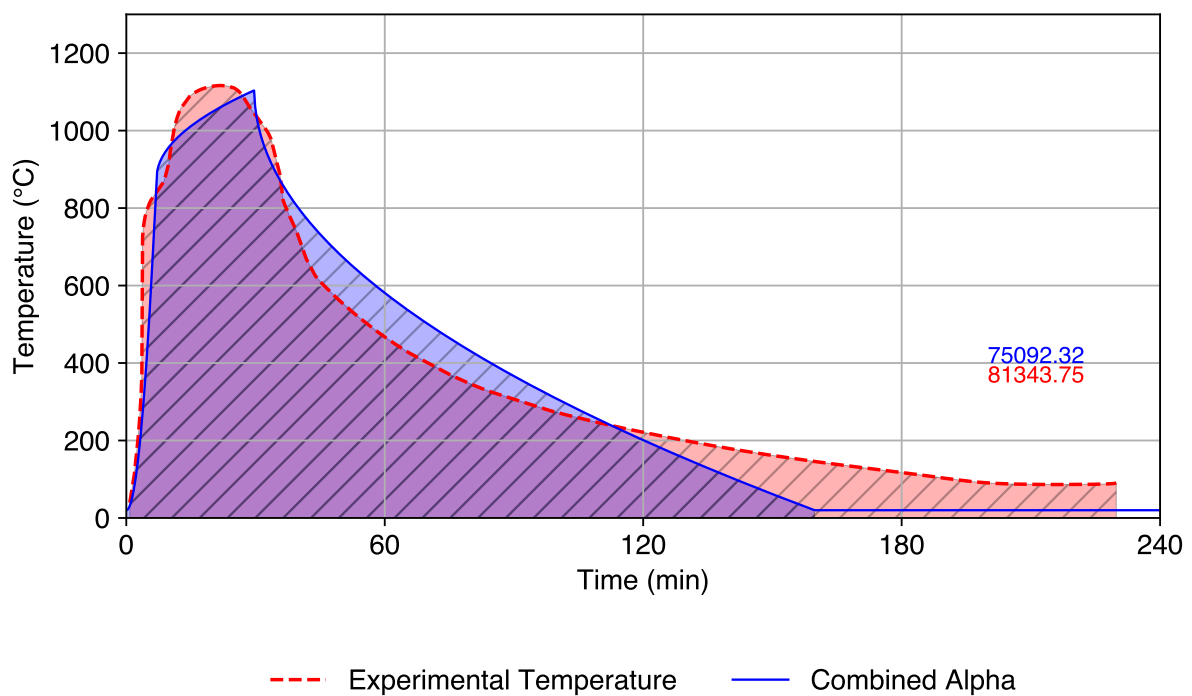
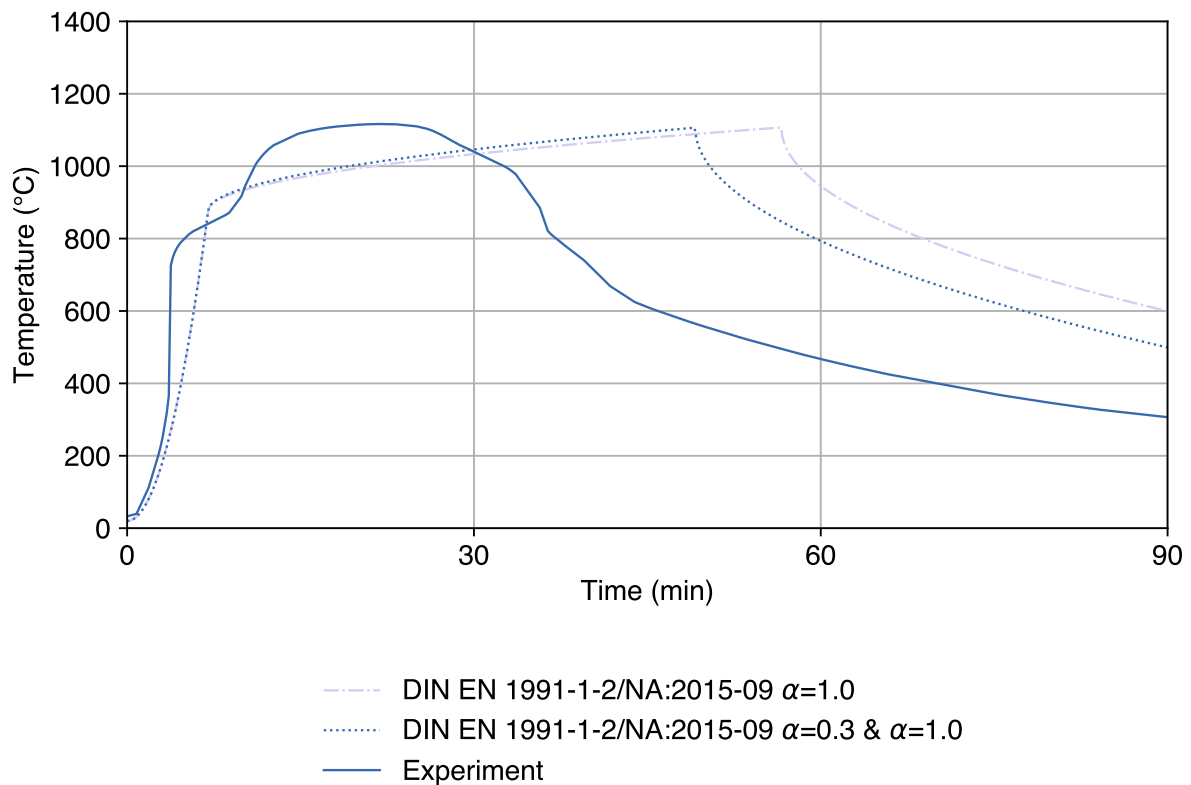


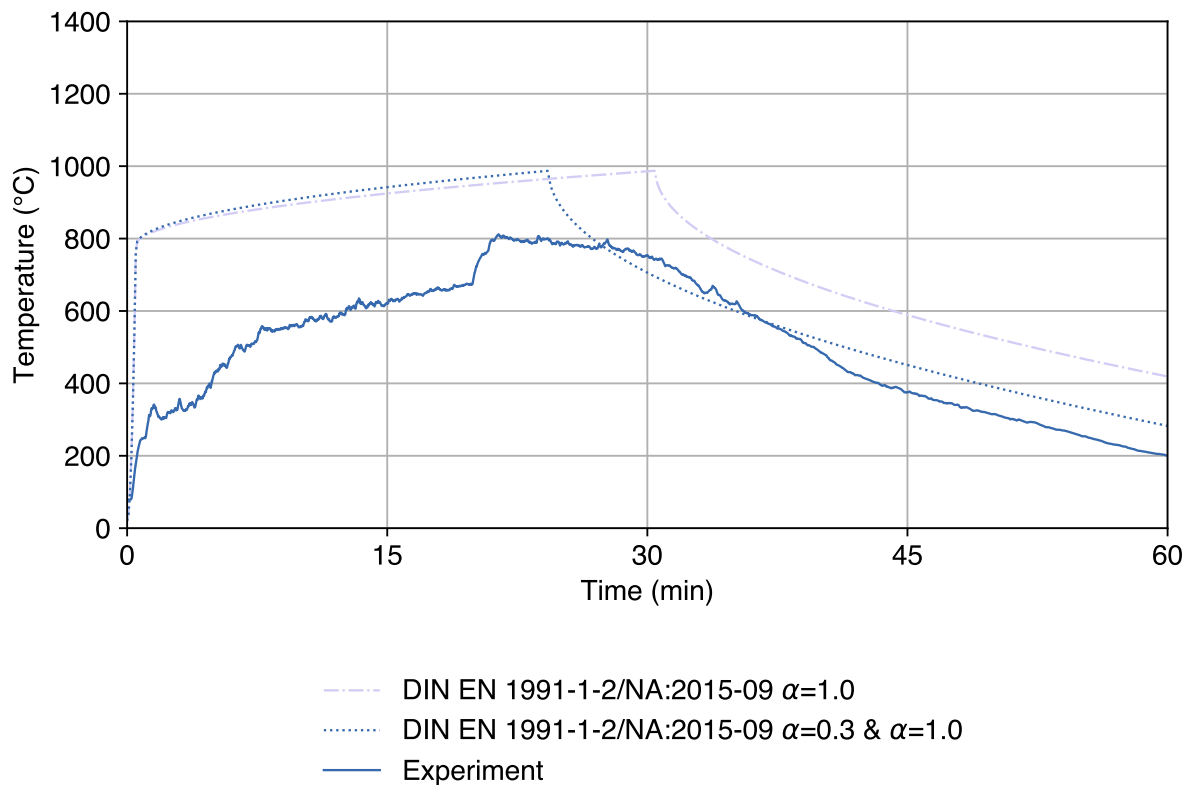
Figure 3.18: Temperatures for two time dependent modification factor for Test 5



The difference in peaks are caused by having different $q_{x,d}$ values which are calculated by using total fuel load which is predicted by using char depth. In the updated version which has two time dependent modification factors (α), the value of $q_{x,d}$ is smaller than the one in previous version which has only one time dependent modification factor (α).

The reason is that the predicted char depth is smaller when two time dependent modification factors (α) are used. This is caused by having lower time dependent modification factor (α) for the decay phase which leads to less efficient conversion of char depth to additional fuel load.

Figure 3.19: Temperatures for two time dependent modification factor for Test C9

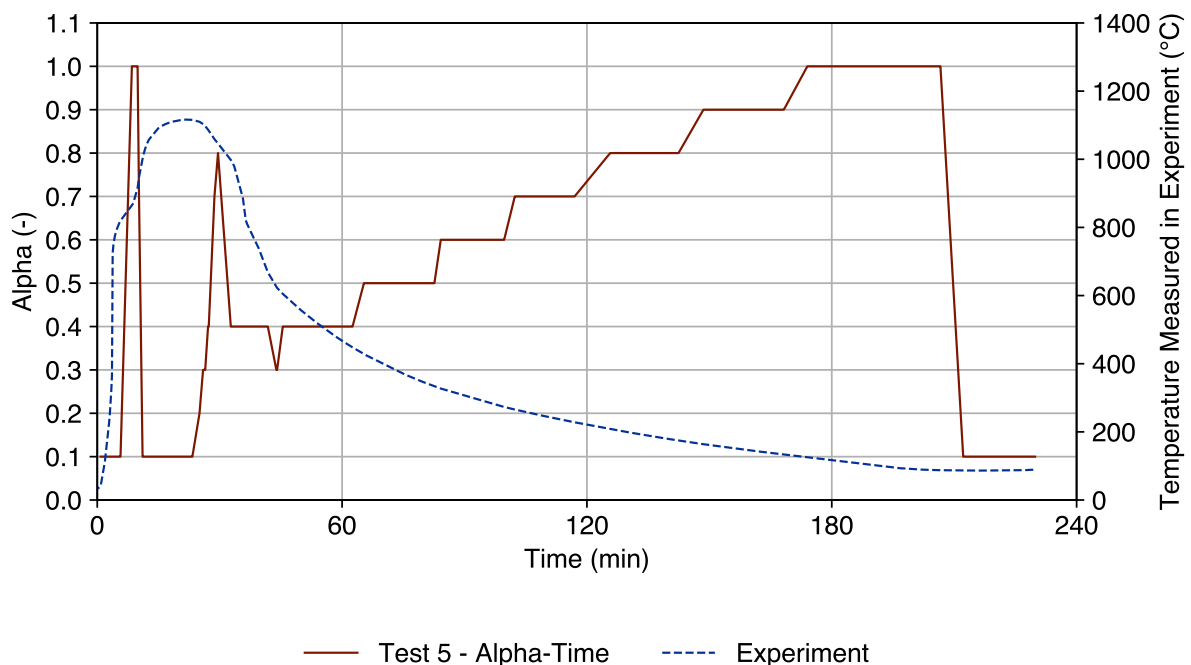


The same discussion of having different $q_{x,d}$ values applies for ETH Zurich Test C9. The comparison can be seen above in Figure 3.19.

3.10 Creating time dependent modification factor (α) - Time Graphs

As it has been seen that using two α values are reasonably better than using only one alpha, the next step is using more than two α 's. In this section a α -time curve is created by using a process where α value is calculated for each time step. This calculation is done by selecting the α value which gives the closest prediction compared to the experimental temperature for that time step. As the α values are calculated from 0.1 to 1.0 the resulting graphs are rather coarse.

Figure 3.20: Alpha - Time Graph for Test 5



It can be seen that the α value reaches to peak value of 1.0 two times, one before the maximum temperature is reached and the other after the maximum temperature is reached. In order to explain this phenomenon the meaning of α should be inspected. α factor is used to take account of energy stored in char layer and the efficiency of char layer's combustion. For a higher α value the char combusts more compared to a case where the α value is low.

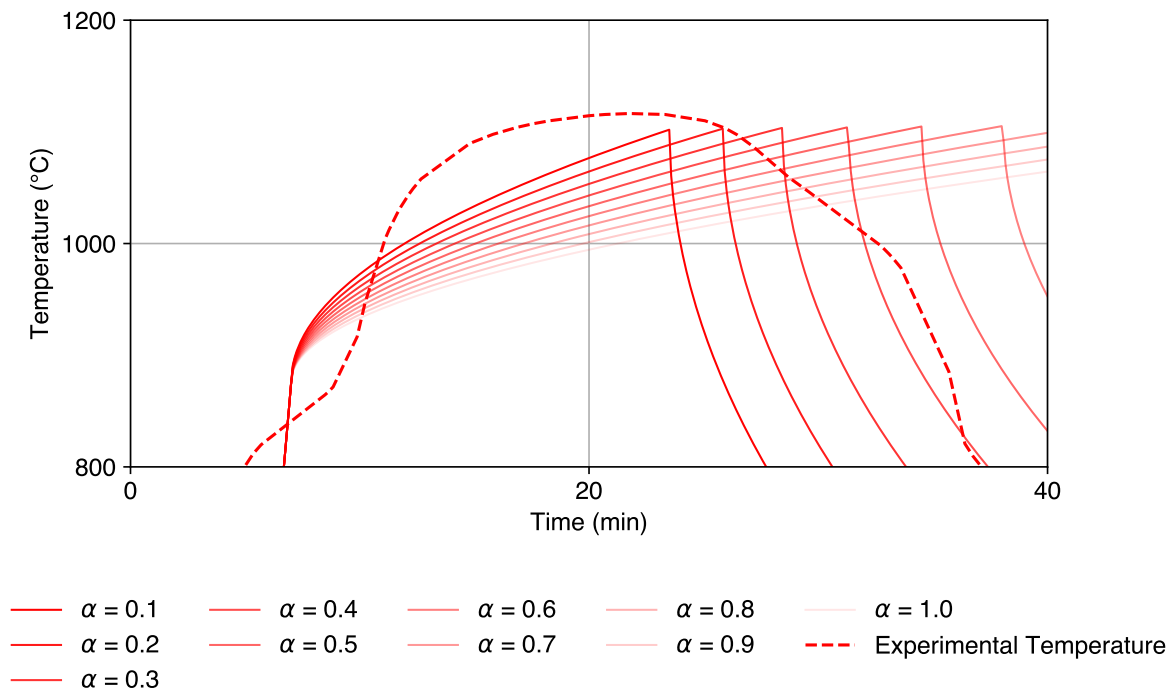
For example in the growth phase of a ventilation controlled fire the expected value for α is lower, as the oxygen in the compartment will not be enough to combust the char layer efficiently. However in the decay phase where the oxygen content gets higher again, the α value gets higher also as the energy stored in char gets released by combustion.

In the Figure 3.20, it can be seen that α value augments as the decay phase progresses. This can be explained by the discussion above. Note that normally α should be zero when the fire extincts, but as the α value of 0 is not defined previously the closest value which is 0.1 is taken for that period.

The peaks of α value that occur in the same figure can be explained by the movable fire load. The experimental temperature curve takes account of both the movable fire load and the structural fire load coming from the combustion of the timber boundaries of the compartment. However α value is defined to deal with only the latter part. So when the α is chosen by using the experimental temperature curve, it tends to be higher than expected. If the temperature curve for structural fire load was available and was used, the α curve will not had this peak in the growth phase.

The other reason of these peaks is the method used to select the α , the α is chosen by comparing the temperature predictions given by α and the experimental temperature measurement. However if Figure 3.21 inspected it can be seen for the location of first peak, the α 1.0 (the curve located at the bottom of the curve bundle) gives closest result. The second peak which occurs in the early stage of decay phase can be explained in the same way, as the curves cross each other their order according to the distance to the experimental temperature curve changes.

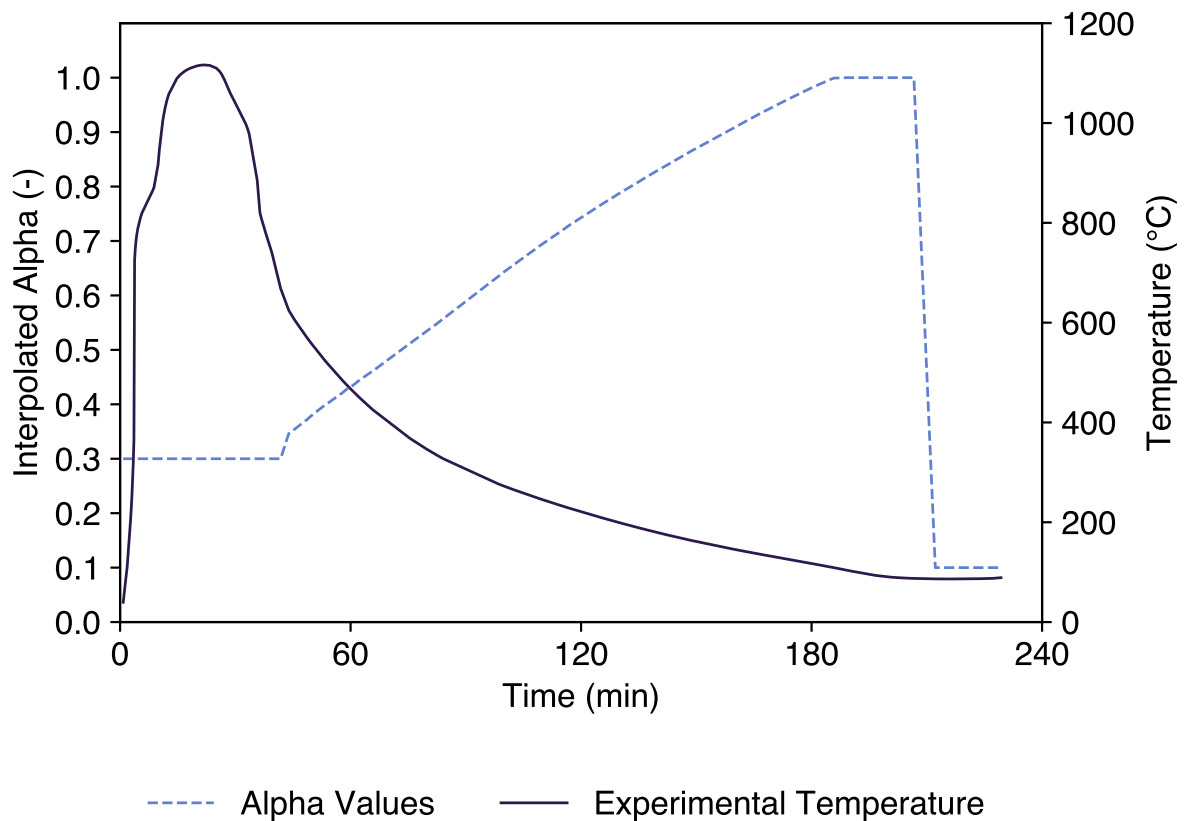
Figure 3.21: Alpha - Time Graph Zoomed for Test 5



In order to make the α -time curve smoother an interpolation process is applied. Also to take account of the problem of peaks mentioned previously, α is taken as a fixed value of 0.3 for the time period from the start of fire to the $1.5 \times$ the time to reach the maximum temperature.

The resulting α -time curve can be seen in the Figure 3.22.

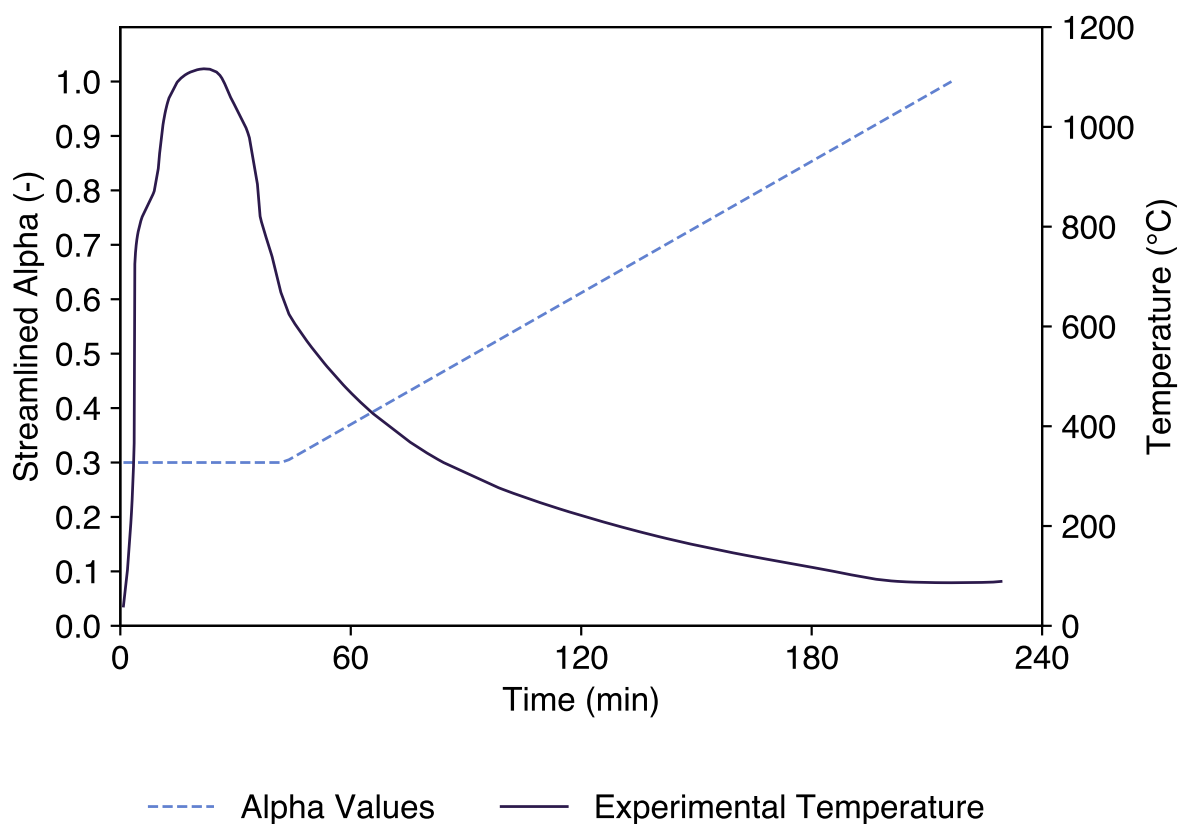
Figure 3.22: Alpha - Time Graph for Test 5



Note that using more than two α values to create a temperature-time curve by using the combined model is not possible as the DIN EN 1991-1-2/NA does not permit to use more than one α for decay phase. (For more information please review DIN EN 1991-1-2/NA Appendix AA) However, if it would be possible to define as many as α , then it would be possible to use these α -time curves and predict the temperature curve which fits very well to the experimental temperature curve.

But the experimental temperature measurement is still required for doing this. So in order to predict the temperature without having an experimental temperature measurement, a fixed α -time curve which can be used is created as seen in Figure 3.23 below. The first part has fixed value for α as 0.3 from the start of fire to the 1.5 \times the time required to reach maximum temperature. The second part is a straight line from 0.3 to 1.0. Note that this curve is produced by using the experimental data available, if more experiments are used this curve could be better.

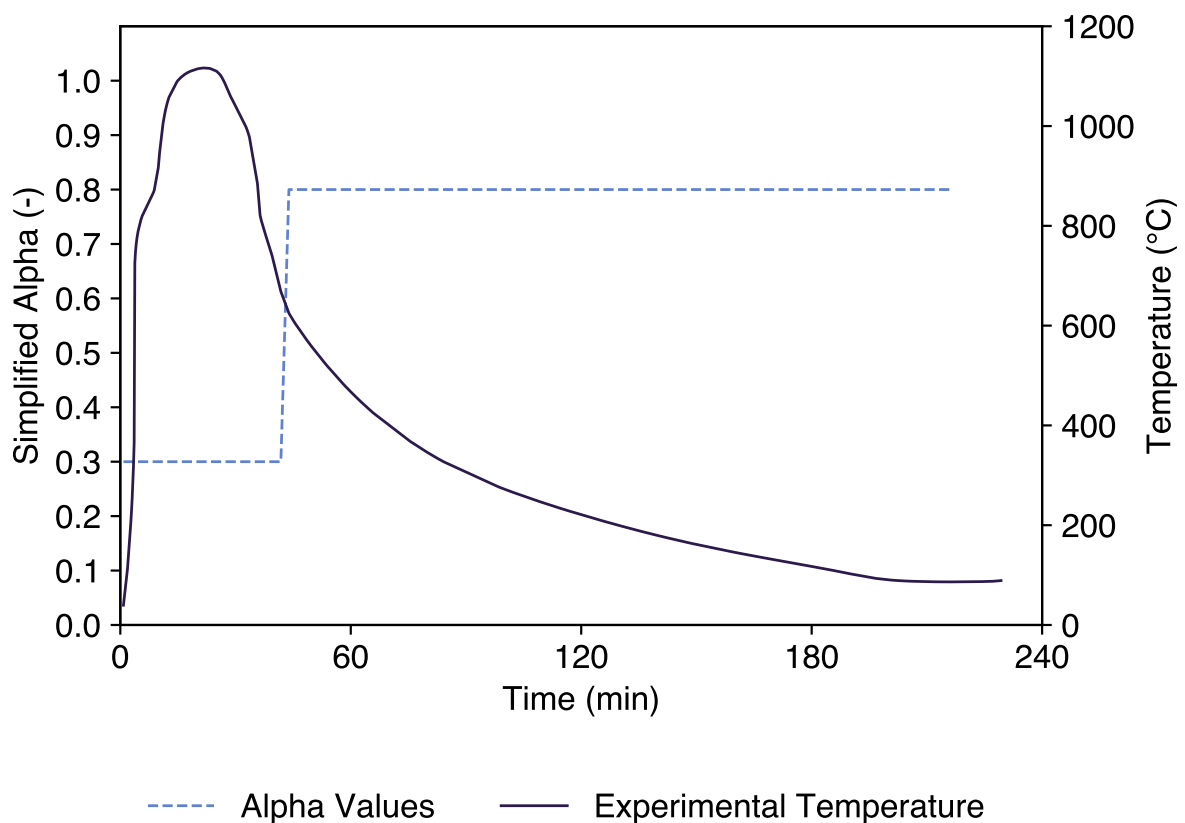
Figure 3.23: Streamlined Alpha - Time Graph for Test 5



As a last step this curve is simplified to make it possible to be used in combined model which uses DIN EN 1991-1-2/NA. The simplified plot has two time dependent modification factors (α) as seen in Figure 3.24 below.

This plot's first segment which has α as 0.3 is defined from the start of fire to the $1.5 \times$ the time required to reach maximum temperature.

Figure 3.24: Simplified Alpha - Time Graph for Test 5



4 Conclusion

In this thesis, charring models of timber have been inspected and three of them are chosen for comparison. Those are the Brandon's model (FSUW book), Eurocode Model (prEN 1995-1-2:20YY + EN 1991-1-2) and Combined Model (Cumulative temperature charring model (prEN 1995-1-2:20YY) + DIN EN 1991-1-2/NA). The discussed combined model does not exist in current codes, it is a combination of two different codes. The creation of this new method is inspired by the parametric temperature curve of German National Annex to EN 1991-1-2 (DIN EN 1991-1-2/NA). Because this parametric temperature curve's equations are defined more detailed compared to the ones for the EN 1991-1-2's parametric temperature curve. Especially the decay phase is defined by an equation which creates a curve instead of a line. However the EN 1991-1-2's parametric temperature curve's decay phase is defined by a set of equations which give lines with different slopes. Also the parametric temperature curve of German National Annex to EN 1991-1-2 (DIN EN 1991-1-2/NA) allows to define two time dependent modification factors. This is used to create a new version of the combined model.

The comparison is made by using three sets of experimental data which are from FSUW book, RISE research paper and compartment tests conducted in ETH Zurich. First two sets are conducted on full scale compartments, the latter one conducted in small scale compartments. The models' predicted values for compartment temperature and char depth at the end of the fire are compared with the ones measured in the experiments. Also a sensitivity analysis is done to see the effect of selected parameters such as combustion factor and time dependent modification factor (α). It is seen that the effect of the time dependent modification factor is important as it changes the shape of temperature curve in the decay phase. Further modifications with this parameter are decided to be done.

A new method of using two different time dependent modification factors for the combined model is created. In this new version, for the first part of the fire (defined by $1.5 \times$ [the time required to reach maximum temperature]), the different time dependent modification factor is set to be constant 0.3. This small value relates with the high amount of energy stored in the char which is caused by the low oxygen content in the compartment. But as the fire starts to decay more oxygen becomes available inside the compartment and therefore char can combust more efficiently. But this does not happen instantly after the decay starts, there is a required time for the oxygen content to get higher. The 1.5 factor that used to define the 0.3 time dependent modification factor (α) region decided according to this extra time. For the rest of the duration of fire the time dependent modification factor is set to be 1.0 which dictates that the char combust very efficiently.

This new version of the combined model is compared with the older version which uses only one (α) value for entire duration of fire. The results suggest that using the updated version of combined model which has two α values gives closer predictions to the experimental measurements. The predictions are close to the mean of the experimental measurements. This is the outcome that is decided why creating this model in this thesis. A safety factor can be added to these predictions according to the specifications of the design case such as the purpose of the building and the number of the occupants. However, further study with different compartment tests can be useful to get more precise results to decide on these safety factors. This model has a potential to be used in the practice of timber building sector.

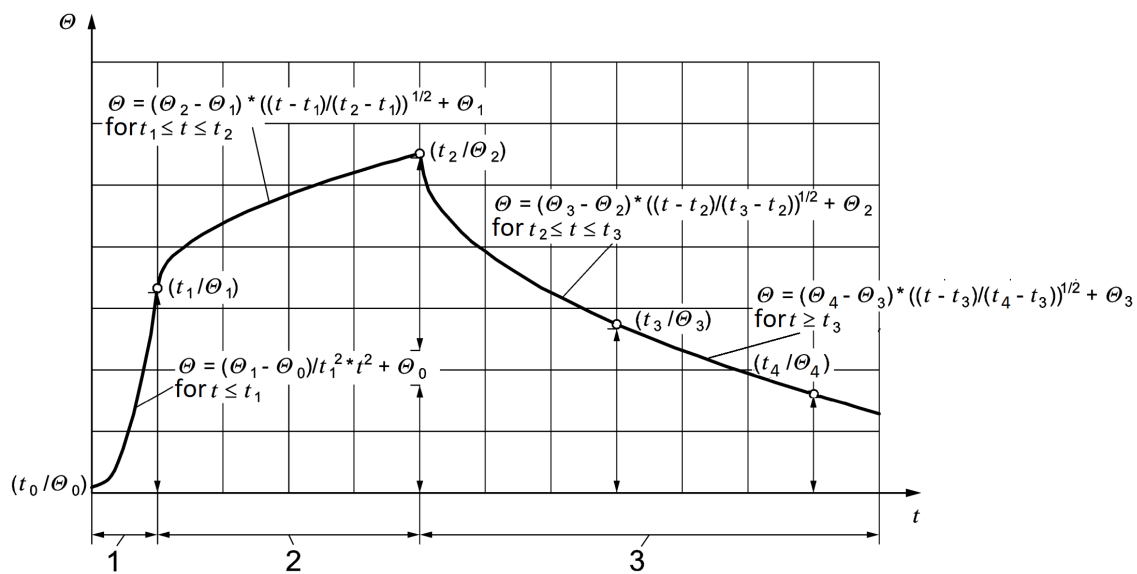
In conclusion, this thesis examines, analyses, and compares current charring models for timber which are used in practice, with the goal of enhancing understanding in this field. A novel approach, referred to as the 'Combined Model,' is developed and later refined following comprehensive sensitivity analyses. This updated version of the Combined Model shows promising potential.

4.1 Recommendations for future work

The discussed multiple time dependent modification factor (α) for the combined model would be an interesting topic to further improve. The author of this thesis is optimistic and anticipates that the proposed future work will bring about significant advancements in this area of study.

In order to do this an additional point can be added to the decay part of the temperature curve as point 4 which is defined by t_4 and Θ_4 . The proposed updated version of the temperature curve can be seen in Figure 4.1.

Figure 4.1: Schematic representation of proposed updated version of the temperature-time curve according to the simplified natural fire model with the points (t_i, Θ_i) described by equations and the curve segments in between



A third value of time dependent modification factor (α) can be assigned to the added part which is after the point 3 which is defined by t_3 and Θ_3 . So now instead of one α value for growth and one α value for decay, the model has one α value for growth phase and two α values for the decay phase.

To create the point 4, the t_4 and Θ_4 values should be determined. This can be done by using the experimental data. Given that the equations for the newly added part are the same as those of the previous part, it is anticipated that an analysis for the time dependent modification factor (α) will suffice to determine the values necessary for locating point 4.

Once the updated model incorporating the 4th point is established, additional points could be introduced to the decay phase. This improvement aims to refine the temperature curve during the decay phase further. There's no necessity to incorporate additional points into the growth phase. This is because assuming a constant value for α has shown to yield satisfactory results for the growth phase of the model.

5 Bibliography

- Abed, J., S. Rayburg, J. Rodwell and M. Neave (2022) A review of the performance and benefits of mass timber as an alternative to concrete and steel for improving the sustainability of structures, *Sustainability*, **14**, 5570.
- Barber, D., L. Sieverts, R. Dixon and J. Alston (2018) A methodology for quantifying fire resistance of exposed structural mass timber elements, paper presented at the *Proceedings of the 10th International Conference on Structures in Fire*, 217–224, Belfast, UK.
- Brandon, D. (2018a) Engineering methods for structural fire design of wood buildings structural integrity during a full natural fire, *Technical Report*, **RISE Report No. 2018:44**, RISE Research Institutes of Sweden, Stockholm.
- Brandon, D. (2018b) Fire safety challenges of tall wood buildings phase 2: Task 4 engineering methods, *Technical Report*, **Report No. FRPF-2018-04**, Fire Protection Research Foundation, Quincy, MA.
- Brandon, D. and R. RISE (2018) Fire safety challenges of tall wood buildings - phase 2: Task 4 - engineering methods, *Technical Report*, Fire Protection Research Foundation, Quincy, MA, March 2018.
- Brandon, D., J. Sjostrom, A. Temple, E. Hallberg and F. Kahl (2021) Fire safe implementation of visible mass timber in tall buildings—compartment fire testing, *Technical Report*, **RISE Report No. 2021:40**, Research Institutes of Sweden (RISE).
- Buchanan, A. and B. E. Ostman (2022) *Fire Safe Use of Wood in Buildings: Global Design Guide (1st ed.)*, CRC Press.
- CEN, E. C. F. S. (2002-10) En 1991-1-2 - eurocode 1: Actions on structures part 1-2: Actions on structures exposed to fire, *Technical Report*, Brussels.

- CEN, E. C. F. S. (2019-05) Timber structures - strength graded structural timber with rectangular cross section - part 1: General requirements, *Technical Report*, Brussels.
- CEN, E. C. F. S. (2023-01) Eurocode 5 design of timber structures part 1-2: Structural fire design, *Technical Report*, Brussels.
- Glauser, T., D. Nadig and D. Rubis (2021) Compartment fires, *Technical Report*, Institute of Structural Engineering (IBK), Swiss Federal Institute of Technology Zurich (ETH Zurich), Zurich, 7 2021.
- Hadvig, S. (1981) Charring of wood in building fires, *Technical Report*, Technical University of Denmark, Kongens Lyngby, Denmark.
- Horowitz, C. A. (2016) Paris agreement, *International Legal Materials*, **55** (4) 740755.
- IEA (2023) Co2 emissions in 2022, *Technical Report*, Paris. License: CC BY 4.0.
- International Organization for Standardization (2014) ISO 834-11:2014 Fire resistance tests Elements of building construction Part 11: Specific requirements for the assessment of fire protection to structural steel elements.
- Karacabeyli, E. and B. Douglas (2013) *CLT Handbook: Cross-Laminated Timber*, FPInnovations, Quebec, QC, Canada.
- Klippel, M. and Frangi, A. (2011) Einfluss des klebstoffes auf das brandverhalten von holzbauteilen, paper presented at the 17. *Internationales Holzbau-Forum IHF*, Garmisch-Partenkirchen, Germany, December 7-9 2011.
- MacLeod, C. E., A. Law and R. M. Hadden (2023) Quantifying the heat release from char oxidation in timber, *Fire Safety Journal*, **138**, 103793, ISSN 0379-7112.
- NABau, D.-N. B. (2015-09) Nationaler anhang national festgelegte parameter eurocode 1: Einwirkungen auf tragwerke teil 1-2: Allgemeine einwirkungen brandeinwirkungen auf tragwerke, *Technical Report*.
- Reid Middleton (2017) Timber construction using clt, <https://www.reidmiddleton.com/reidourblog/timber-construction-using-clt/>.

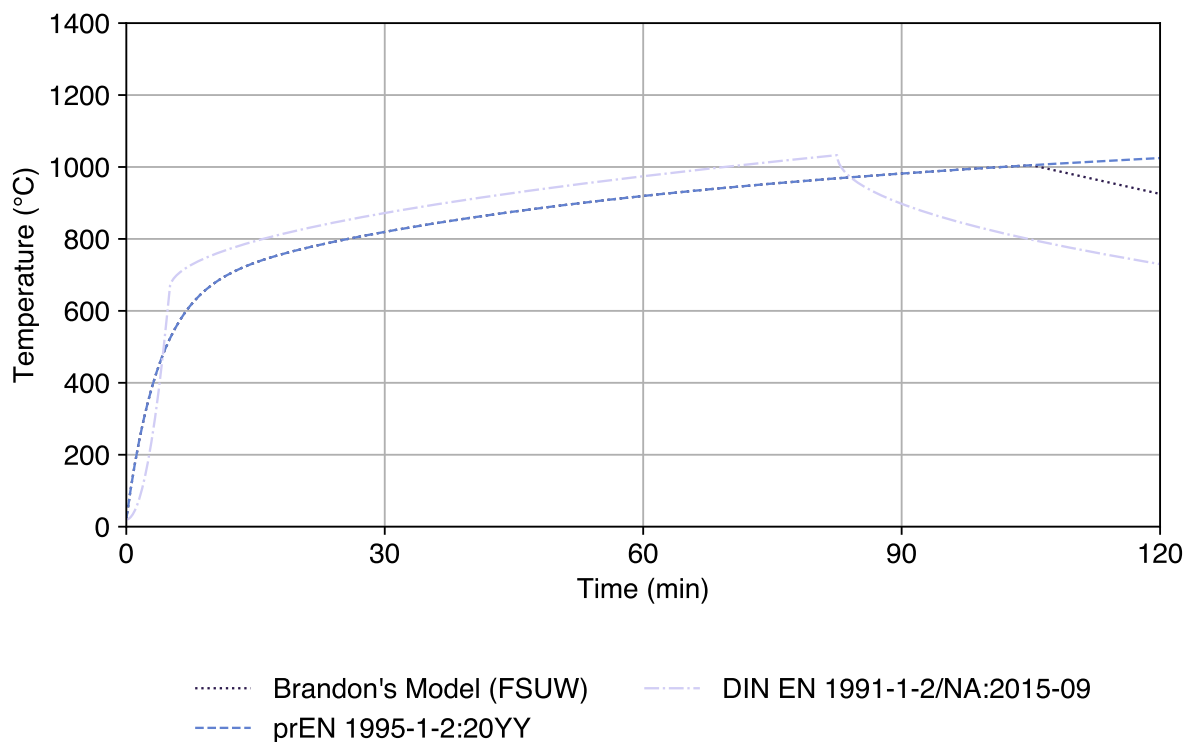
- Schmid, J., D. Brandon, A. Santomaso, U. Wickström and A. Frangi (2016) Timber under real fire conditions the influence of oxygen content and gas velocity on the charring behavior, paper presented at the *Proceedings of the 9th International Conference on Structures in Fire*, Lancaster, Pennsylvania, USA.
- Schmid, J. and A. Frangi (2021) Structural timber in compartment fires the timber charring and heat storage model, *Open Engineering*, **11**, 435–452.
- United Nations Environment Programme (2022) *2022 Global Status Report for Buildings and Construction: Towards a Zeroemission, Efficient and Resilient Buildings and Construction Sector*, UNEP, Nairobi.
- Wade, C. A. (2019) A theoretical model of fully developed fire in mass timber enclosures, Ph.D. Thesis, University of Canterbury, Department of Civil and Natural Resources Engineering, Christchurch.
- Wade, C. A., G. B. Baker, K. Frank, R. Harrison and M. J. Spearpoint (2016) B-risk 2016 user guide and technical manual, *Technical Report, Study Report No. SR364*, BRANZ, Porirua.
- Wade, C. A., D. Hopkin, J. Su, M. J. Spearpoint and C. M. Fleischmann (2019) Enclosure fire model for mass timber construction benchmarking with a kinetic pyrolysis submodel, paper presented at the *Interflam 2019: 15th International Conference on Fire Science and Engineering*, Royal Holloway College, Nr Windsor.
- Wade, C. A., M. J. Spearpoint, C. M. Fleischmann, G. B. Baker and A. K. Abu (2018) Predicting the fire dynamics of exposed timber surfaces in compartments using a two-zone model, *Fire Technology*, **54**, 893–920.

Appendix A Graphs for the Other Tests

A.1 FSUW Tests

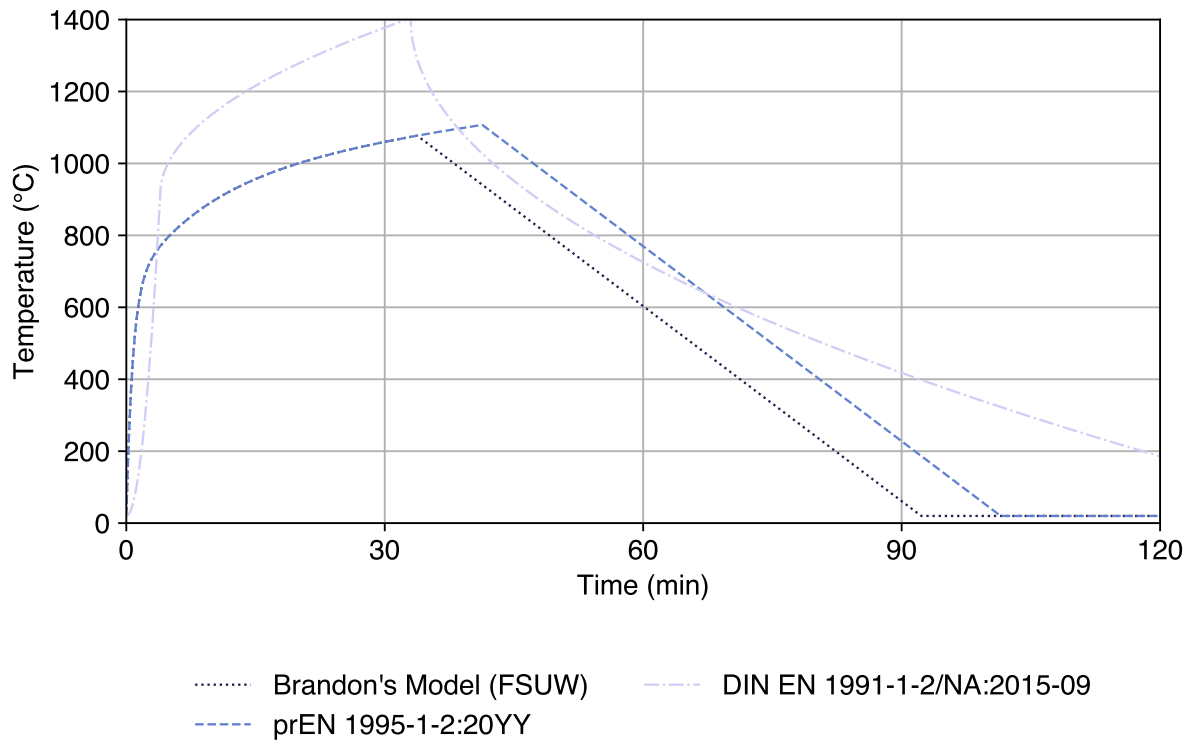
A.1.1 Test 2

Figure A.1: Temperature for Test 2



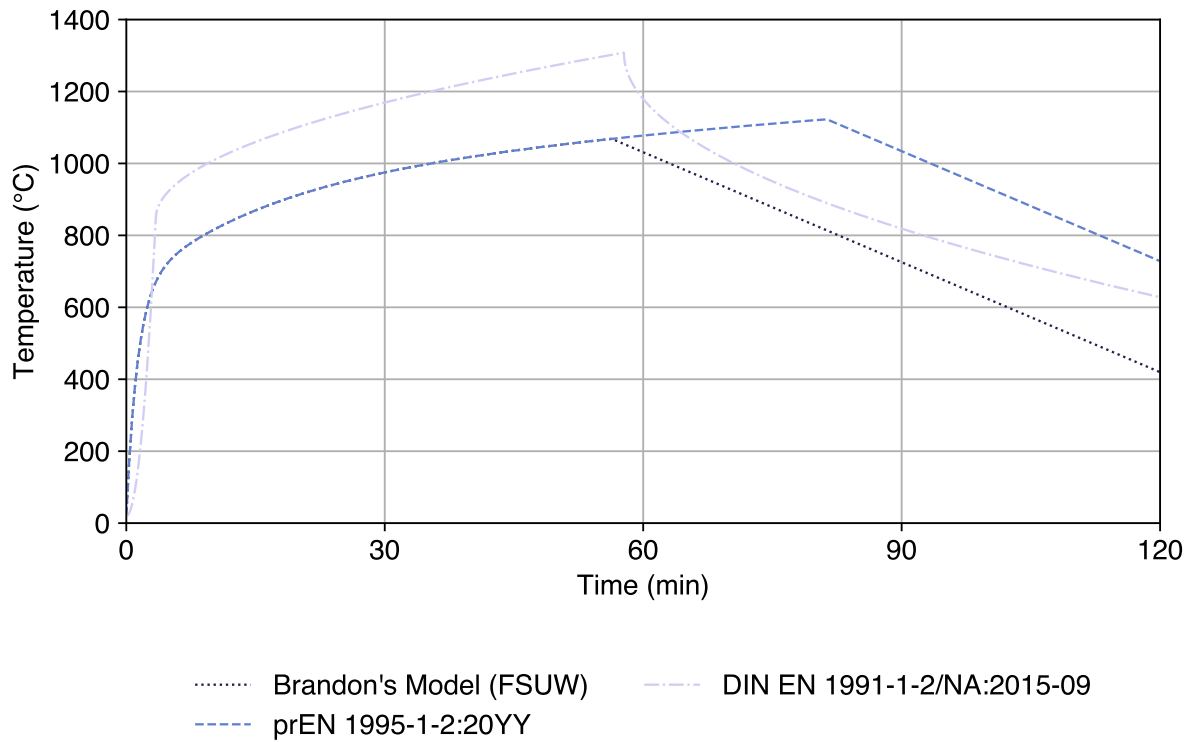
A.1.2 Test 3

Figure A.2: Temperature for Test 3



A.1.3 Test 4

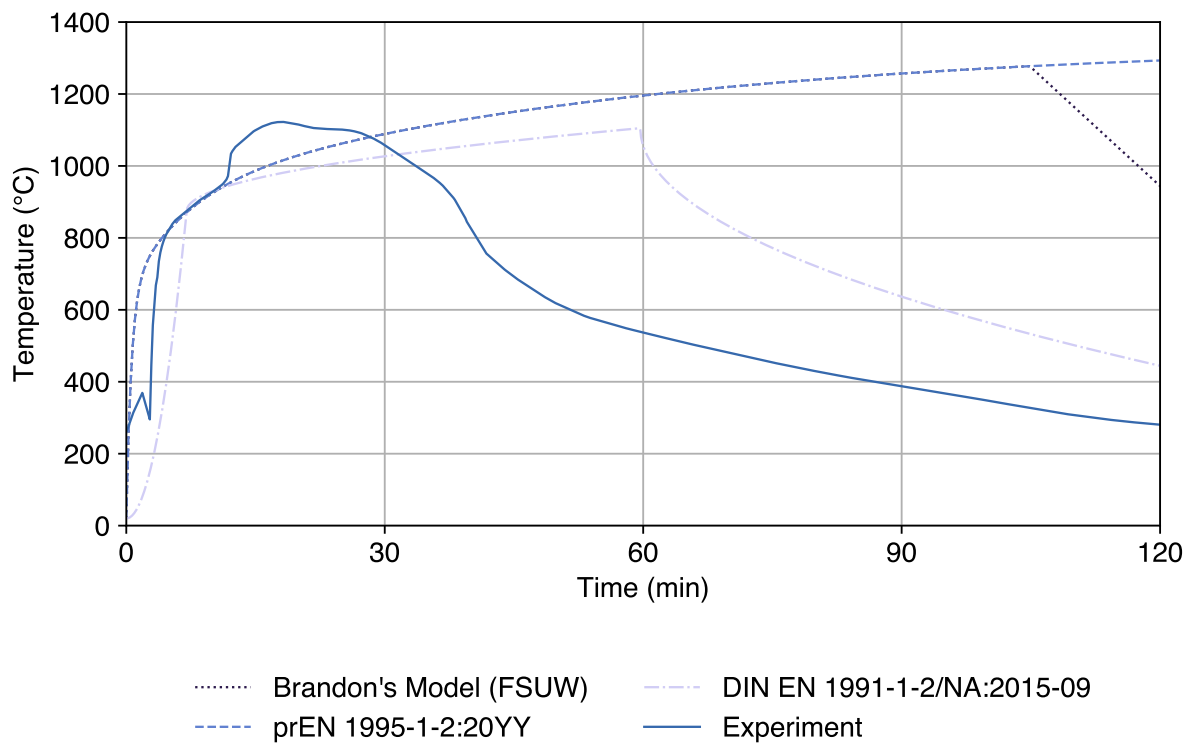
Figure A.3: Temperature for Test 4



A.2 RISE Tests

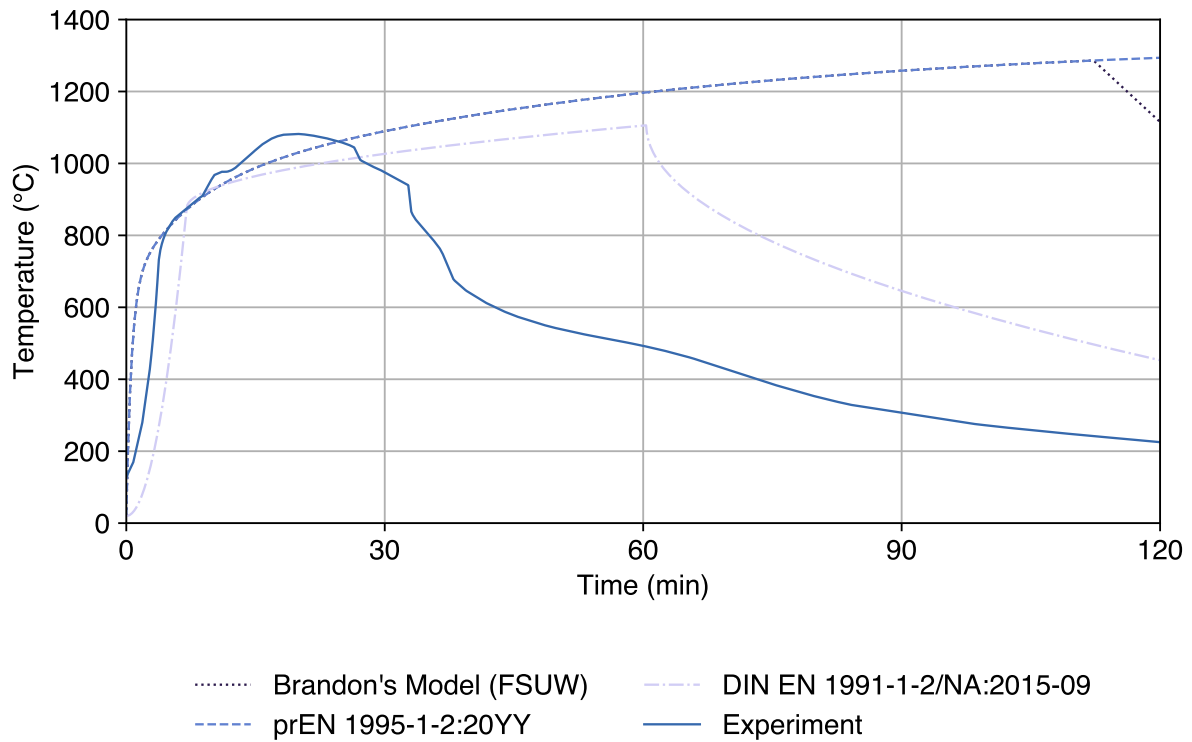
A.2.1 Test 6

Figure A.4: Temperature for Test 6



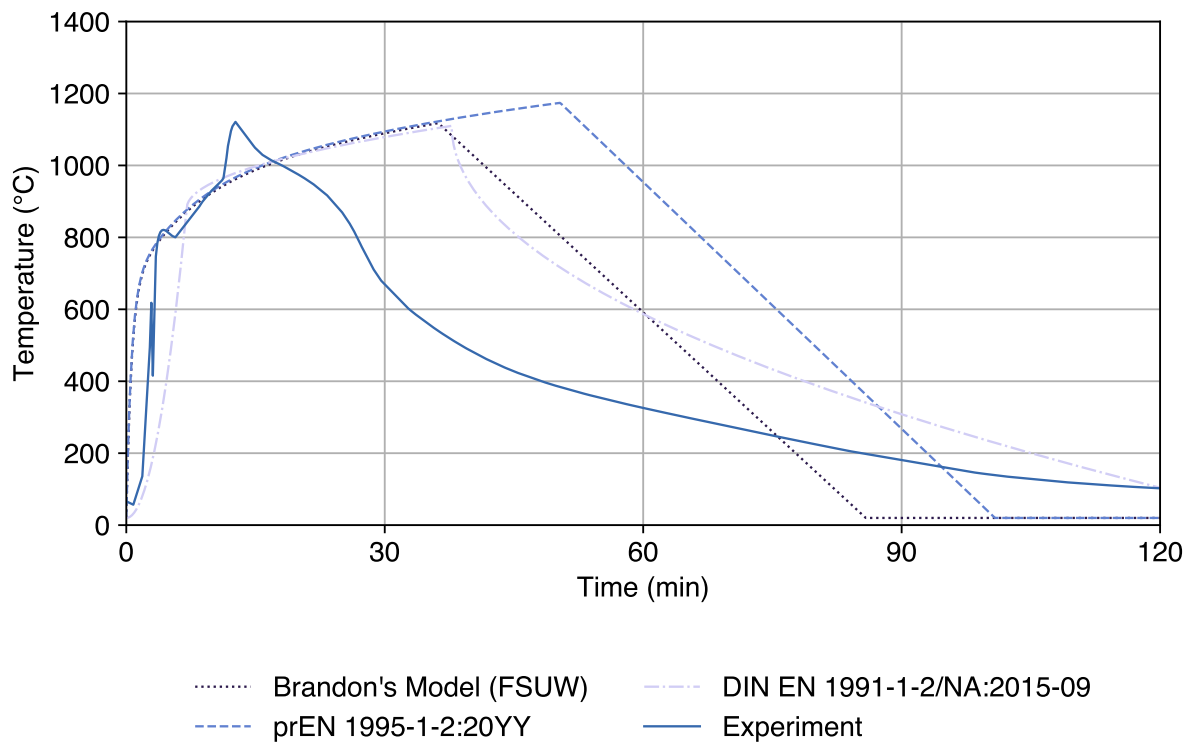
A.2.2 Test 7

Figure A.5: Temperature for Test 7



A.2.3 Test 8

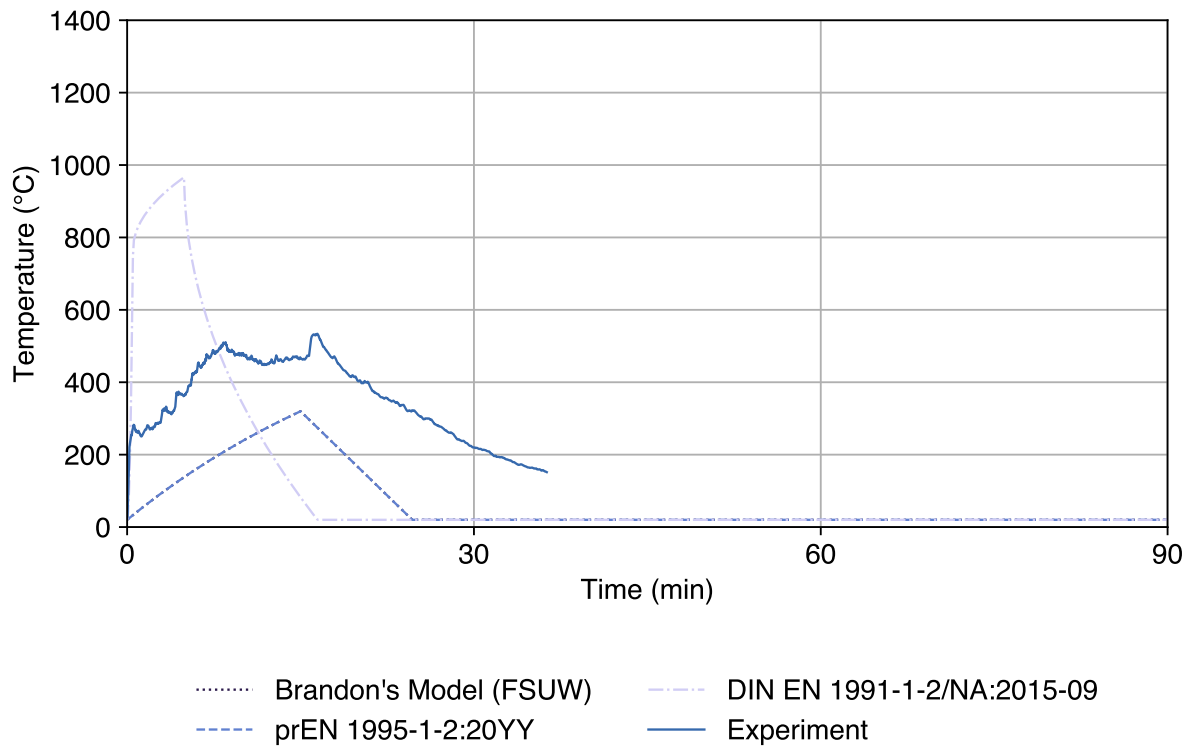
Figure A.6: Temperature for Test 8



A.3 ETH Zurich Tests

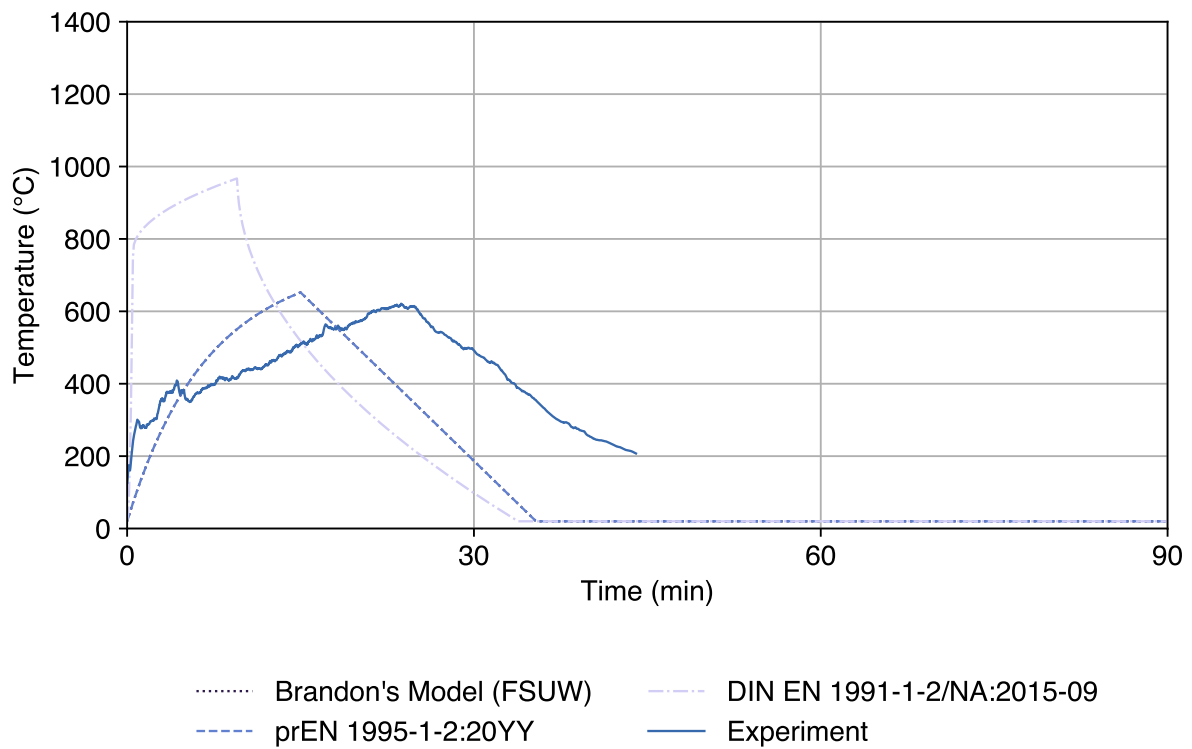
A.3.1 Test C2

Figure A.8: Temperature for Test C2



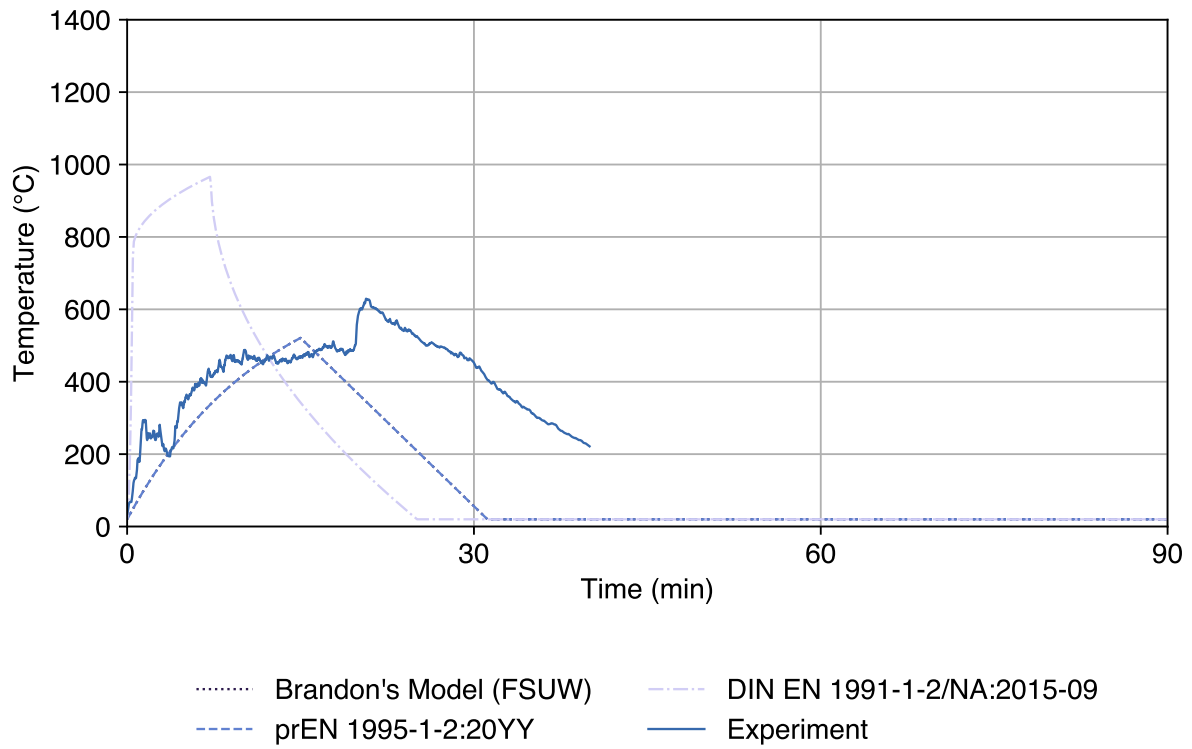
A.3.2 Test C3

Figure A.9: Temperature for Test C3



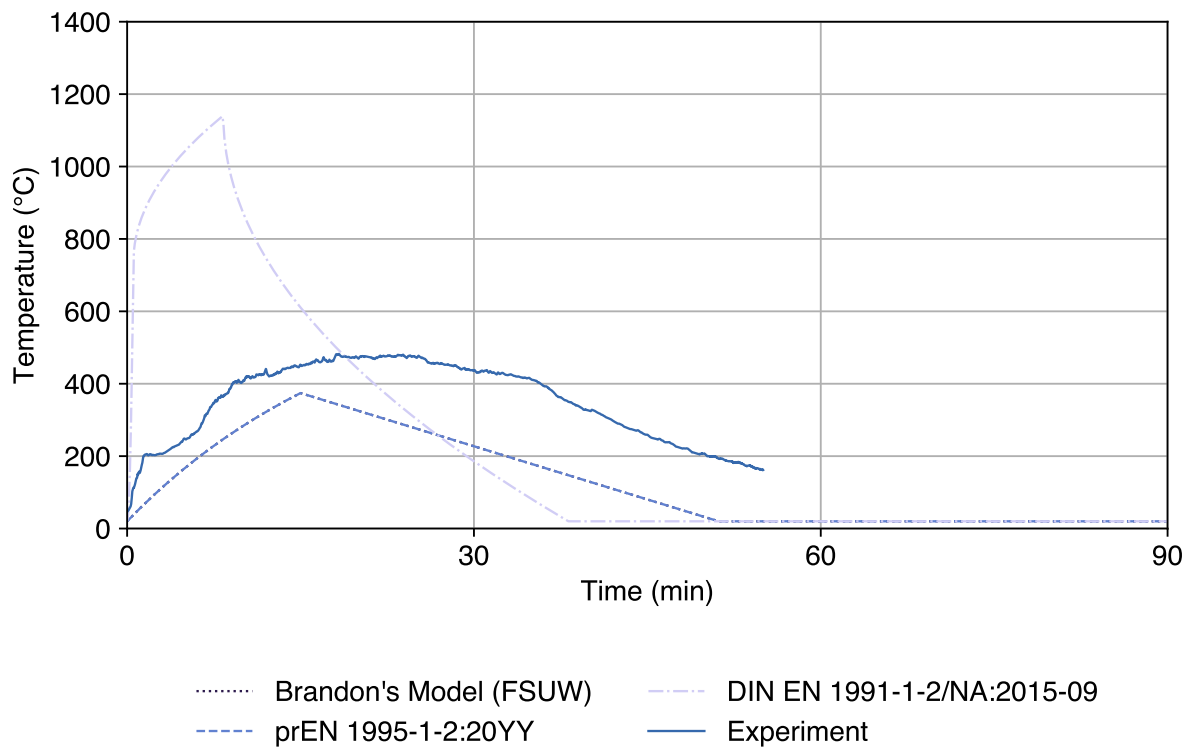
A.3.3 Test C4

Figure A.10: Temperature for Test C4



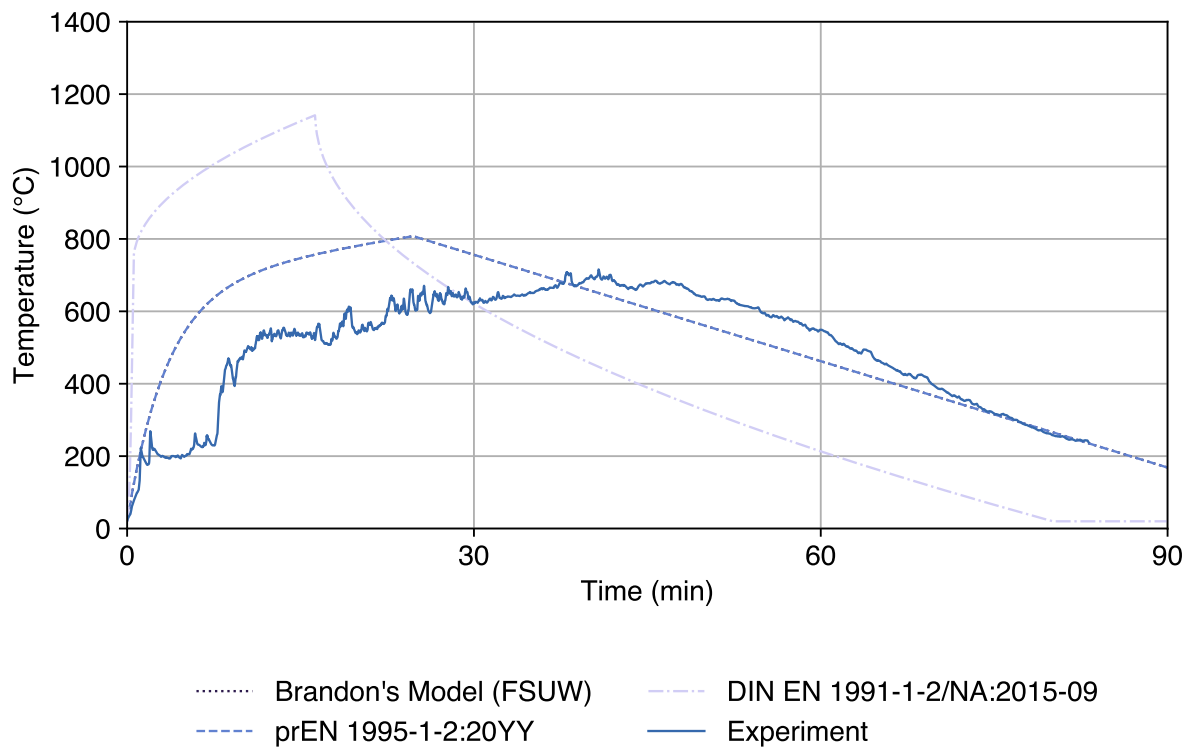
A.3.4 Test C5

Figure A.11: Temperature for Test C5



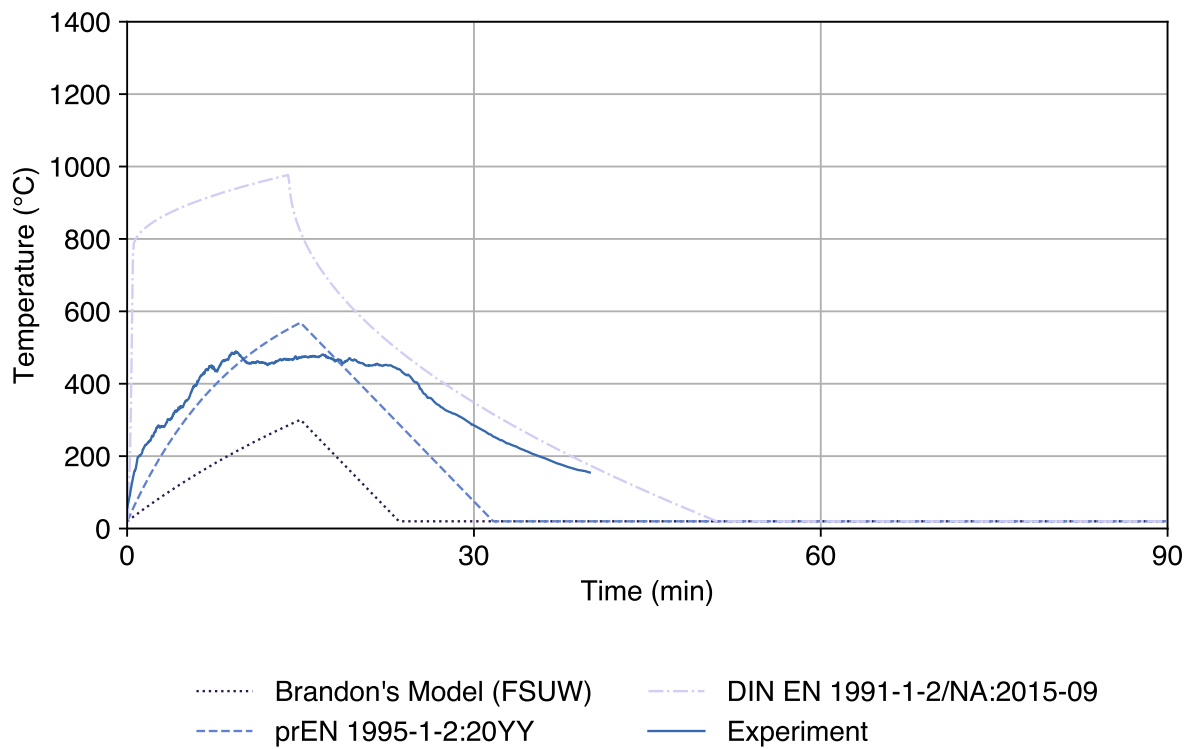
A.3.5 Test C6

Figure A.12: Temperature for Test C6



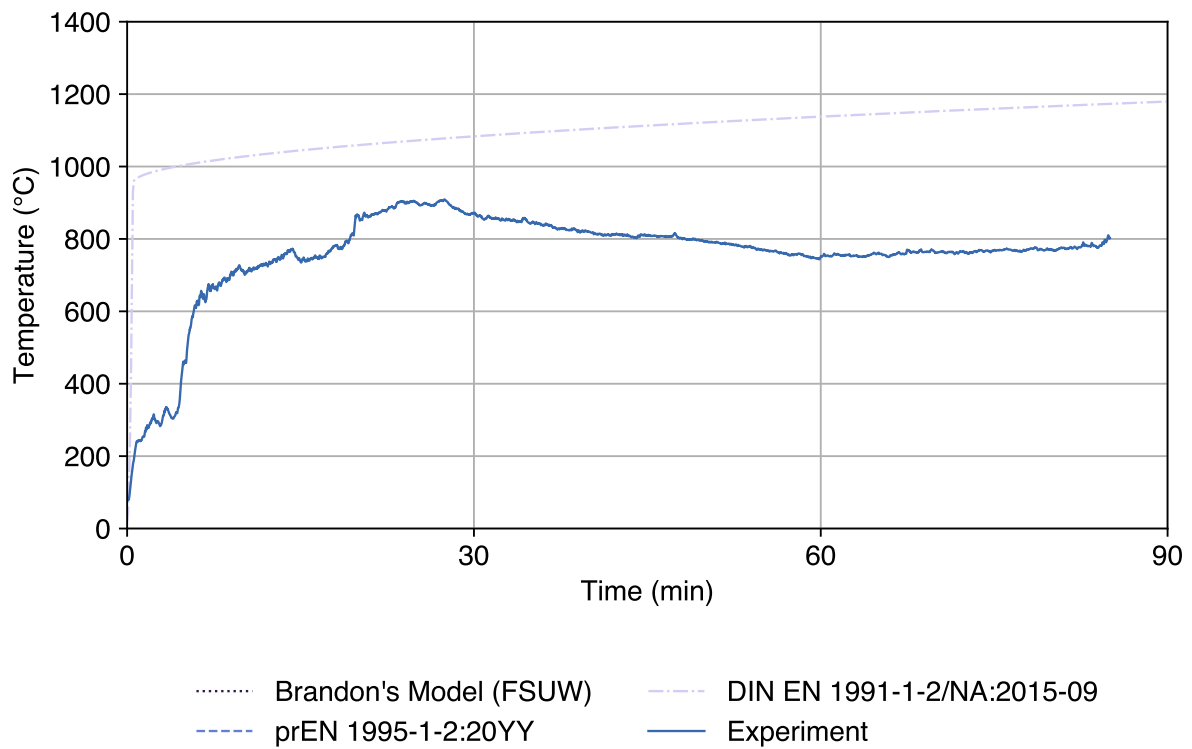
A.3.6 Test C7

Figure A.13: Temperature for Test C7



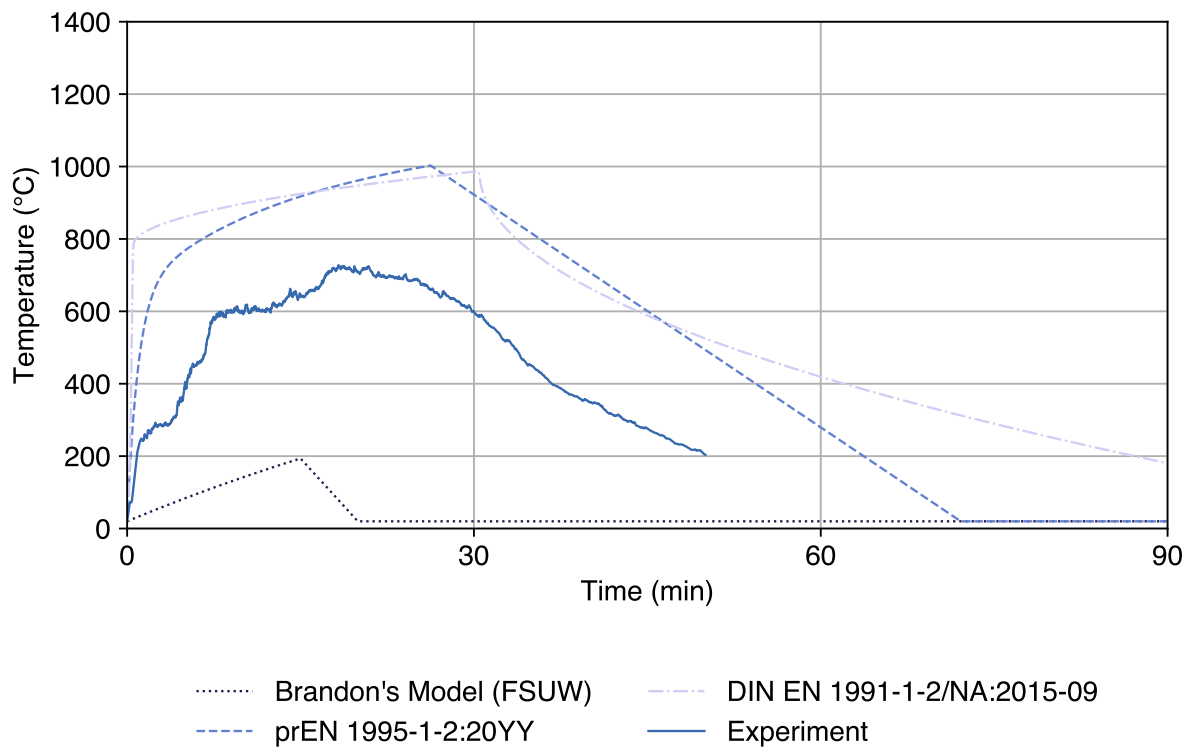
A.3.7 Test C8

Figure A.14: Temperature for Test C8



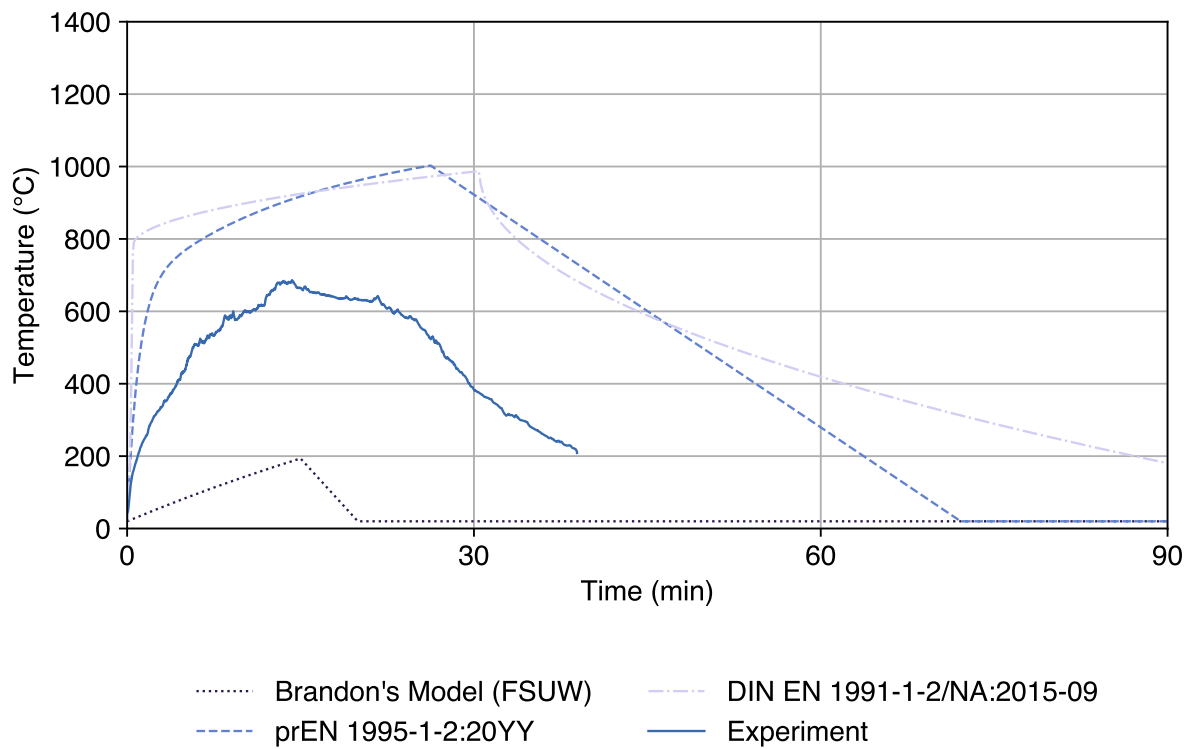
A.3.8 Test C10

Figure A.15: Temperature for Test C10



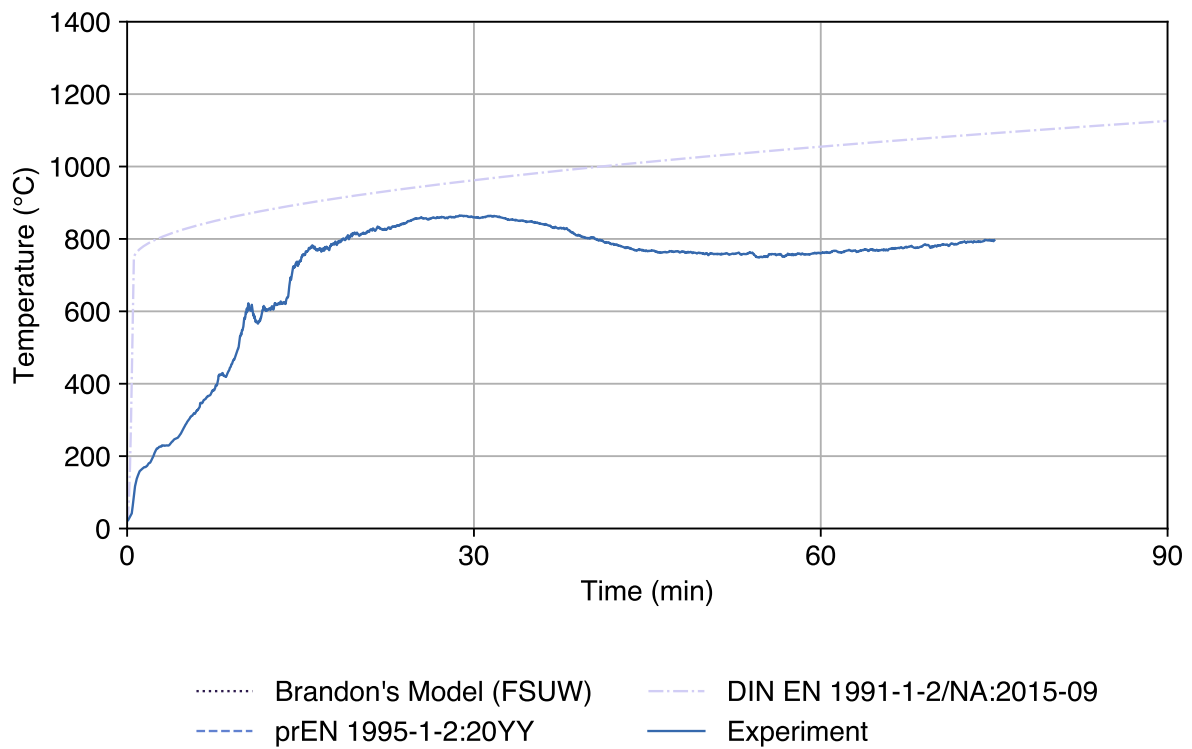
A.3.9 Test C11

Figure A.16: Temperature for Test C11



A.3.10 Test C12

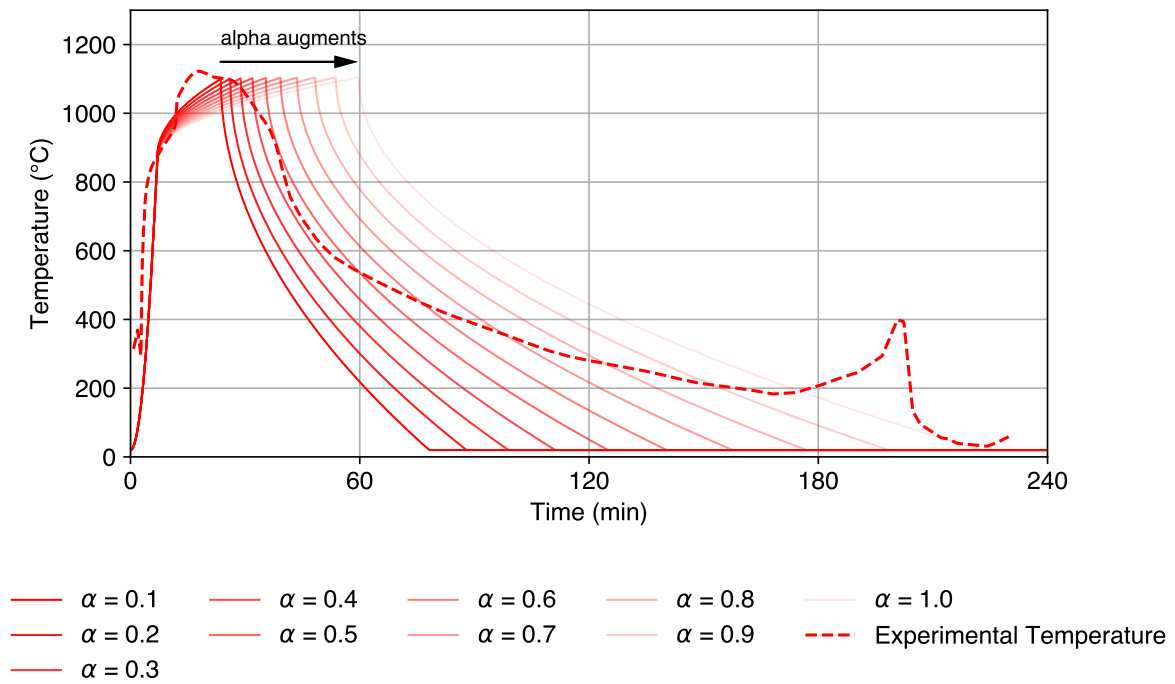
Figure A.17: Temperature for Test C12



A.4 Time dependent modification factor (α) Analysis

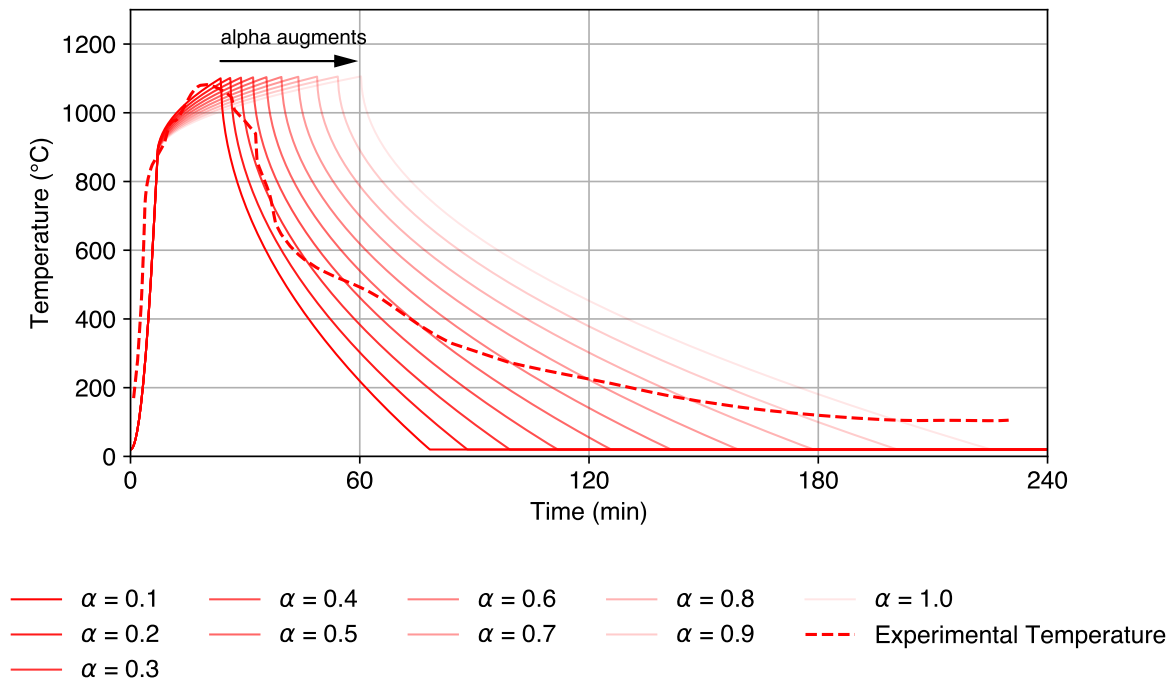
A.4.1 Test 6

Figure A.18: Alpha Analysis for Test 6



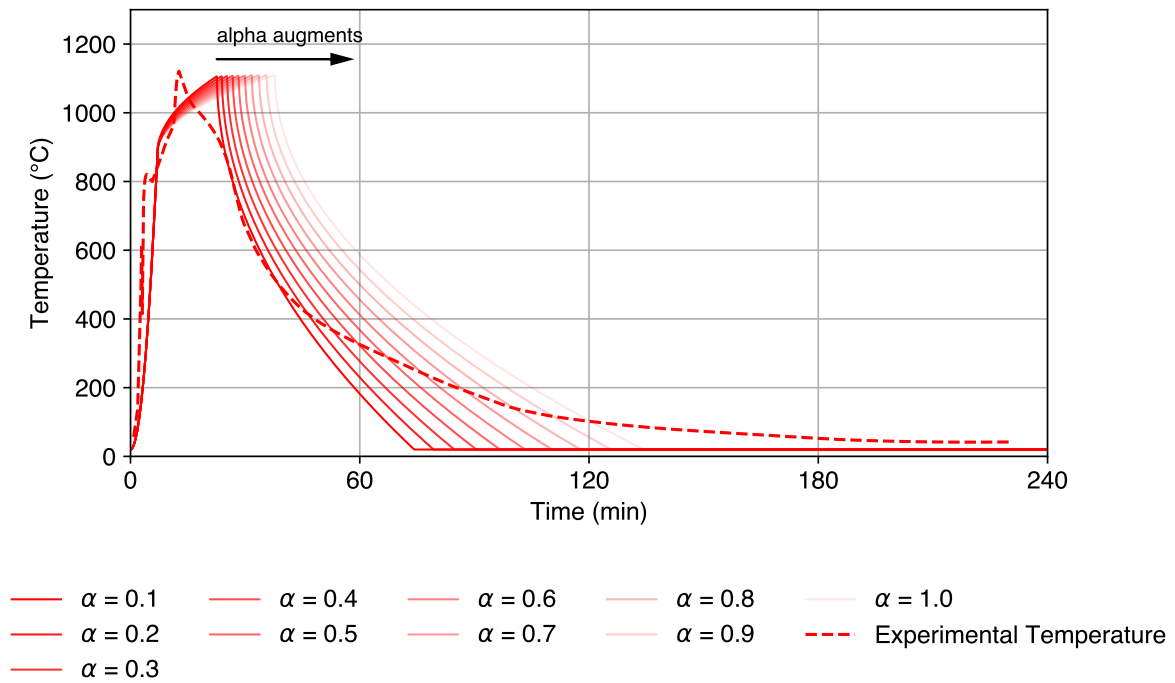
A.4.2 Test 7

Figure A.19: Alpha Analysis for Test 7



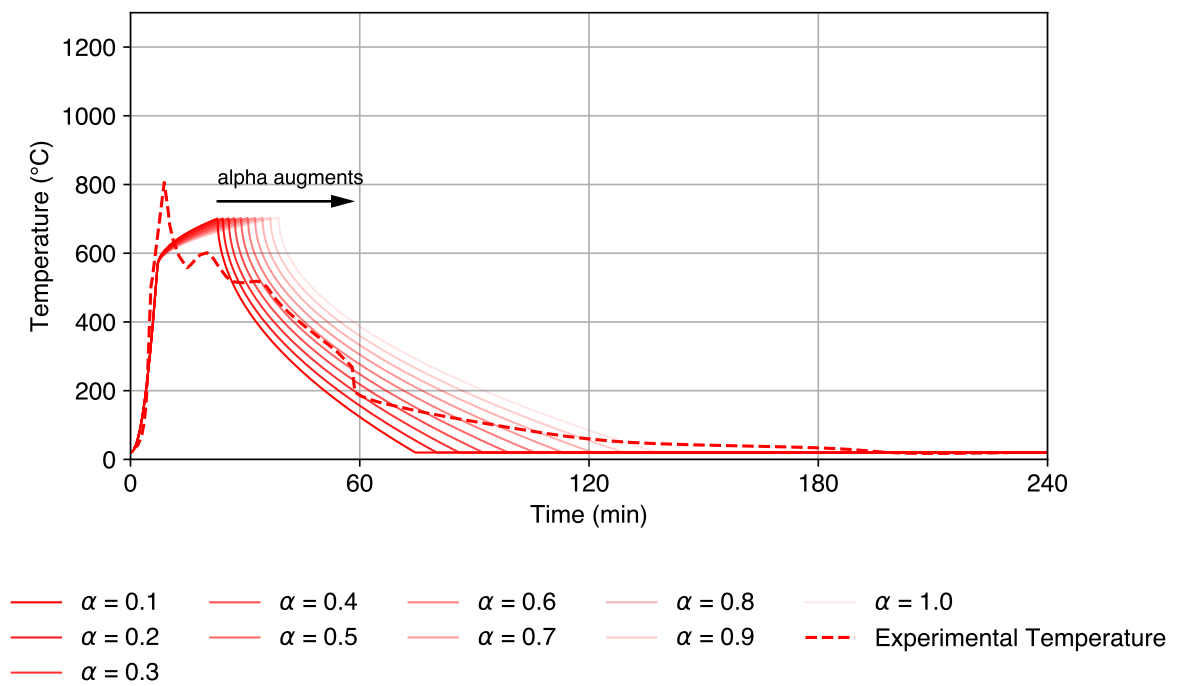
A.4.3 Test 8

Figure A.20: Alpha Analysis for Test 8



A.4.4 Test 9

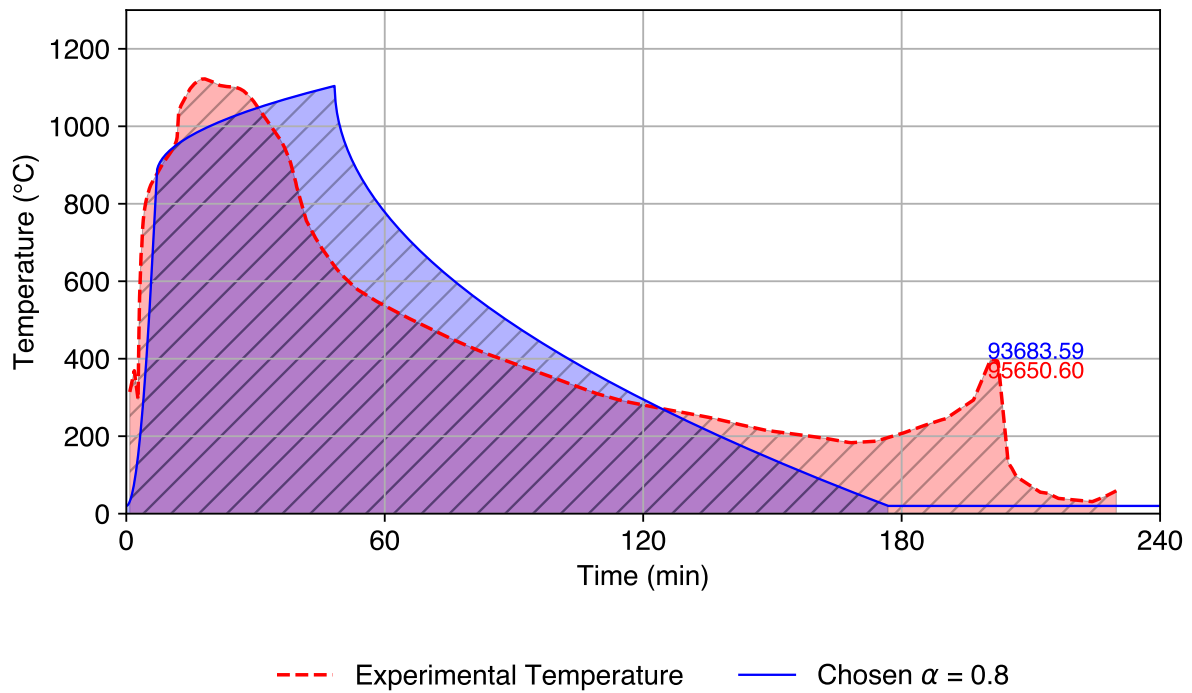
Figure A.21: Alpha Analysis for Test 9



A.5 Choosing time dependent modification factor (α)

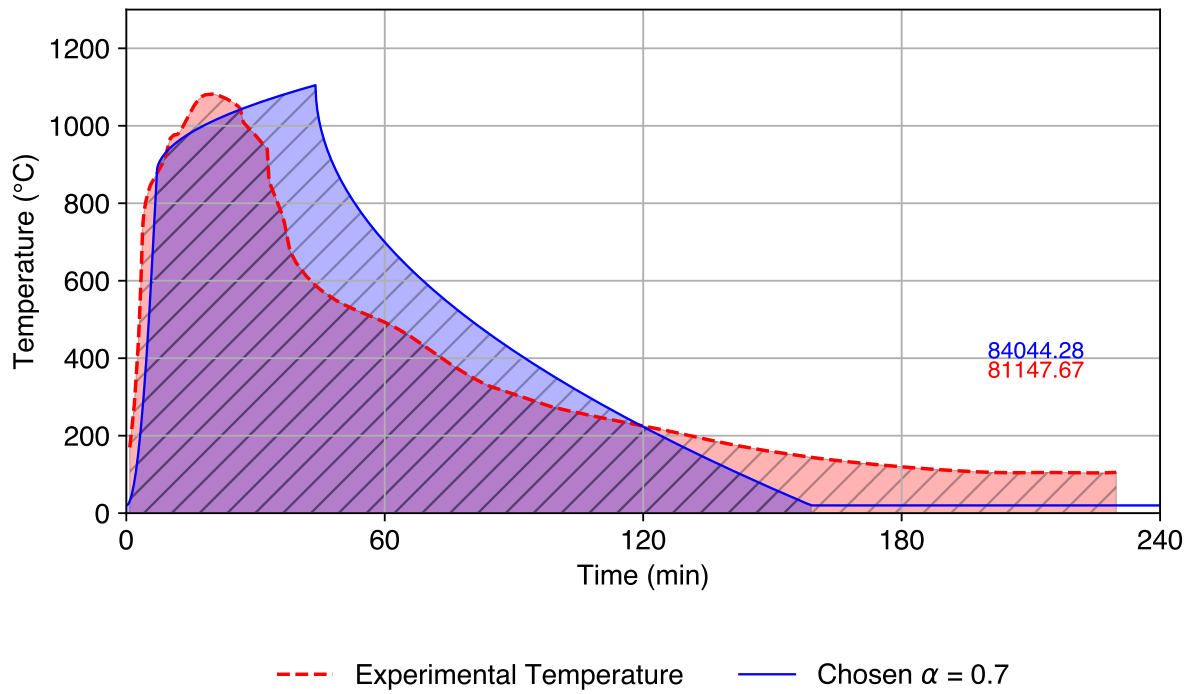
A.5.1 Test 6

Figure A.22: Choosing Alpha for Test 6



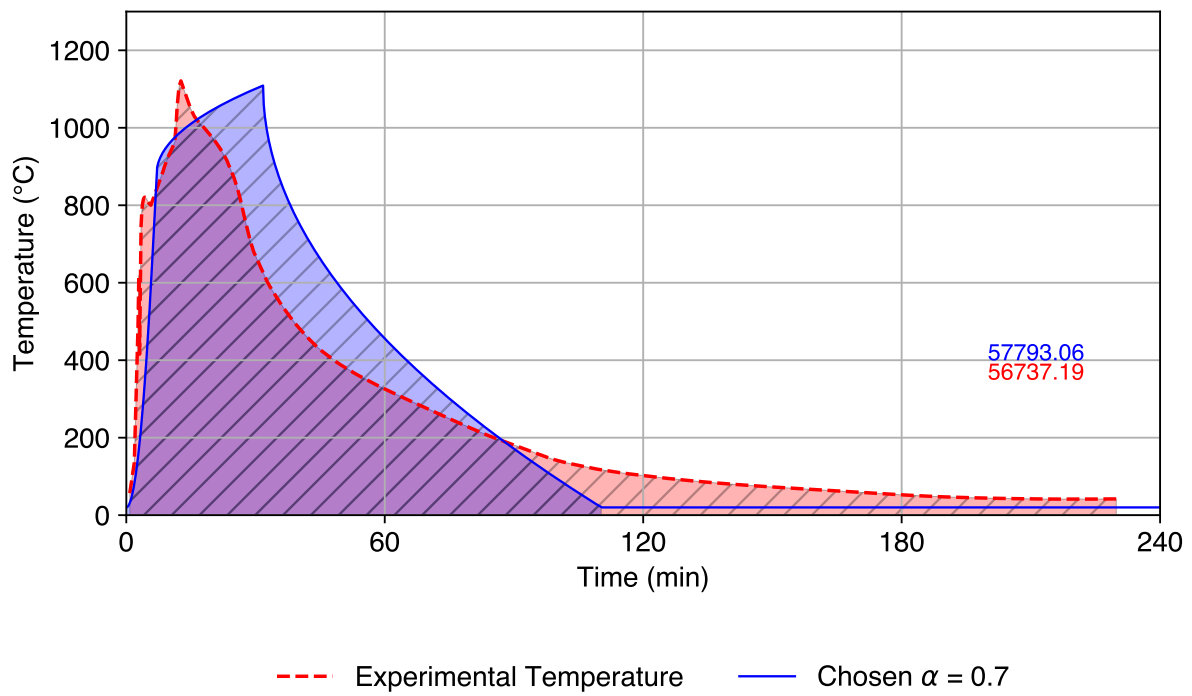
A.5.2 Test 7

Figure A.23: Choosing Alpha for Test 7



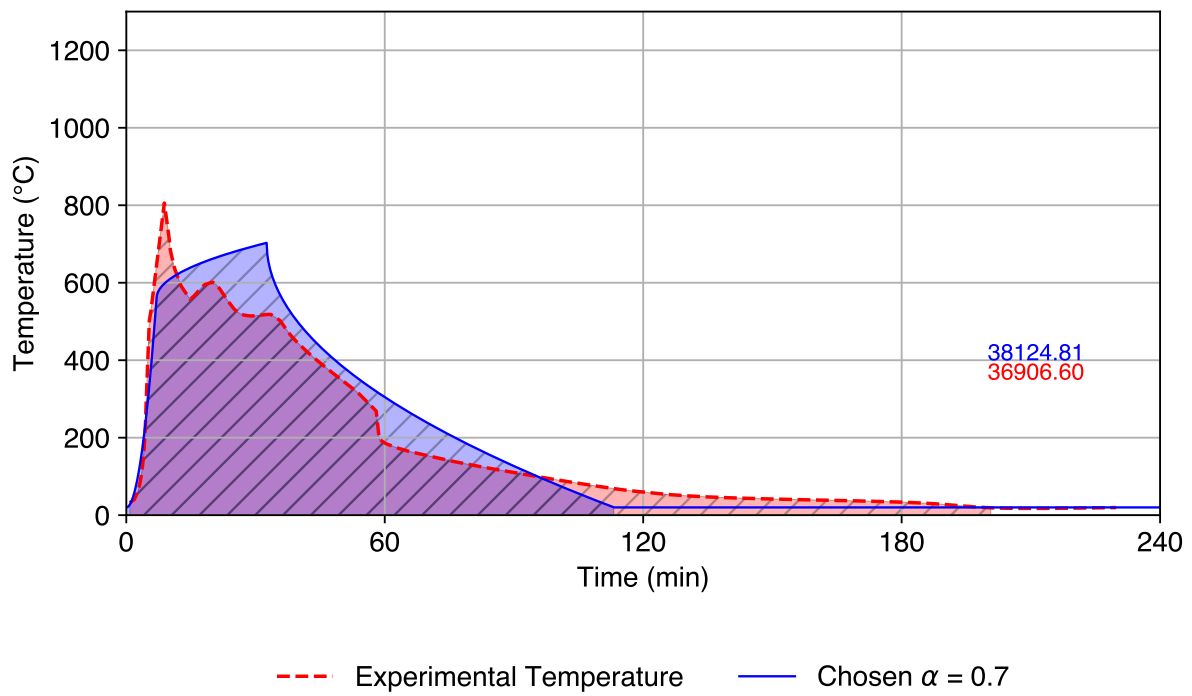
A.5.3 Test 8

Figure A.24: Choosing Alpha for Test 8



A.5.4 Test 9

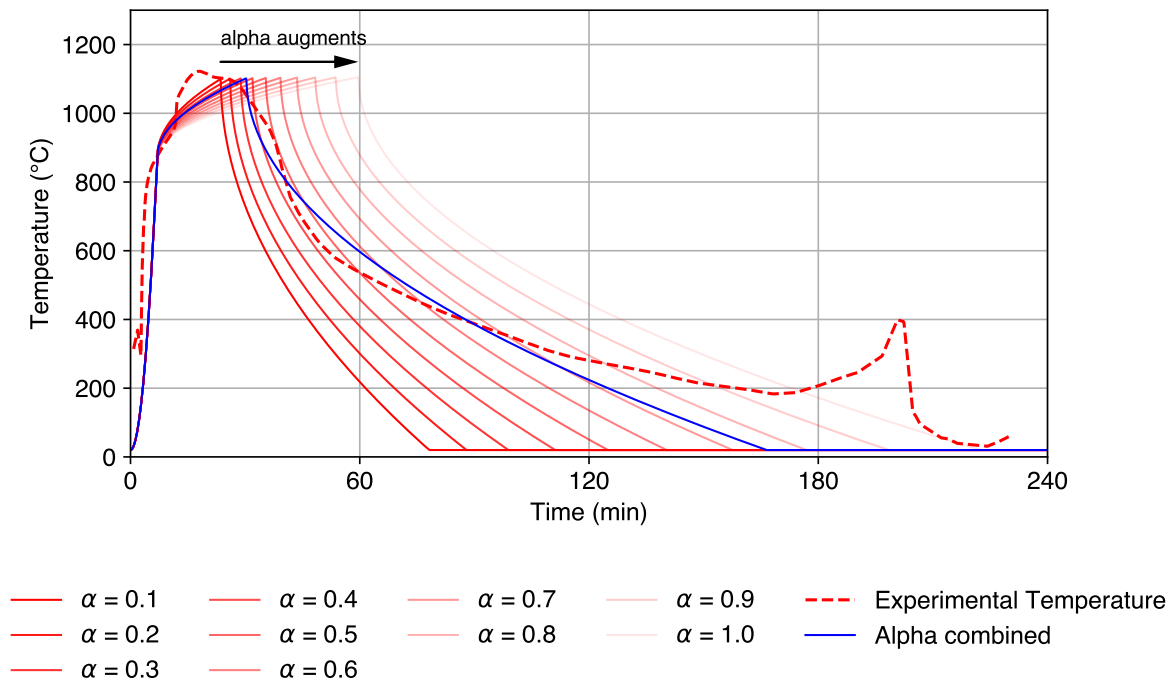
Figure A.25: Choosing Alpha for Test 9



A.6 Using two time dependent modification factors (α)

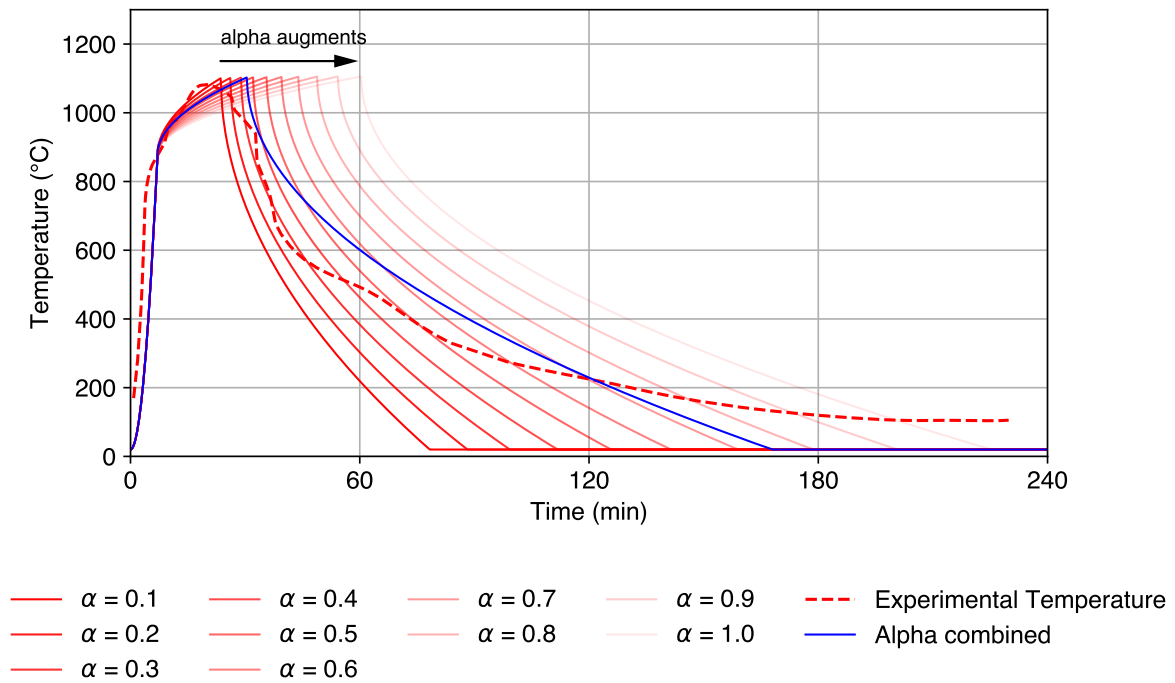
A.6.1 Test 6

Figure A.26: Combined Alpha Method for Test 6



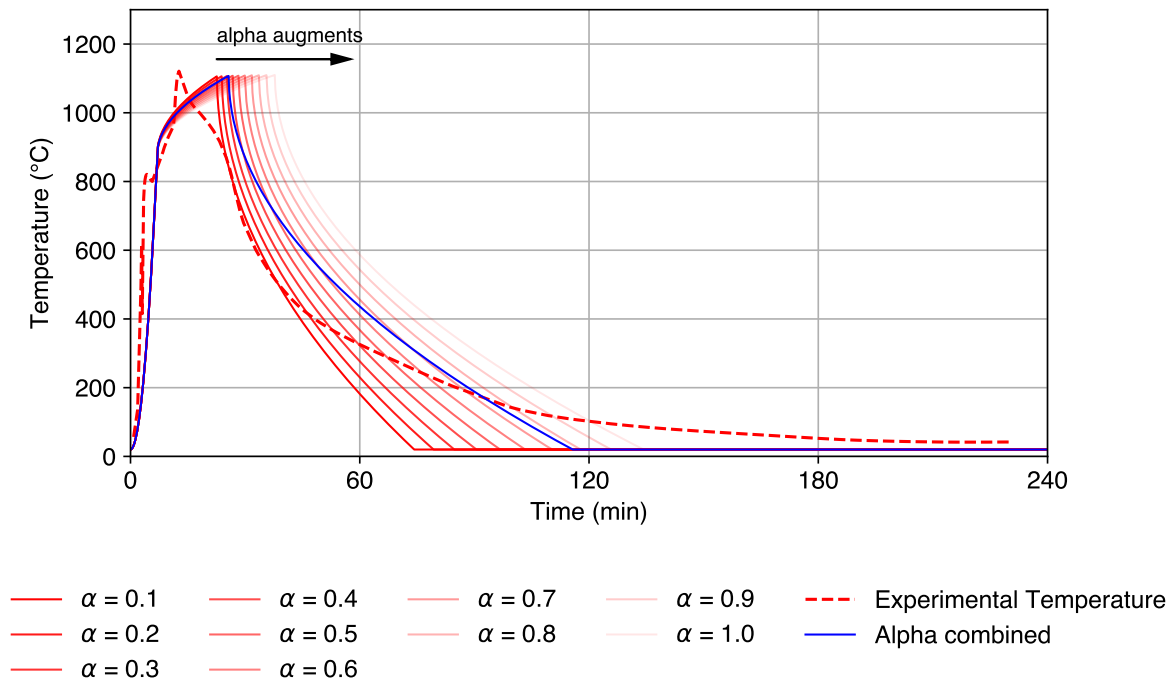
A.6.2 Test 7

Figure A.27: Combined Alpha Method for Test 7



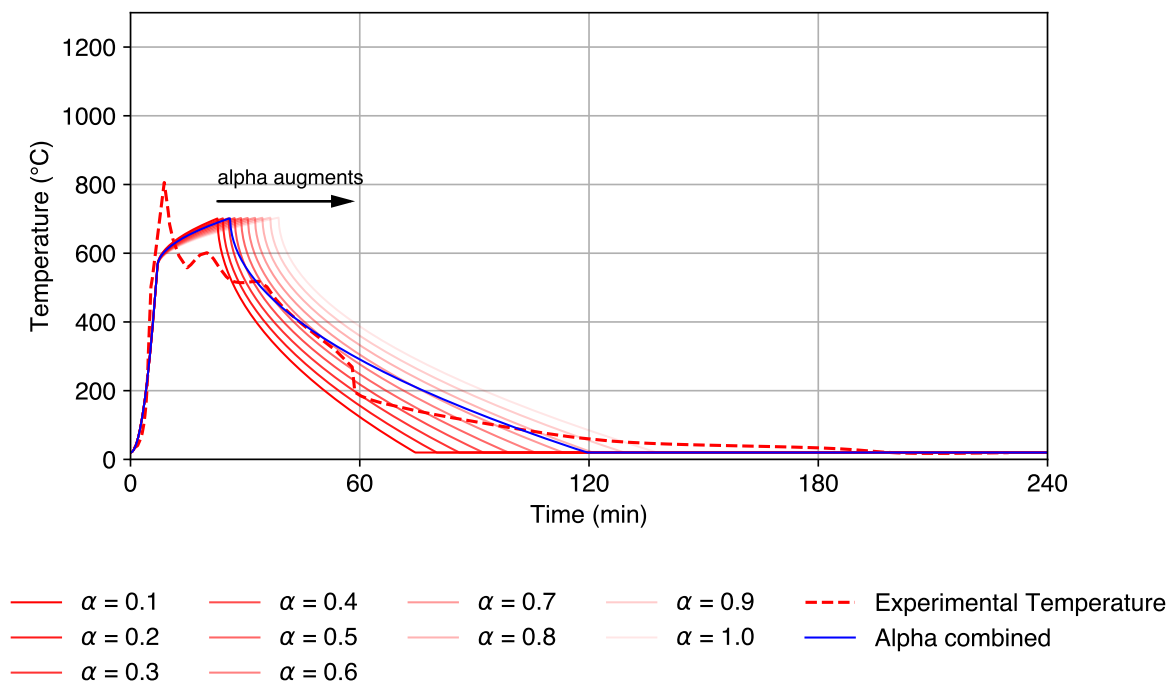
A.6.3 Test 8

Figure A.28: Combined Alpha Method for Test 8



A.6.4 Test 9

Figure A.29: Combined Alpha Method for Test 9



A.7 Two time dependent modification factors (α) comparison

A.7.1 Test 6

Figure A.30: Combined Alpha Method for Test 6

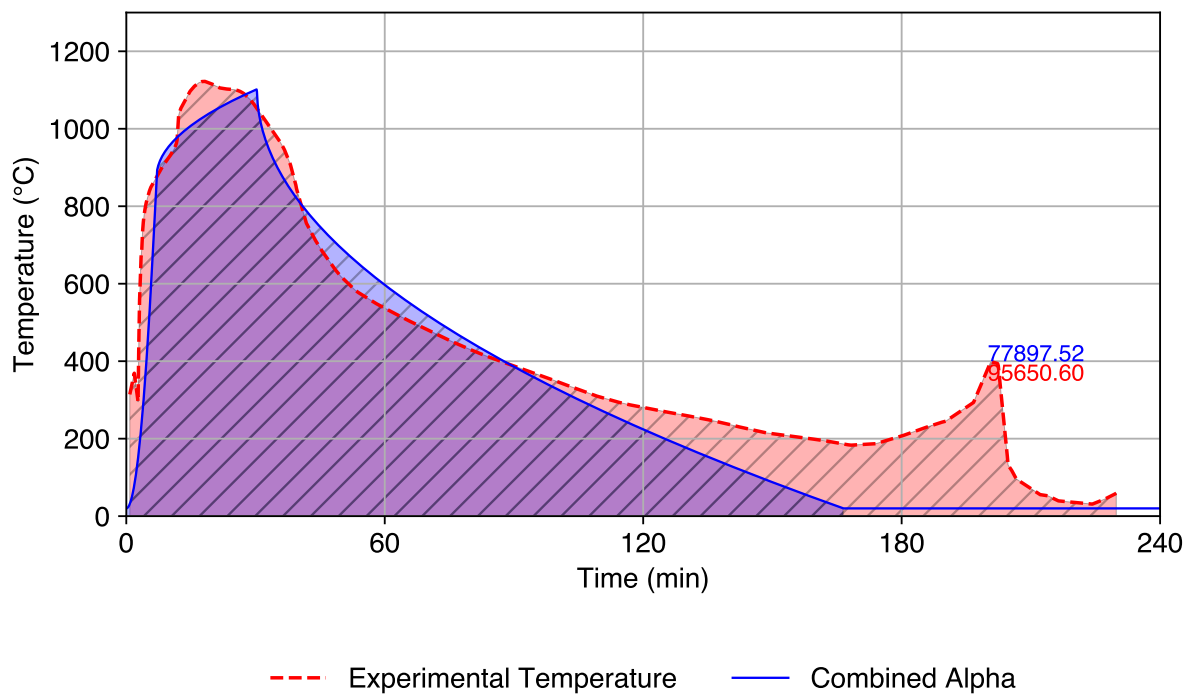
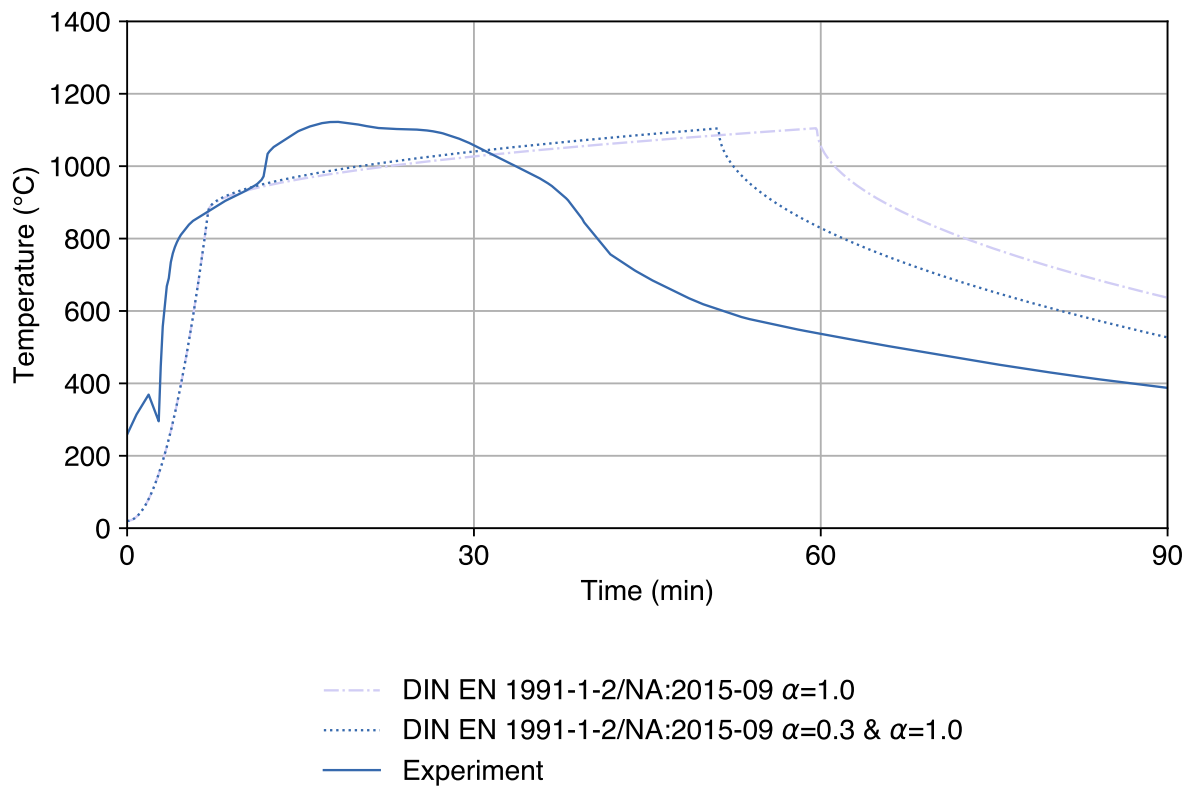


Figure A.31: Temperatures for two time dependent modification factor for Test 6



A.7.2 Test 7

Figure A.32: Combined Alpha Method for Test 7

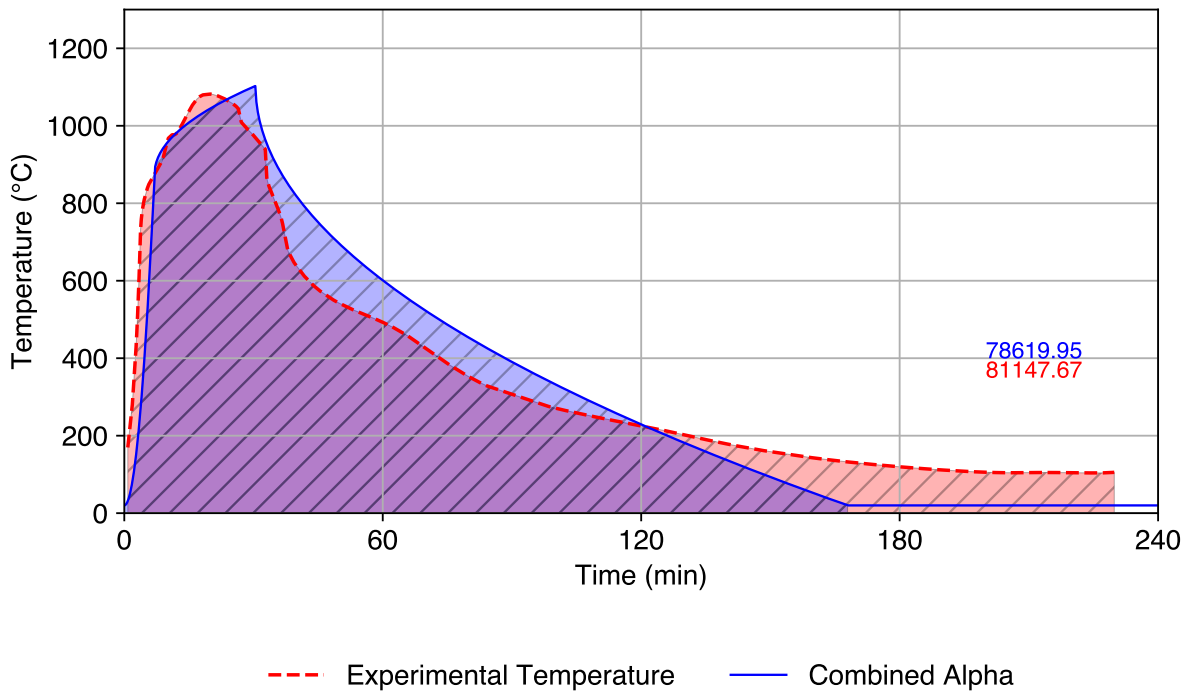
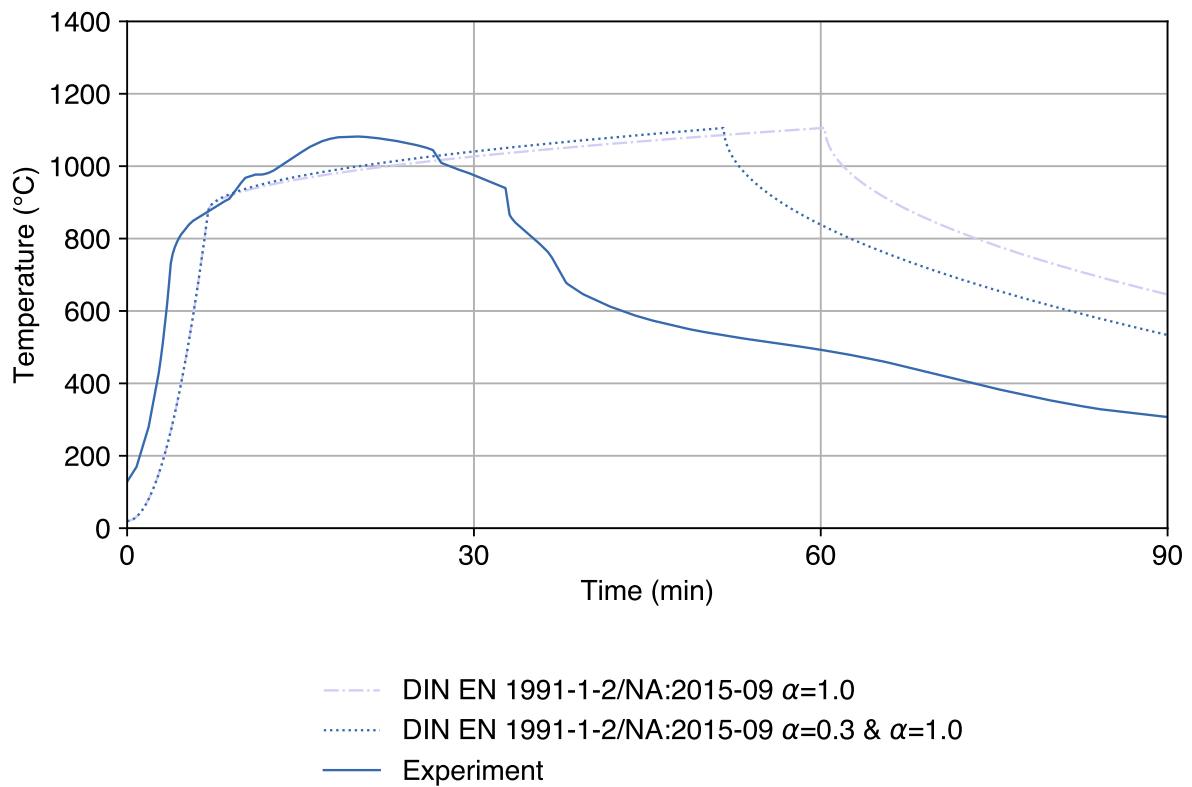


Figure A.33: Temperatures for two time dependent modification factor for Test 7



A.7.3 Test 8

Figure A.34: Combined Alpha Method for Test 8

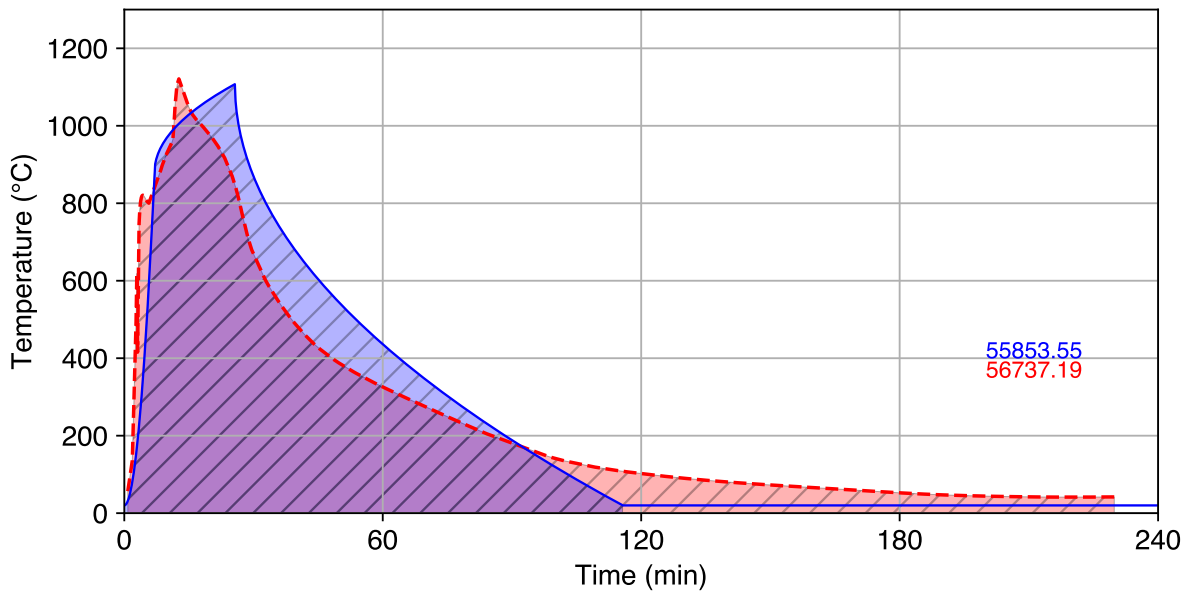
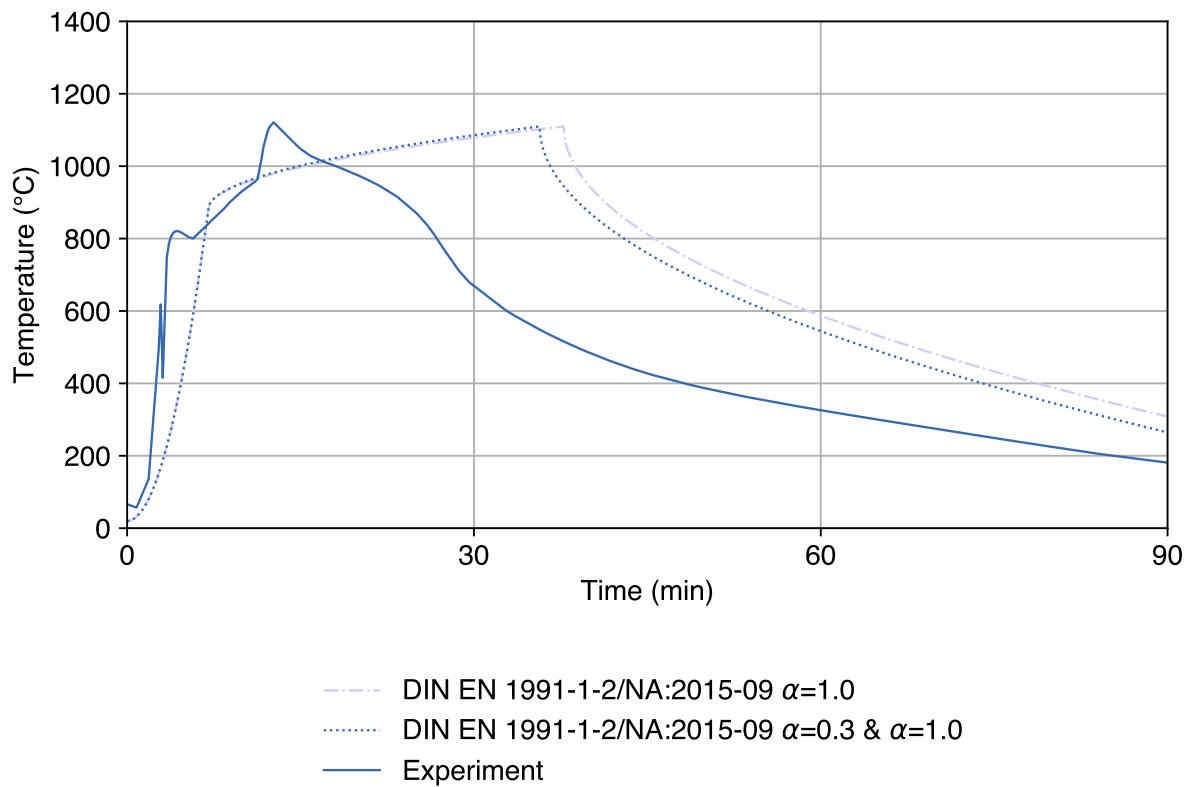


Figure A.35: Temperatures for two time dependent modification factor for Test 8



A.7.4 Test 9

Figure A.36: Combined Alpha Method for Test 9

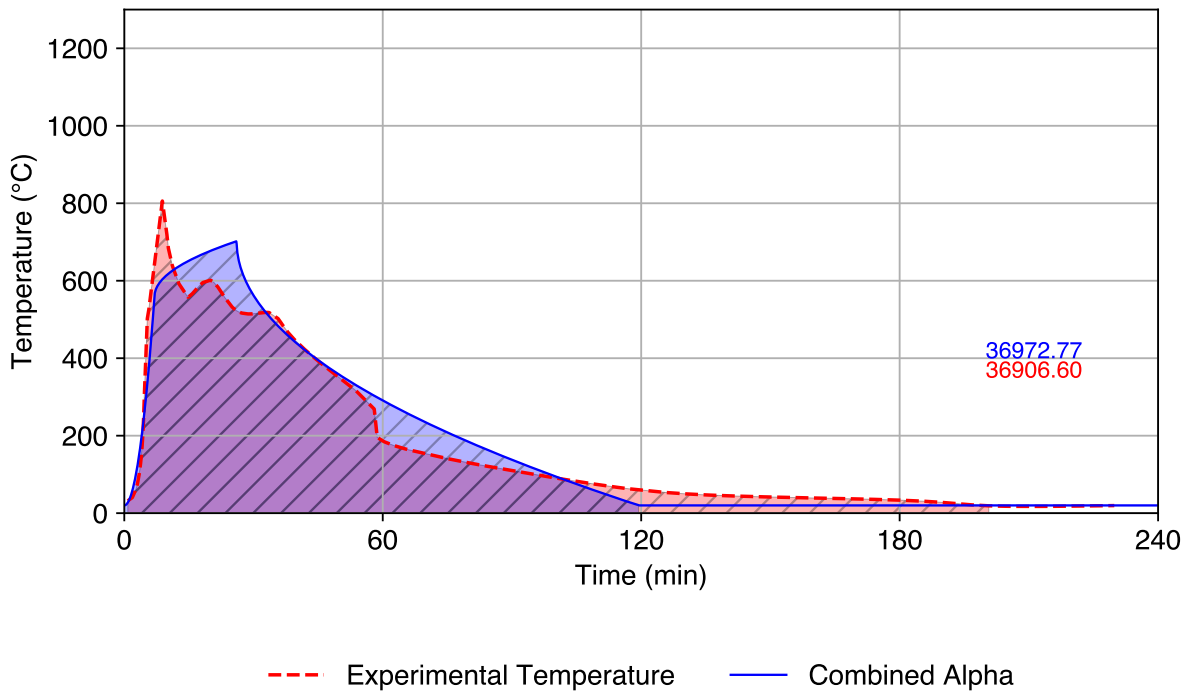
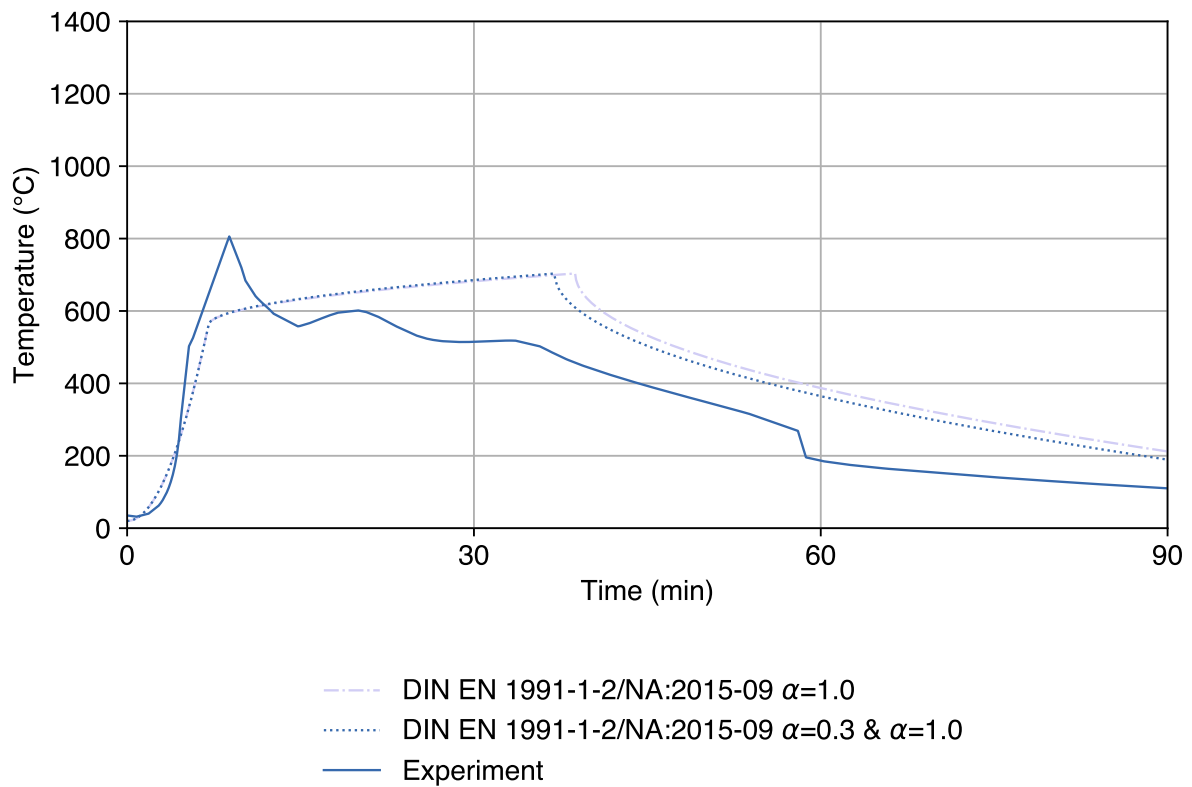
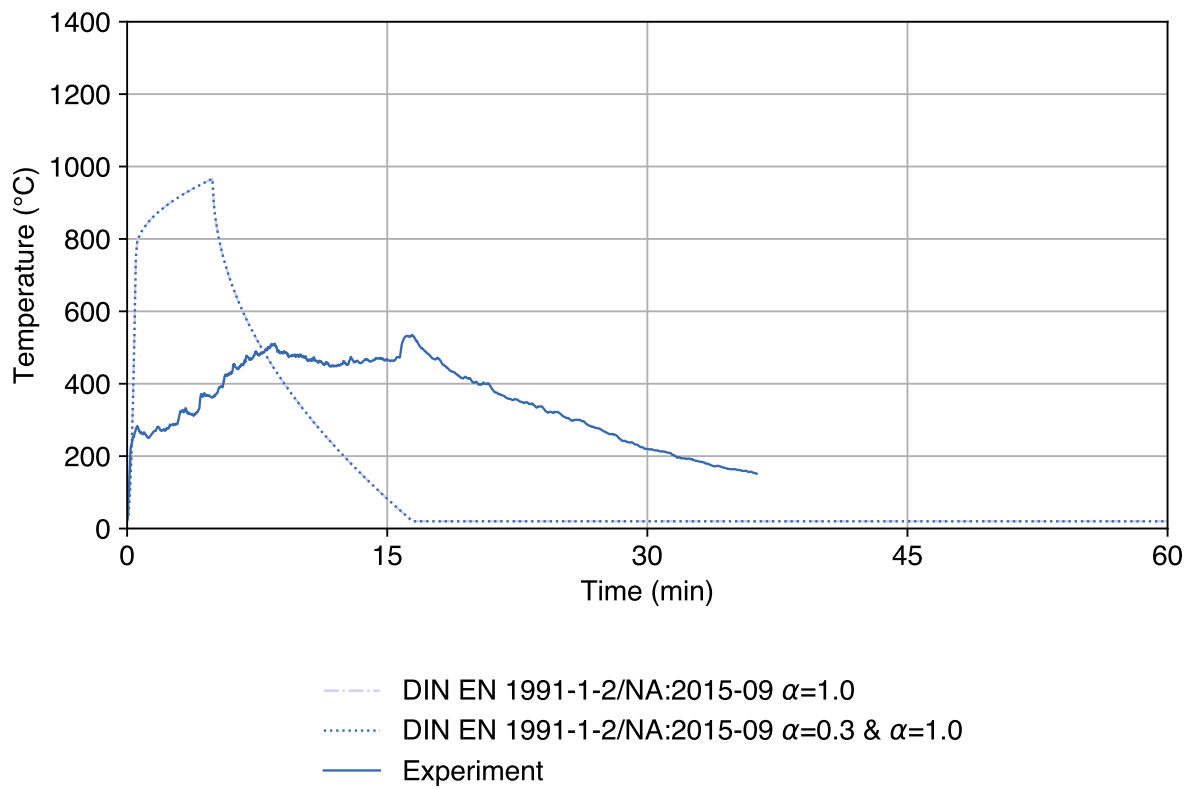


Figure A.37: Temperatures for two time dependent modification factor for Test 9



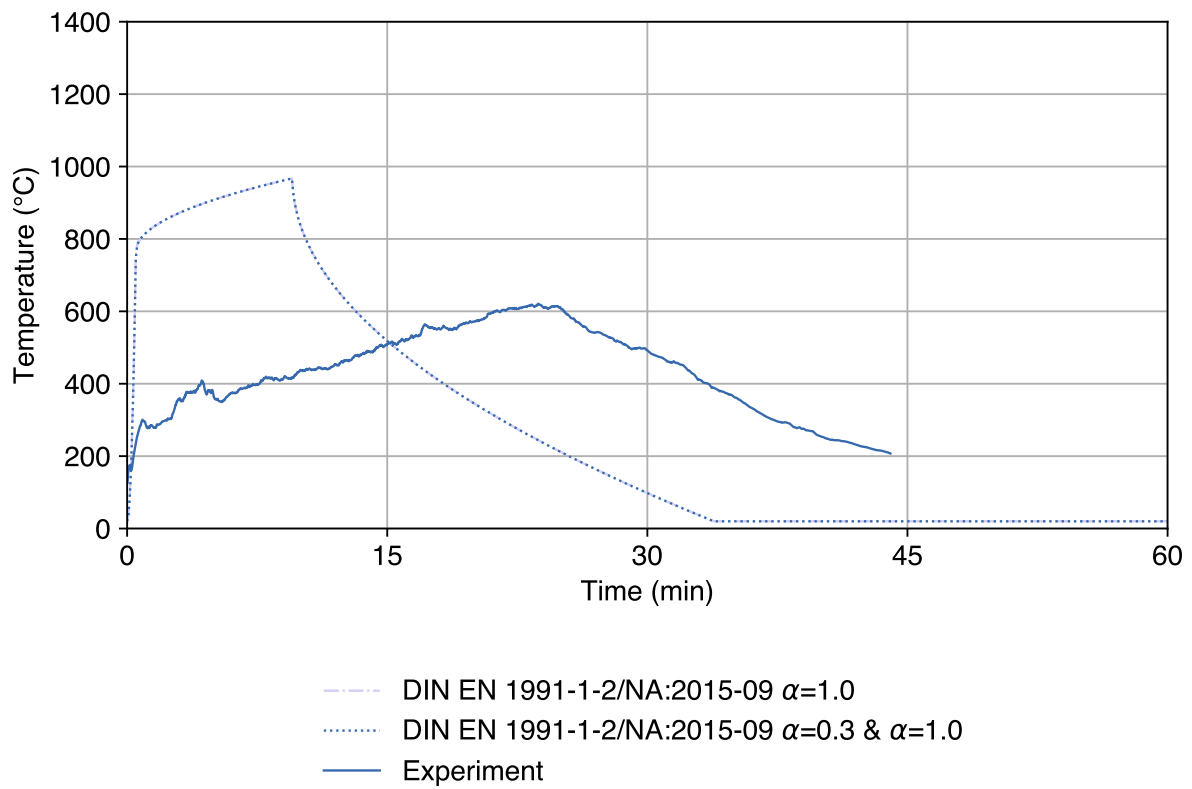
A.7.5 Test C2

Figure A.38: Temperatures for two time dependent modification factor for Test C2



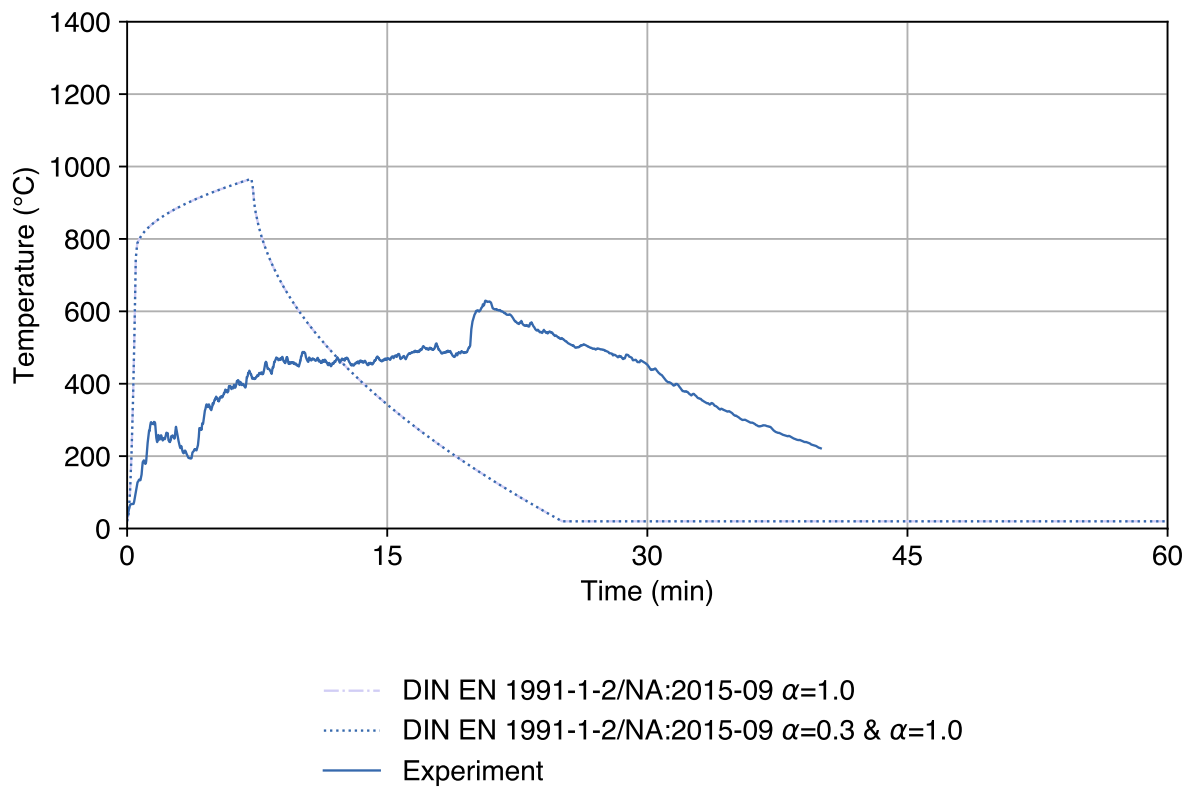
A.7.6 Test C3

Figure A.39: Temperatures for two time dependent modification factor for Test C3



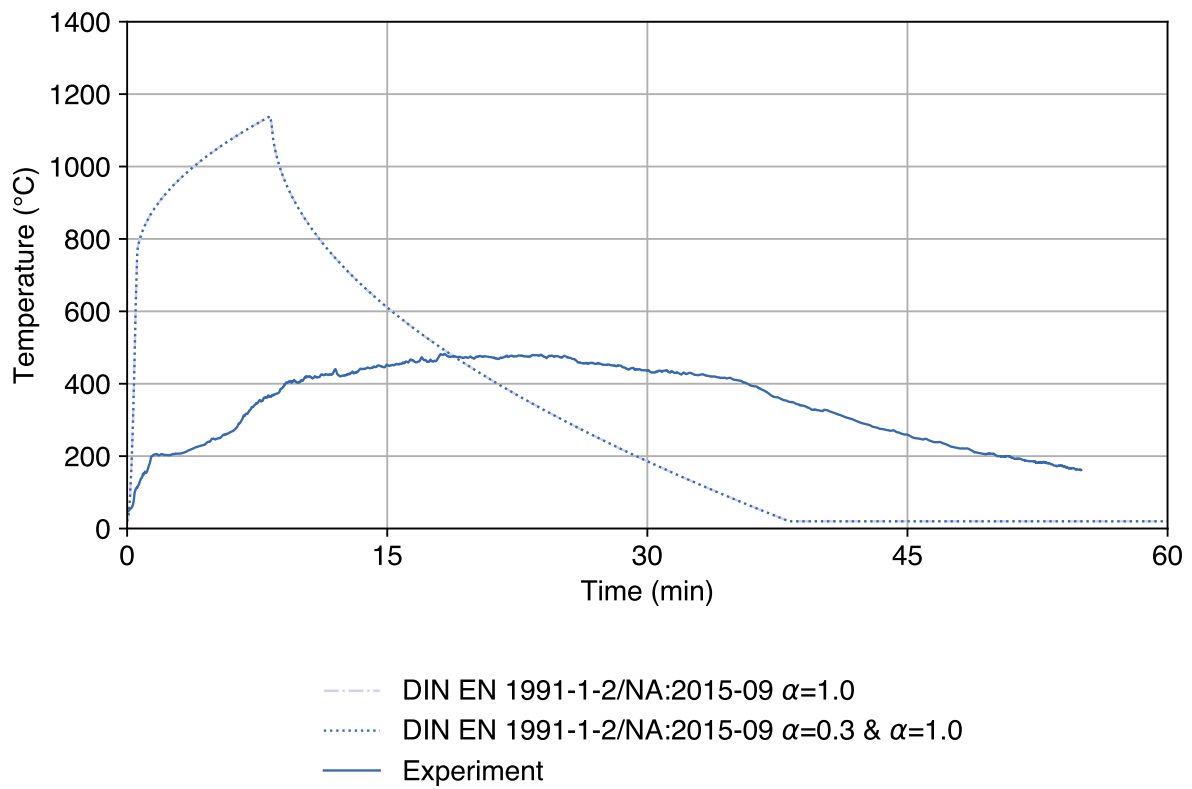
A.7.7 Test C4

Figure A.40: Temperatures for two time dependent modification factor for Test C4



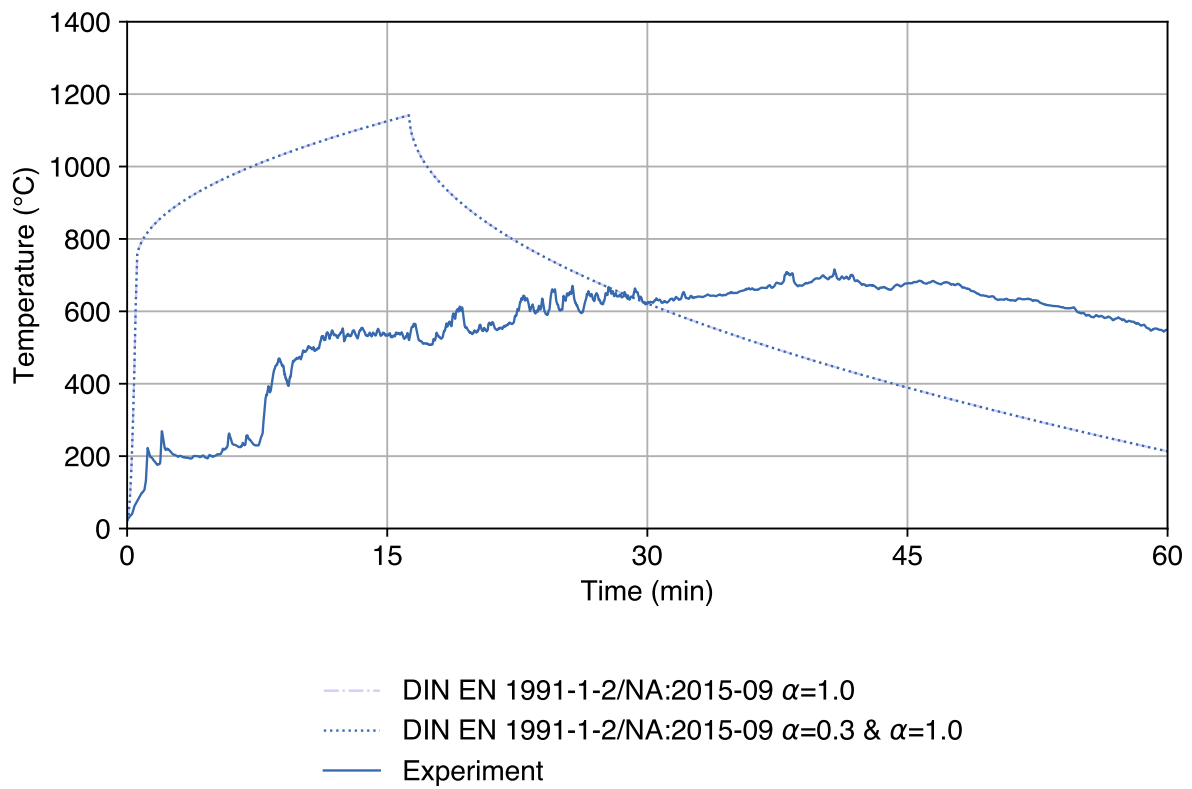
A.7.8 Test C5

Figure A.41: Temperatures for two time dependent modification factor for Test C5



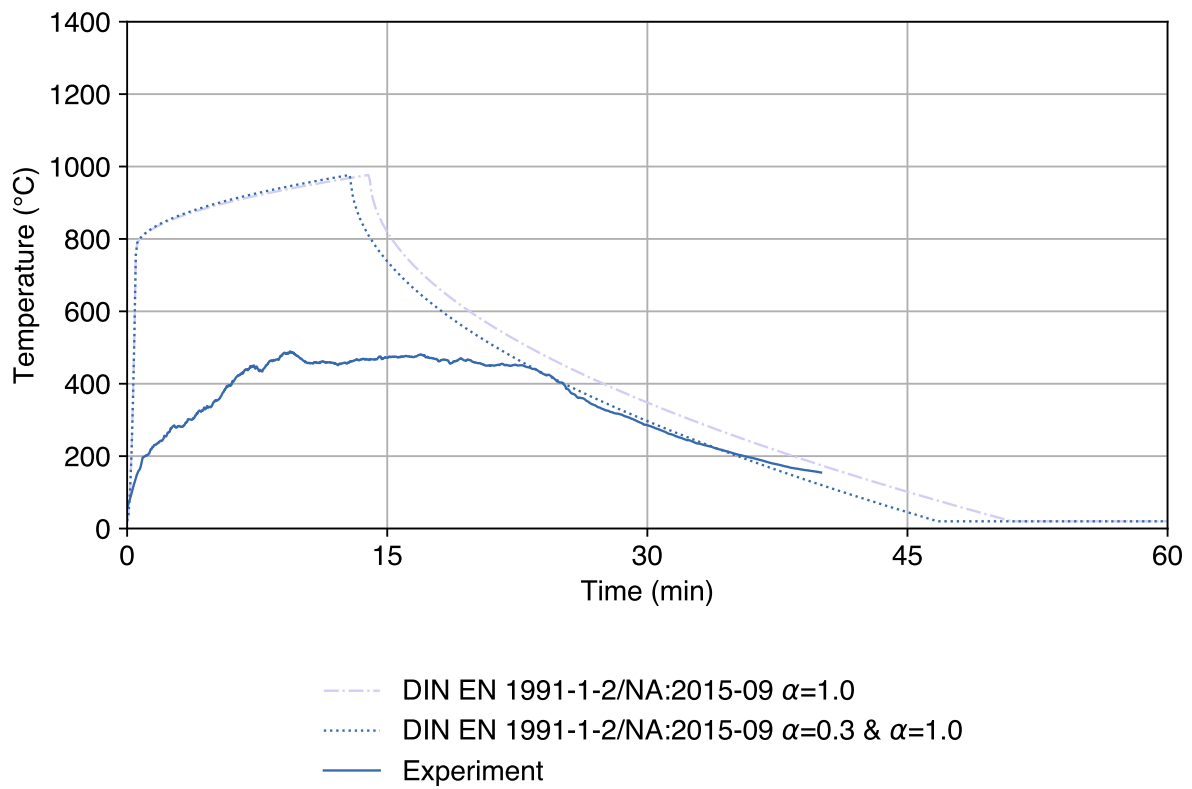
A.7.9 Test C6

Figure A.42: Temperatures for two time dependent modification factor for Test C6



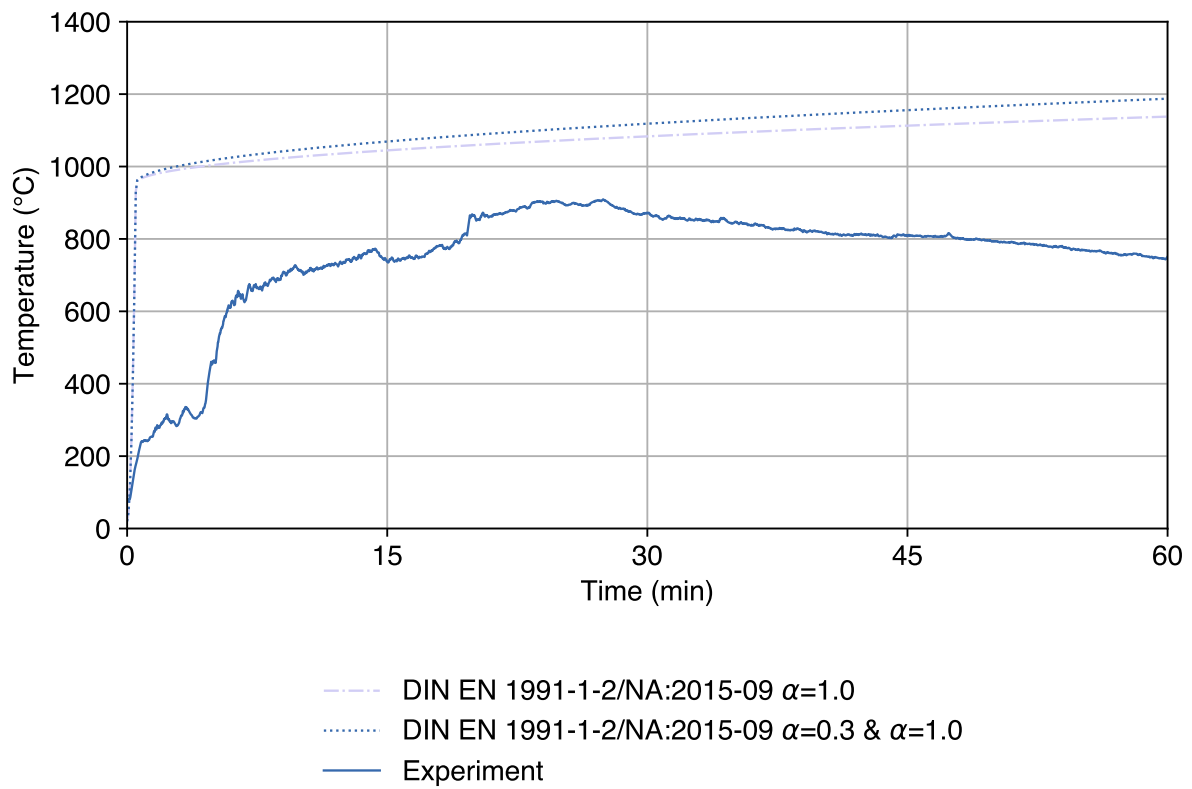
A.7.10 Test C7

Figure A.43: Temperatures for two time dependent modification factor for Test C7



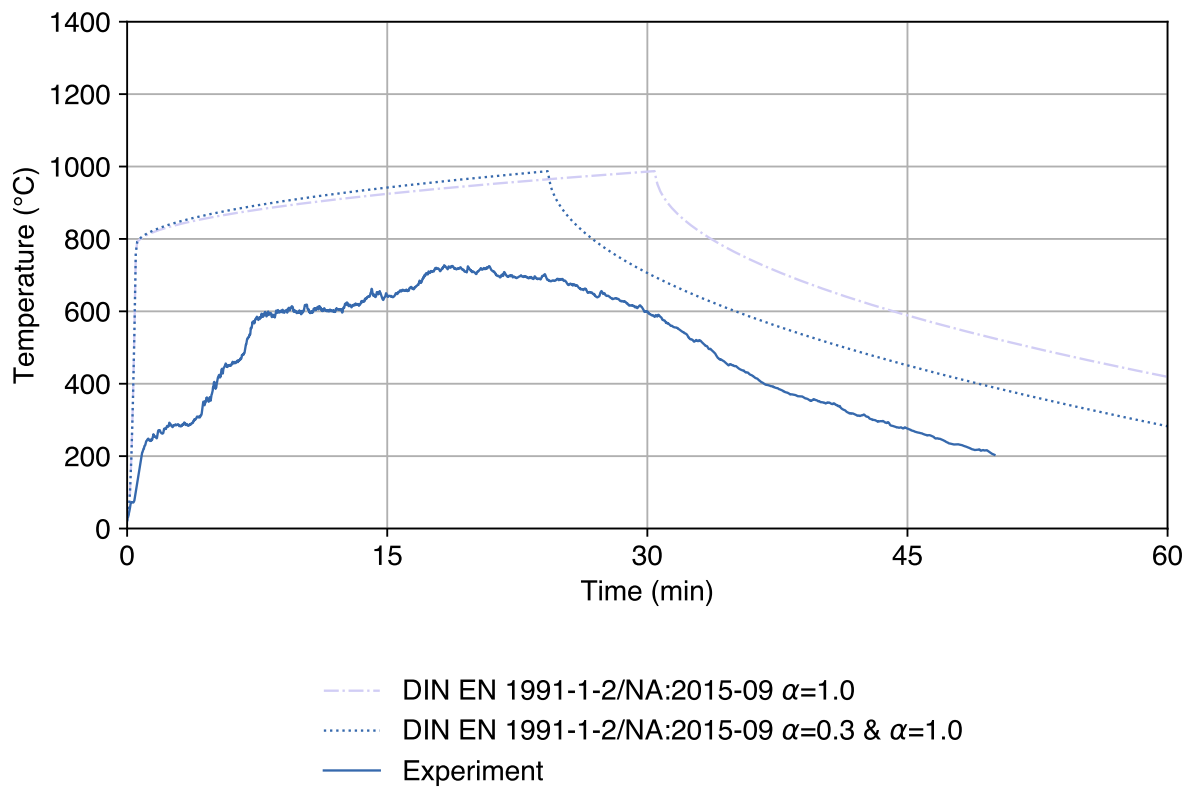
A.7.11 Test C8

Figure A.44: Temperatures for two time dependent modification factor for Test C8



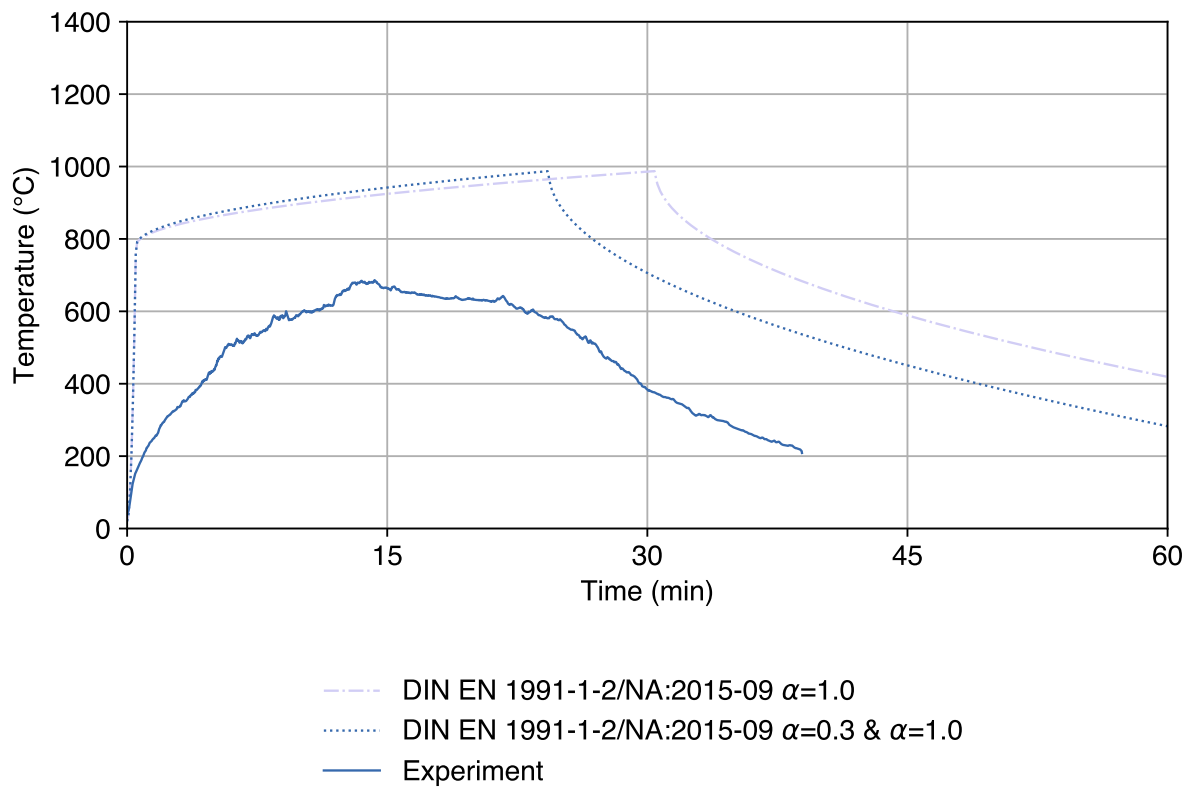
A.7.12 Test C10

Figure A.45: Temperatures for two time dependent modification factor for Test C10



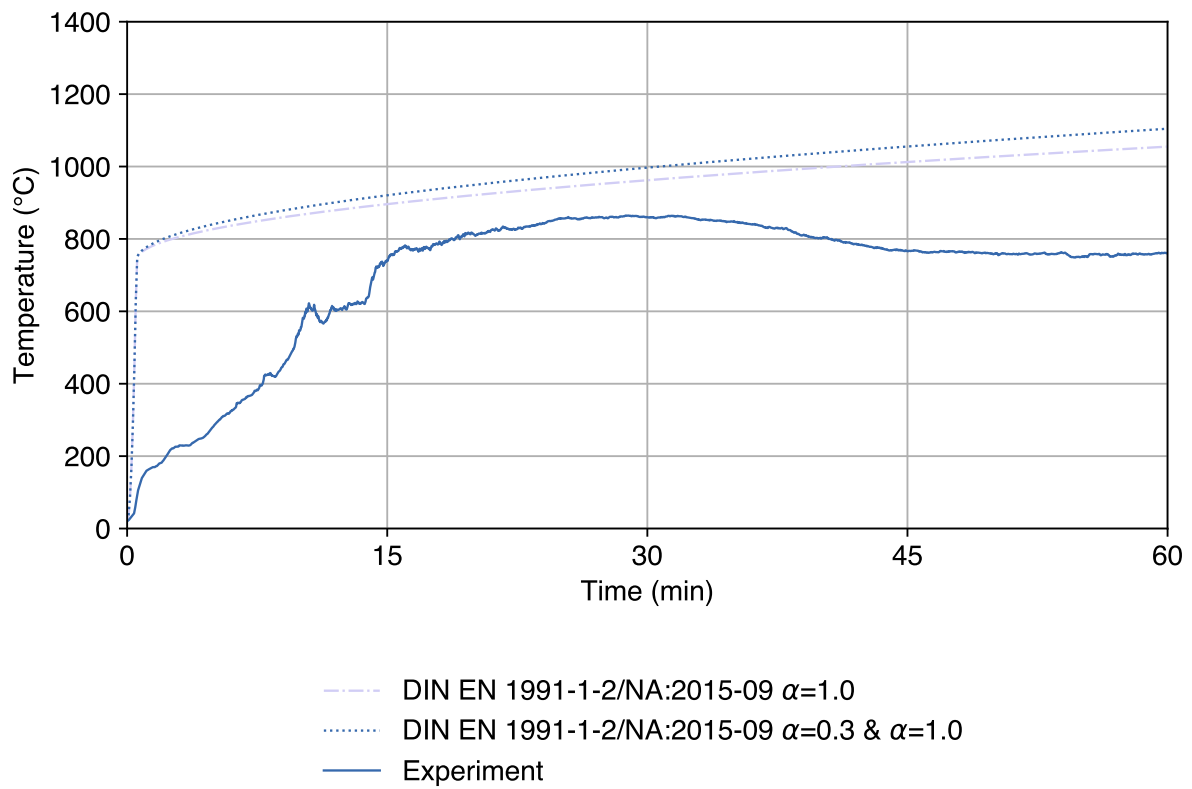
A.7.13 Test C11

Figure A.46: Temperatures for two time dependent modification factor for Test C11



A.7.14 Test C12

Figure A.47: Temperatures for two time dependent modification factor for Test C12



A.8 Creating time dependent modification factor (α) - Time Graphs

A.8.1 Test 6

Figure A.48: Alpha - Time Graph for Test 6

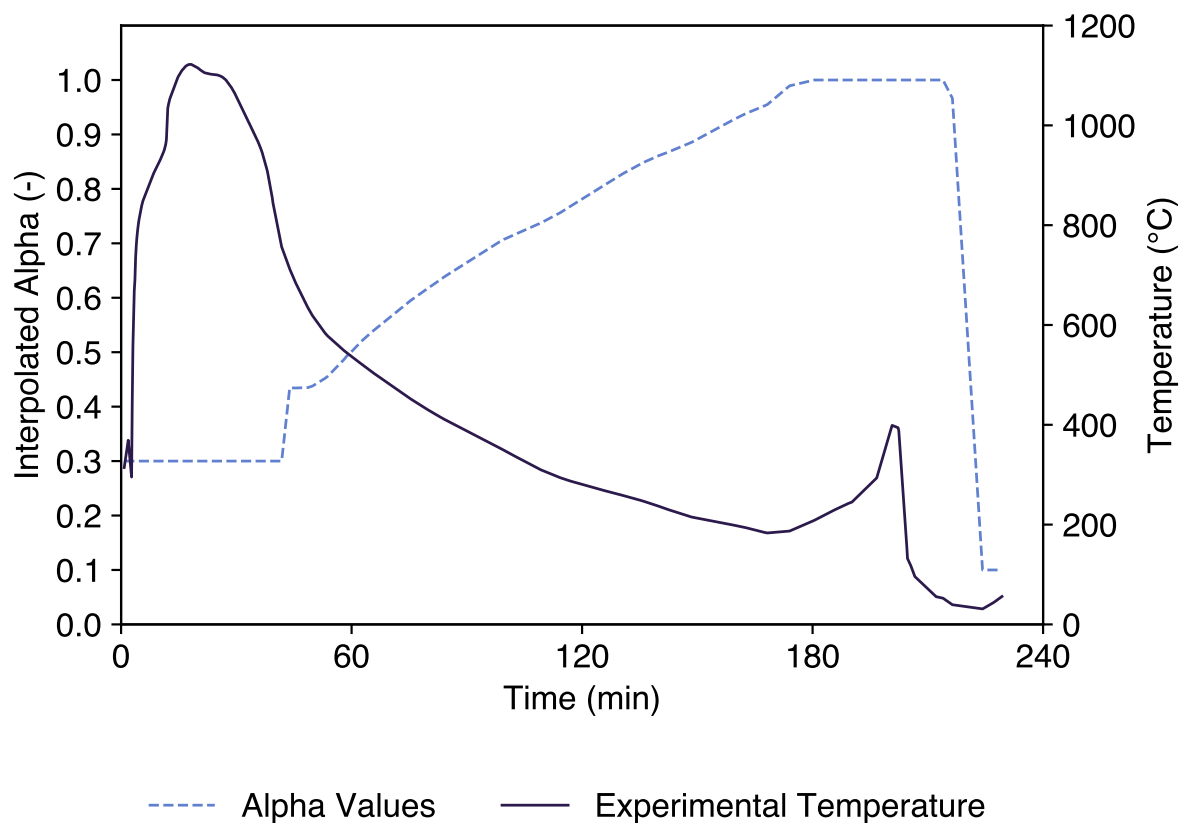


Figure A.49: Streamlined Alpha - Time Graph for Test 6

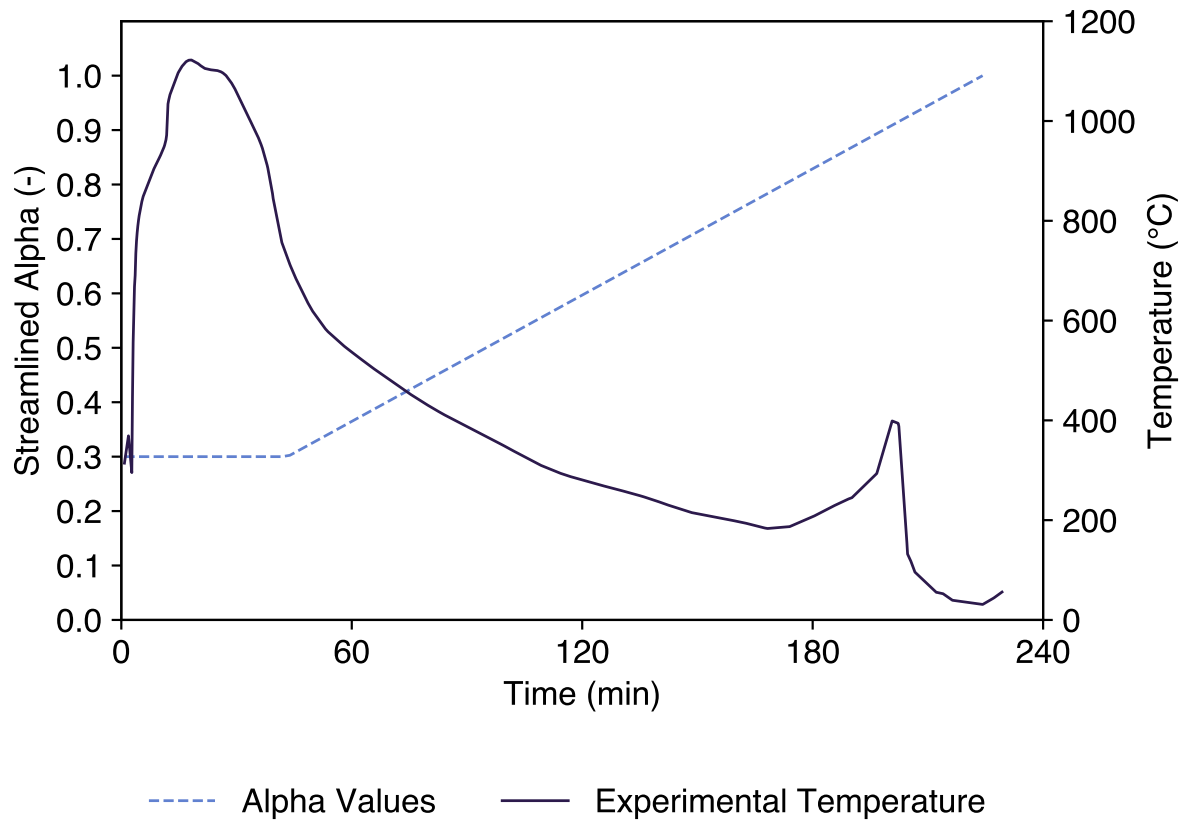
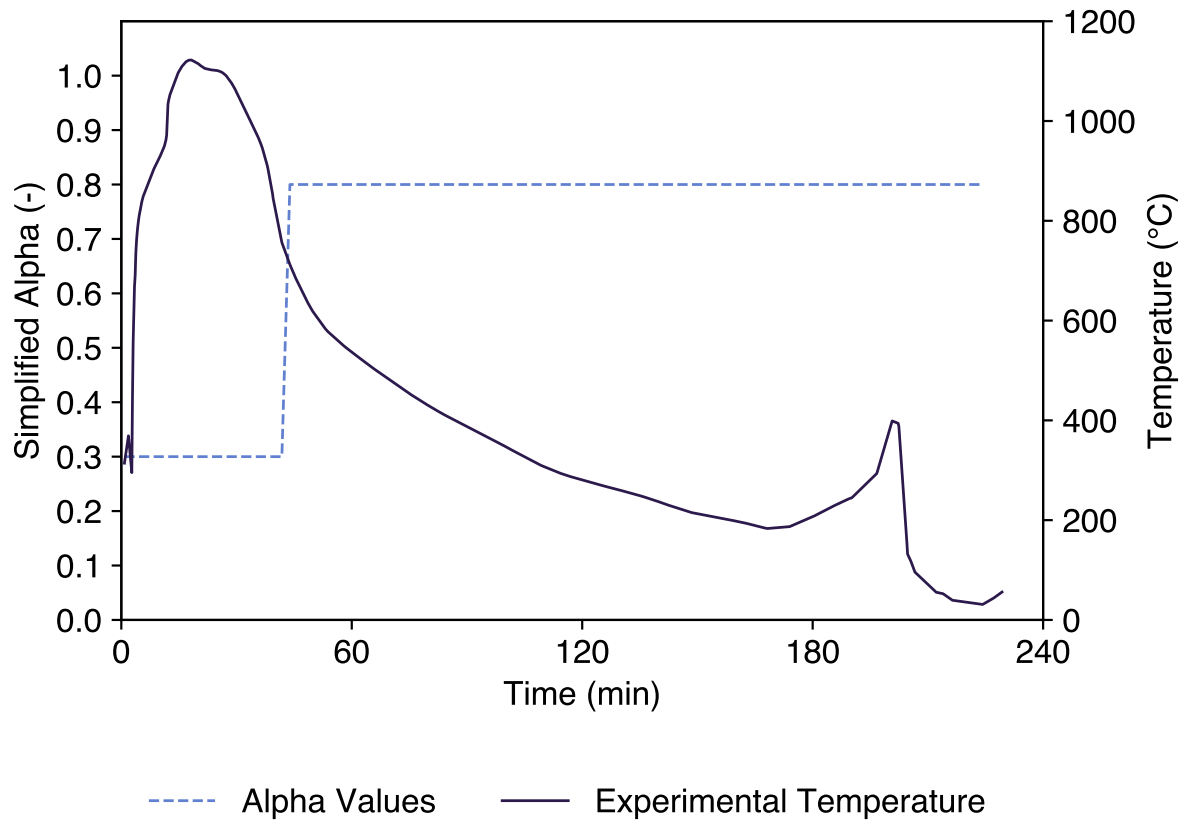


Figure A.50: Simplified Alpha - Time Graph for Test 6



A.8.2 Test 7

Figure A.51: Alpha - Time Graph for Test 7

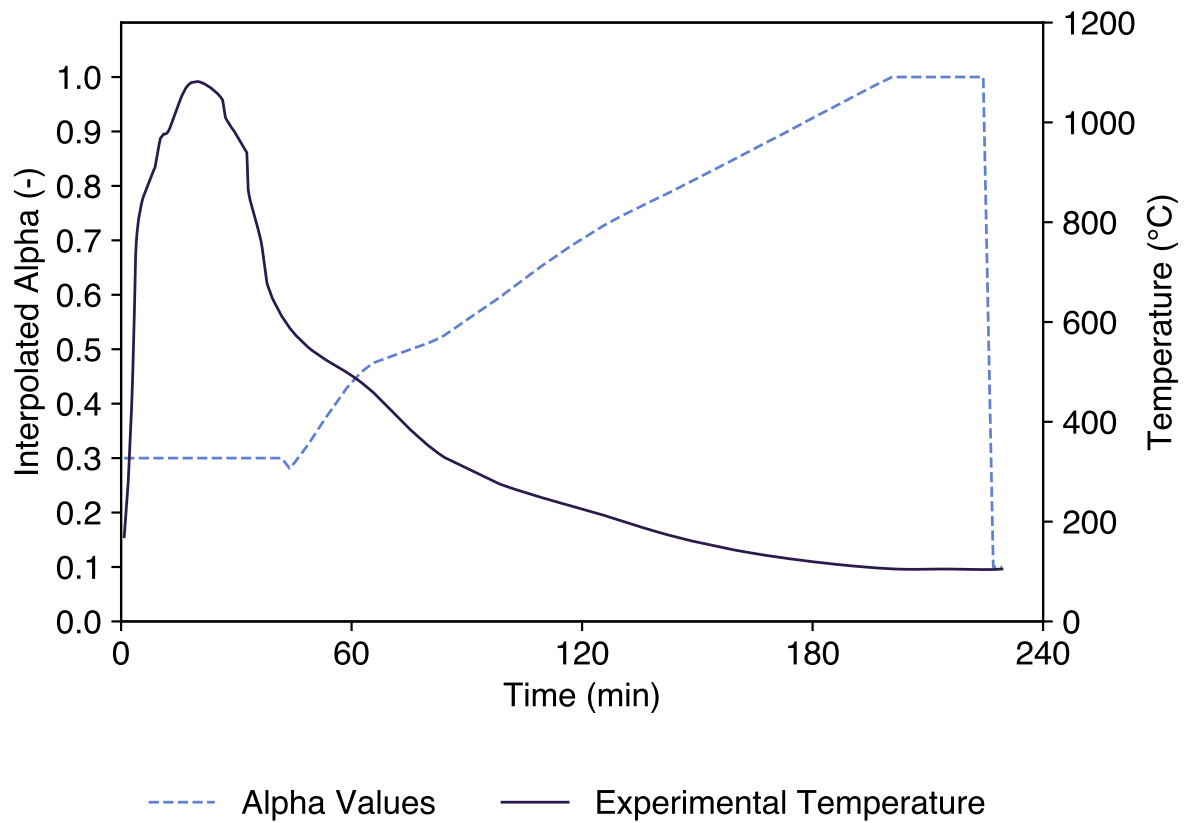


Figure A.52: Streamlined Alpha - Time Graph for Test 7

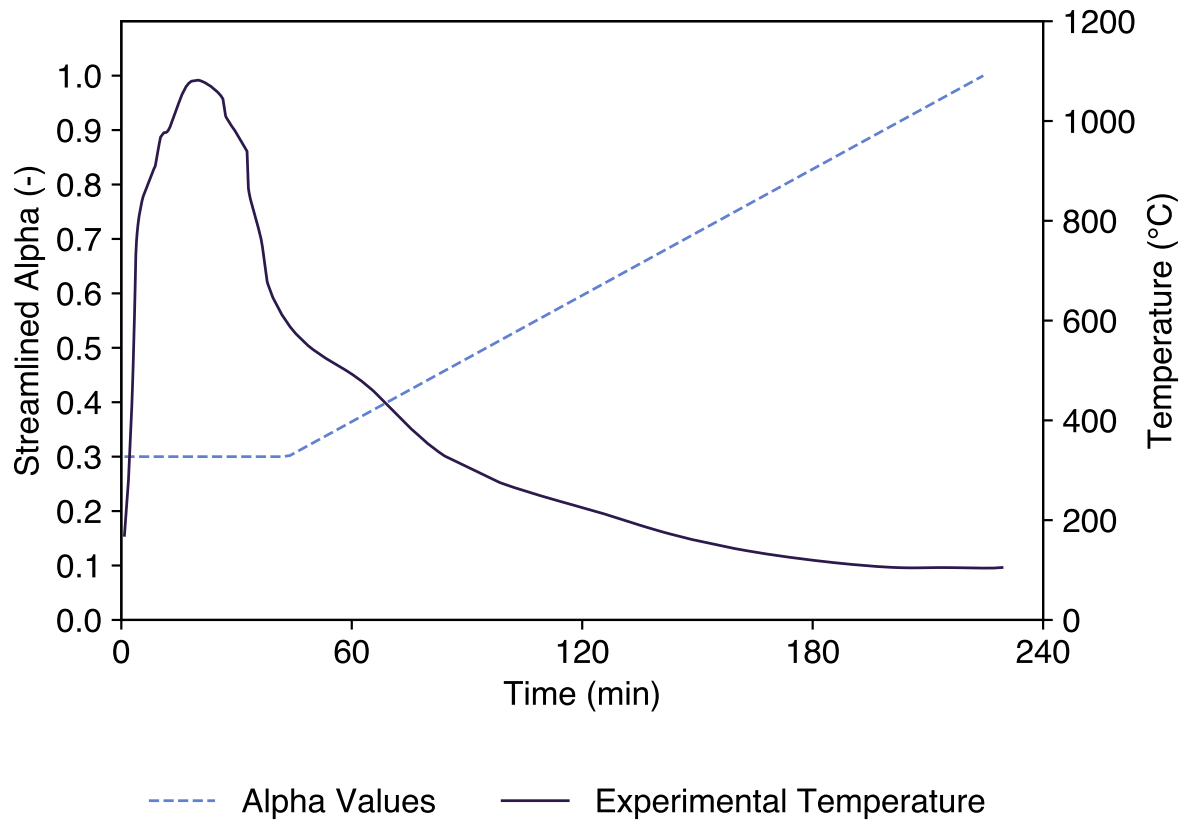
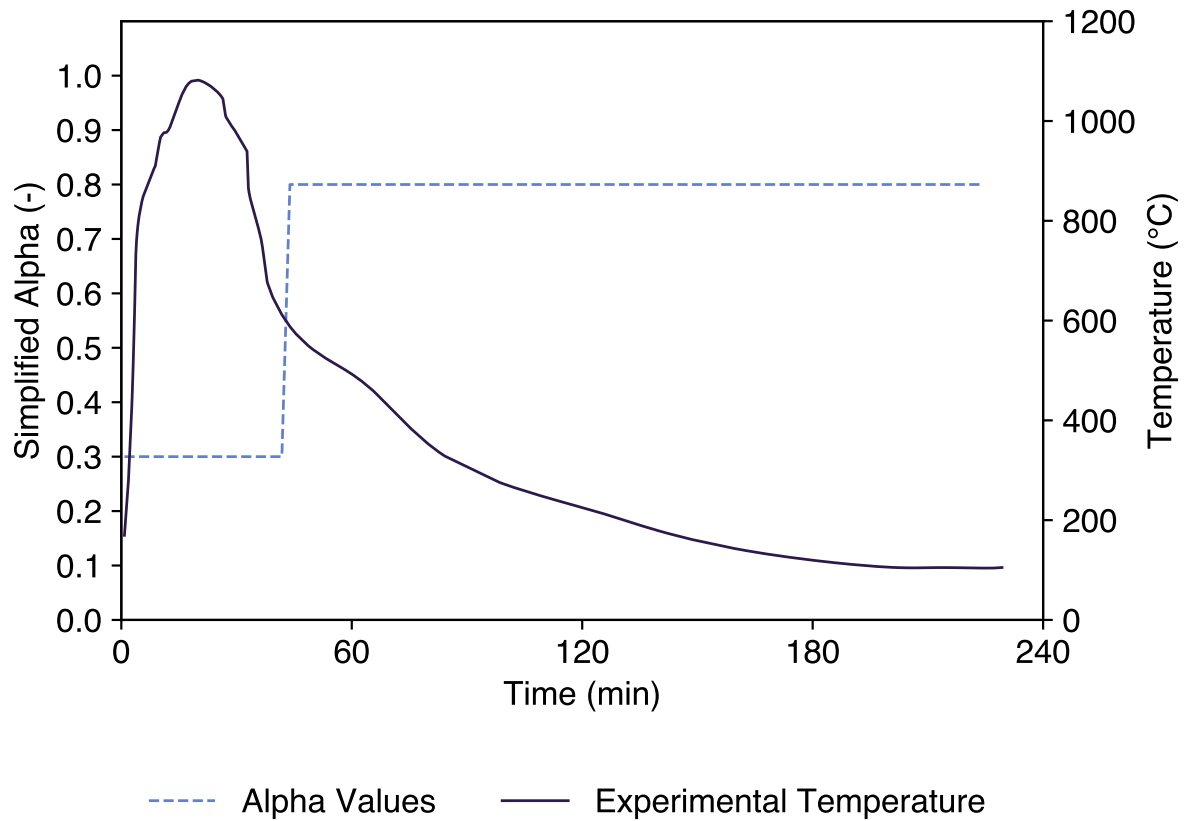


Figure A.53: Simplified Alpha - Time Graph for Test 7



A.8.3 Test 8

Figure A.54: Alpha - Time Graph for Test 8

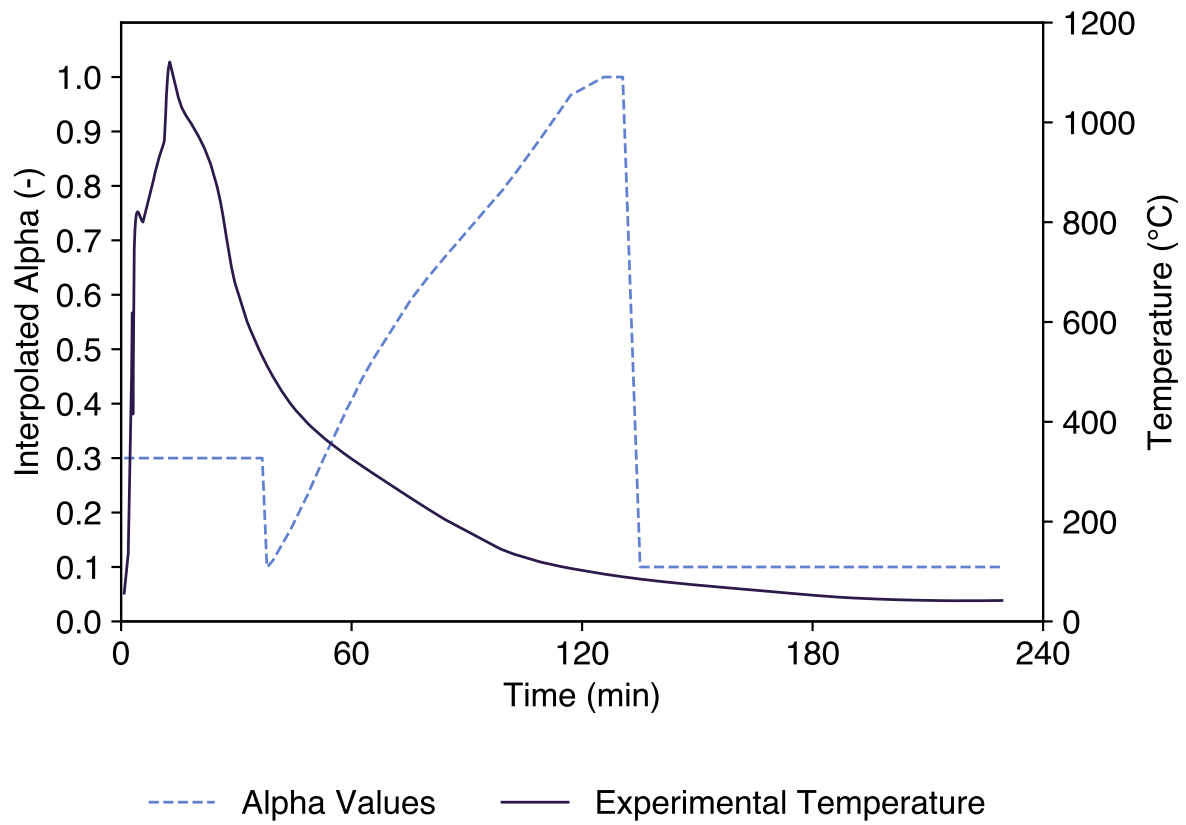


Figure A.55: Streamlined Alpha - Time Graph for Test 8

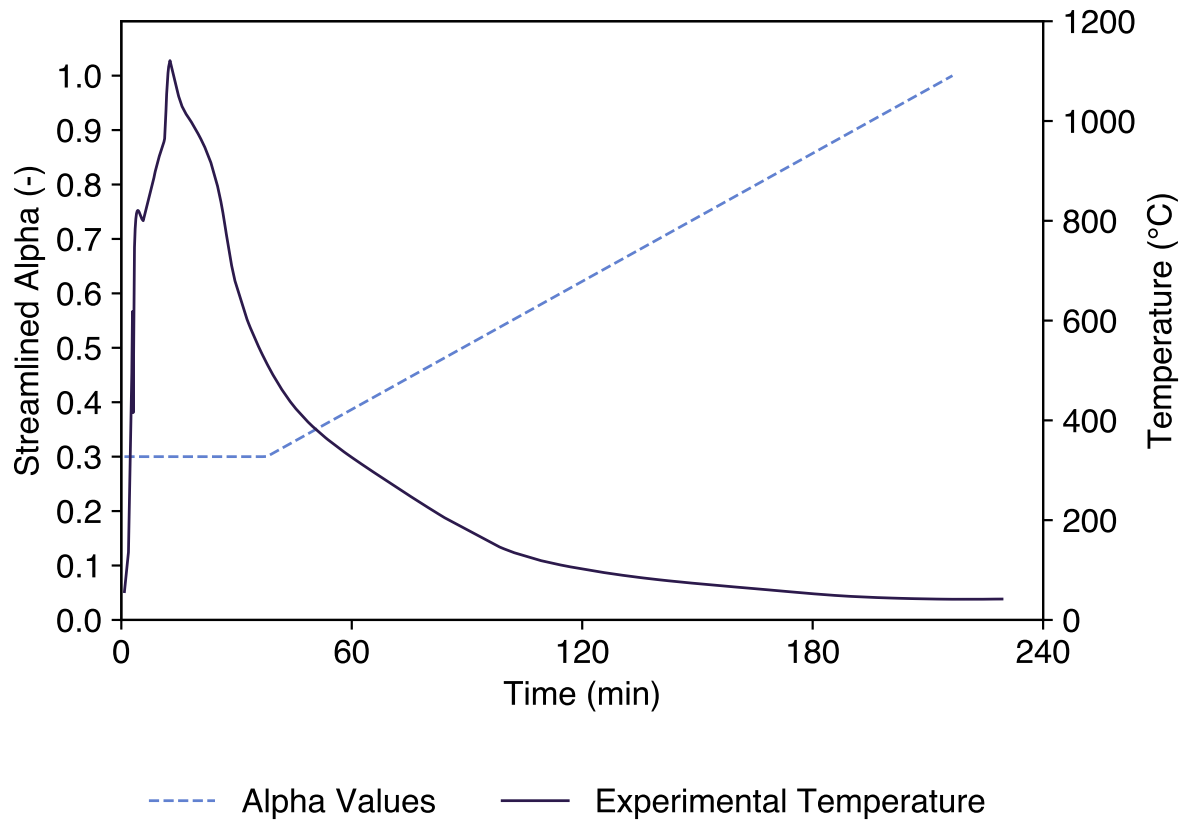
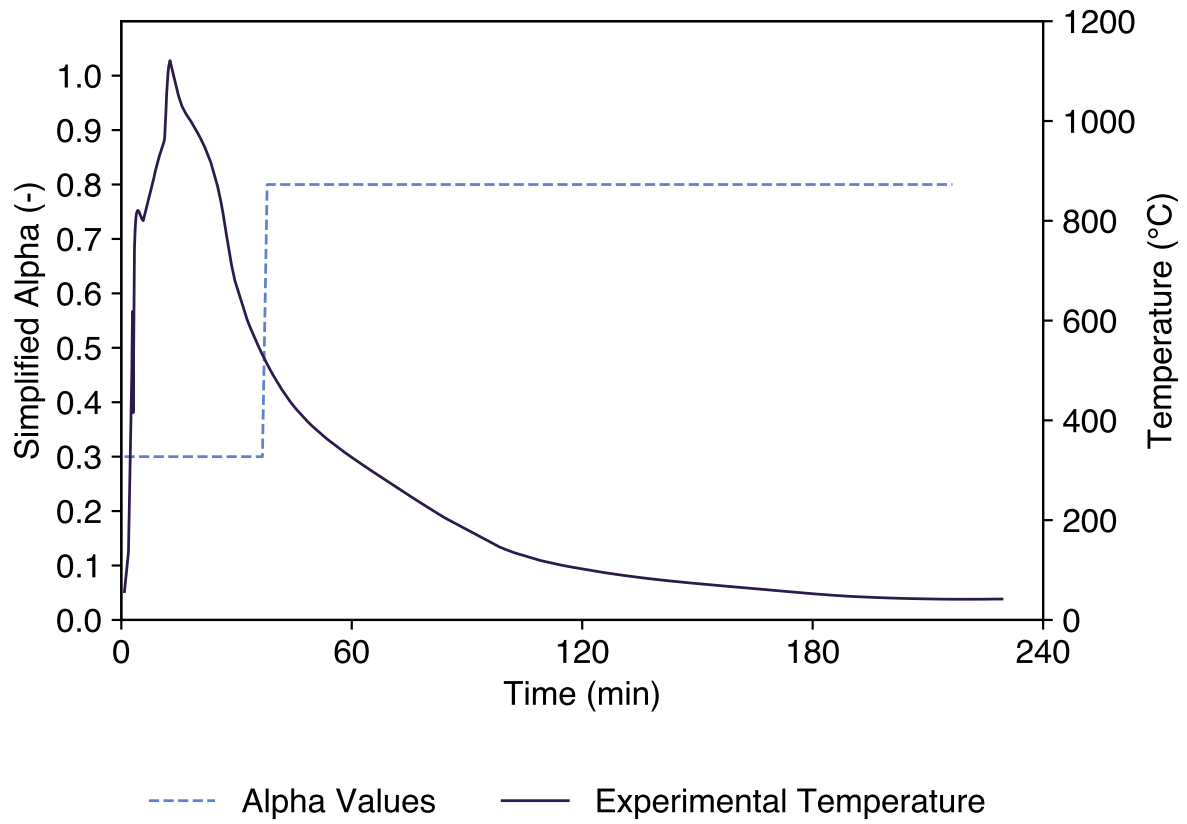


Figure A.56: Simplified Alpha - Time Graph for Test 8



A.8.4 Test 9

Figure A.57: Alpha - Time Graph for Test 9

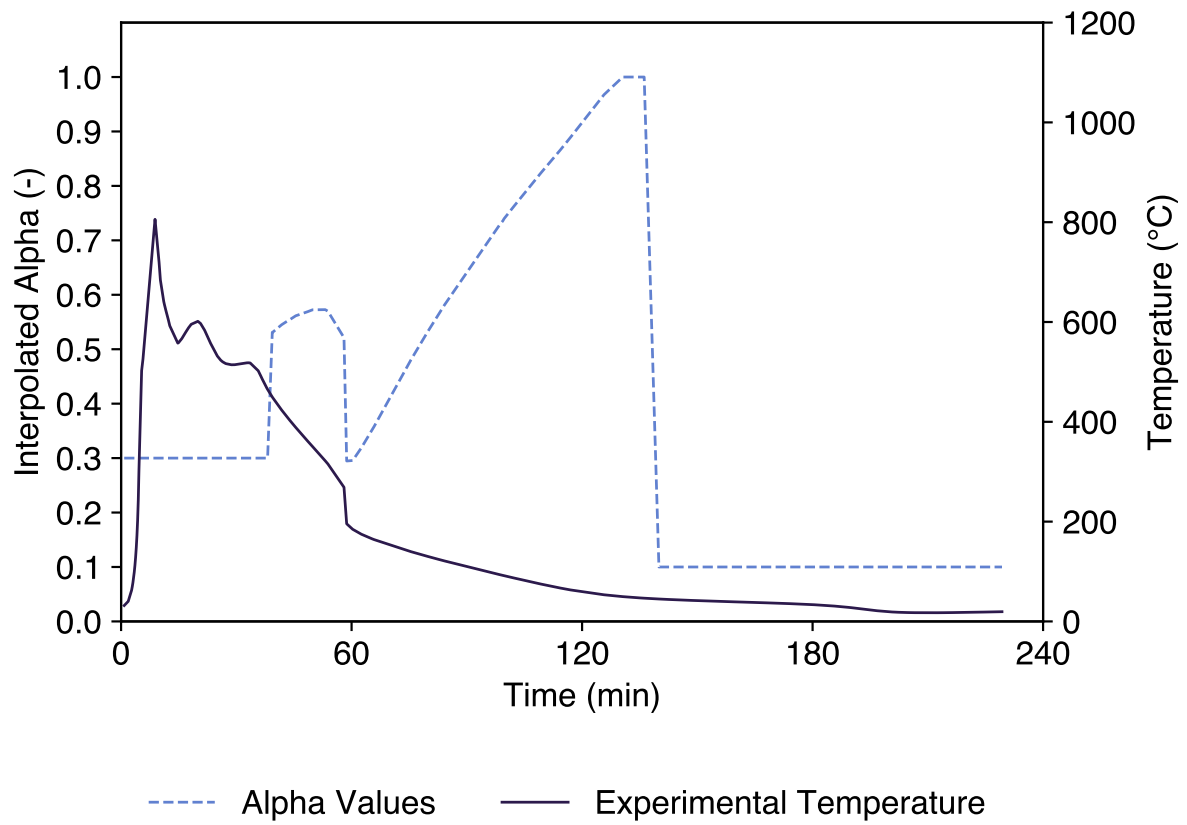


Figure A.58: Streamlined Alpha - Time Graph for Test 9

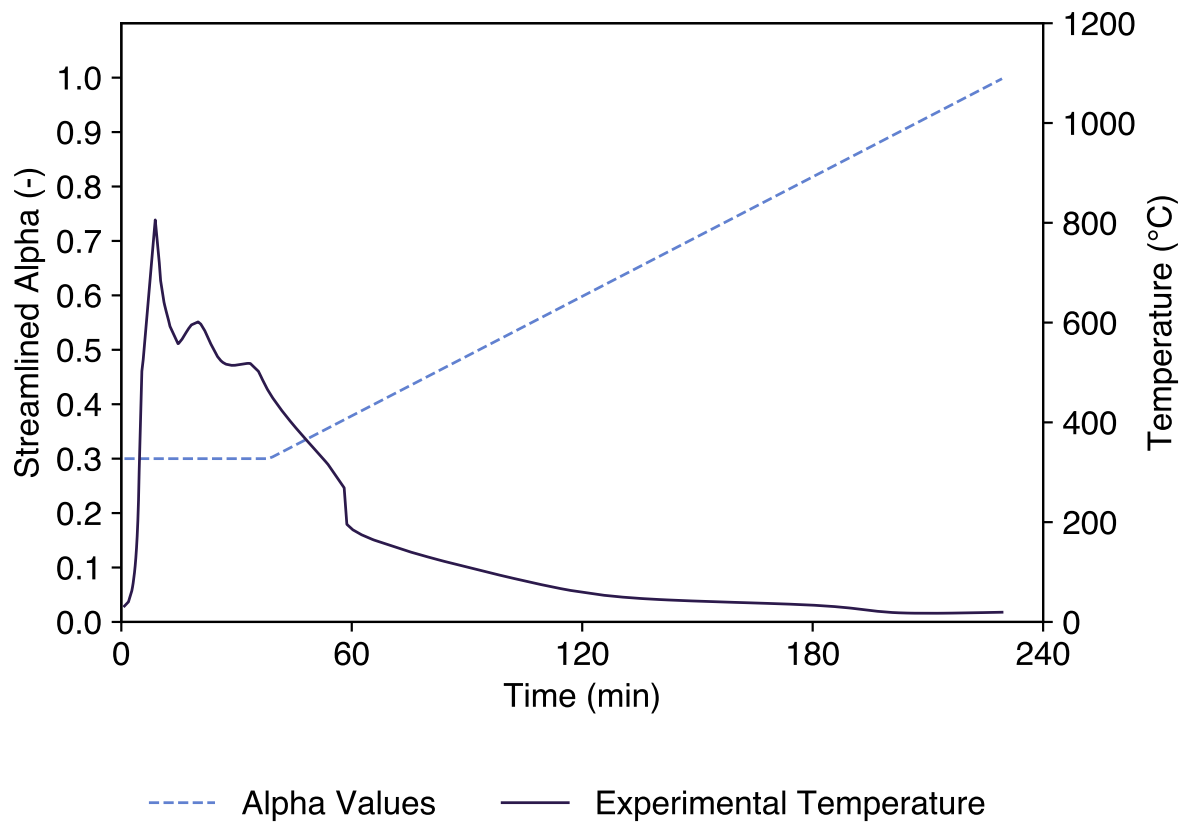


Figure A.59: Simplified Alpha - Time Graph for Test 9

